N73-10931

DEVELOPMENT OF PROCEDURES FOR CALCULATING STIFFNESS AND DAMPING PROPERTIES OF ELASTOMERS IN ENGINEERING APPLICATIONS

PART I: VERIFICATION OF BASIC METHODS

by

Thomas Chiang
Juergen M. Tessarzik
Robert H. Badgley

MECHANICAL TECHNOLOGY INCORPORATED

Prepared for

NATIONAL AERONAUTICS AND SPACE ADMINISTRATION

NASA -- Lewis Research Center

Contract NAS3-15334

Robert E. Cunningham, Project Manager

NOTICE

This report was prepared as an account of Government-sponsored work. Neither the United States, nor the National Aeronautics and Space Administration (NASA), nor any person acting on behalf of NASA:

A.) Makes any warranty or representation, expressed or implied, with respect to the accuracy, completeness, or usefulness of the information contained in this report, or that the use of any information, apparatus, method, or process disclosed in this report may not infringe privately-owned rights; or

B.) Assumes any liabilities with respect to the use of, or for damages resulting from the use of, any information, apparatus, method or process disclosed in this report.

As used above, "person acting on behalf of NASA" includes any employee or contractor of NASA, or employee of such contractor, to the extent that such employee or contractor of NASA or employee of such contractor prepares, disseminates, or provides access to any information pursuant to his employment or contract with NASA, or his employment with such contractor.

Requests for copies of this report should be referred to

National Aeronautics and Space Administration
Scientific and Technical Information Facility
P.O. Box 33
College Park, Md. 20740

1 Report No. NASA CR-120965	2 Government Accession No.	3 Recipient's Catalog No.
4 Title and Subtitle DEVELOPMENT OF PROCEDURES FOR CALCULATING STIFFNESS AND DAMPING PROPERTIES OF ELASTOMERS IN ENGINEERING APPLICATIONS PART I: VERIFICATION OF BASIC METHODS		5 Report Date March 31, 1972 6 Performing Organization Code
7 Author(s) Thomas Chiang; Juergen M. Tessarzik; Robert H. Badgley		8 Performing Organization Report No. MTI 72TR20 10 Work Unit No.
9 Performing Organization Name and Address Mechanical Technology Incorporated 968 Albany-Shaker Road Latham, New York 12110		11 Contract or Grant No. NAS3-15334 13 Type of Report and Period Covered Contractor Report
12 Sponsoring Agency Name and Address National Aeronautics and Space Administration Washington, D. C. 20546		14 Sponsoring Agency Code

15 Supplementary Notes
Project Manager, Robert E. Cunningham, Bearings Branch, NASA Lewis Research Center, Cleveland, Ohio

16 Abstract The primary aim of the efforts reported herein was verification of basic methods which are to be used in cataloging elastomer dynamic properties (stiffness and damping) in terms of viscoelastic model constants. These constants may then be used to predict dynamic properties for general elastomer shapes and operating conditions, thereby permitting optimum application of elastomers as energy absorption and/or energy storage devices in the control of vibrations in a broad variety of applications.

The efforts reported herein involved a (1) literature search; (2) the design, fabrication and use of a test rig for obtaining elastomer dynamic test data over a wide range of frequencies, amplitudes, and preloads; and (3) the reduction of the test data, by means of a selected three-element elastomer model and specialized curve fitting techniques, to material properties.

Material constants thus obtained have been used to calculate stiffness and damping for comparison with measured test data. These comparisons are excellent for a number of test conditions and only fair to poor for others. The results confirm the validity of the basic approach of the overall program and the mechanics of the cataloging procedure, and at the same time suggest areas in which refinements should be made.

17 Key Words (Suggested by Author(s))	18 Distribution Statement
Elastomers Dynamic Properties Vibration Test Rig Vibration Literature Survey Viscoelastic Models Analytical Prediction Methods	Unlimited

19 Security Classif. (of this report)	20 Security Classif. (of this page)	21 No. of Pages	22 Price*
Unclassified	Unclassified	110	$3.00

*For sale by the National Technical Information Service, Springfield, Virginia 22151

FOREWORD

The work described herein was done at Mechanical Technology Incorporated (MTI) under NASA Contract NAS3-15334 with Dr. Robert H. Badgley of the MTI Research and Development Division's Machinery Dynamics Section as Project Manager. Dr. Thomas Chiang of MTI performed the analytical portions of the investigation, while Mr. Juergen M. Tessarzik was responsible for the experimental efforts.

ABSTRACT

The primary aim of the efforts reported herein was verification of basic methods which are to be used in cataloging elastomer dynamic properties (stiffness and damping) in terms of viscoelastic model constants. These constants may then be used to predict dynamic properties for general elastomer shapes and operating conditions, thereby permitting optimum application of elastomers as energy absorption and/or energy storage devices in the control of vibrations in a broad variety of applications.

The efforts reported herein involved a (1) literature search; (2) the design, fabrication and use of a test rig for obtaining elastomer dynamic test data over a wide range of frequencies, amplitudes, and preloads; and (3) the reduction of the test data, by means of a selected three-element elastomer model and specialized curve fitting techniques, to material properties.

Material constants thus obtained have been used to calculate stiffness and damping for comparison with measured test data. These comparisons are excellent for a number of test conditions and only fair to poor for others. The results confirm the validity of the basic approach of the overall program and the mechanics of the cataloging procedure, and at the same time suggest areas in which refinements should be made.

TABLE OF CONTENTS

	Page
FOREWORD	ii
ABSTRACT	iii
LIST OF FIGURES	vi
SUMMARY	1
INTRODUCTION	3
Program Objectives	4
Engineering Configurations of Elastomers	5
LITERATURE SEARCH	9
DESCRIPTION OF ELASTOMER TEST RIG	13
Test Apparatus Requirements	13
Test Rig Mechanical Details	15
Instrumentation	17
Data Acquisition System	19
DESCRIPTION OF TESTS	21
Selection of Elastomers for Testing	21
Description of Tests Conducted	23
Data Taking Procedure	24
DEVELOPMENT OF ANALYTICAL METHODS	26
Dynamic Model Nomenclature	26
Mechanical Impedance and Compliance	31
DATA REDUCTION AND CORRELATION	35
Data Reduction	35
Correlation of Data With Viscoelastic Model	39
DISCUSSION OF RESULTS	44
CONCLUSIONS AND RECOMMENDATIONS	49
APPENDIX I – CALCULATION OF AIR CYLINDER STIFFNESS	53
SYMBOLS	54
REFERENCES	56
FIGURES 1 – 43	59
DISTRIBUTION	

LIST OF FIGURES

Figure Number	
1	Schematic of Elastomer Test Rig
2	Elastomer Test Rig Details
3	Elastomer Test Rig Mounted on Vibration Table
4	Mounting Configurations for Elastomer Test Specimen in Compression, Shear and Combined Compression-Shear Loading (right to left)
5	Radial Guide Bearing
6	Urethane Compression Test Sample After Failure
7	Schematic of Data Acquisition System for Analytical and Experimental Investigations of Elastomeric Damping Materials
8	Data Printout Sample
9	Data Acquisition Instrumentation
10	Resonance Frequency vs. Resonance Mass for Various Spring Rates, Including Approximate Stiffness Values for Neoprene and Urethane Cylindrical Test Specimens 2 Inches (5 cm) In Diameter and 0.50 Inches (1.27 cm) Long
11	A Diagram Illustreting the Dynamic Elements of the Test Rig
12	Three-Element Viscoelastic Model
13	Real Part of Complex Compliance Function Versus Frequency for Urethane Sample Under Shear Loading at Peak-to-Peak Amplitude of 0.001 in. (0.025 mm)
14	Imaginary Part of Complex Compliance Function Versus Frequency for Urethane Sample Under Shear Loading at Peak-to-Peak Amplitude of 0.001 in. (0.025 mm)
15	Real Part of Complex Compliance Function Versus Frequency for Urethane Sample Under Shear Loading at Peak-to-Peak Amplitude of 0.0015 in. (0.038 mm)
16	Imaginary Part of Complex Compliance Function Versus Frequency for Urethane Sample Under Shear Loading at Peak-to-Peak Amplitude of 0.0015 in. (0.038 mm)
17	Real Part of Complex Compliance Function Versus Frequency for Neoprene Sample Under Shear Loading at Peak-to-Peak Amplitude of 0.001 in. (0.025 mm)
18	Imaginary Part of Complex Compliance Function Versus Frequency for Neoprene Sample Under Shear Loading at Peak-to-Peak Amplitude of 0.001 in. (0.025 mm)
19	Real Part of Complex Compliance Function Versus Frequency for Neoprene Sample Under Shear Loading at Peak-to-Peak Amplitude of 0.003 in. (0.076 mm)

LIST OF FIGURES (continued)

Figure Number	
20	Imaginary Part of Complex Compliance Function Versus Frequency for Neoprene Sample Under Shear Loading at Peak-to-Peak Amplitude of 0.003 in. (0.076 mm)
21	Real Part of Complex Complaince Function Versus Frequency for Neoprene Sample Under Compression Loading at Peak-to-Peak Amplitude of 0.001 in. (0.025 mm)
22	Imaginary Part of Complex Compliance Function Versus Frequency for Neoprene Sample Under Compression Loading at Peak-to-Peak Amplitude of 0.001 in. (0.025 mm)
23	Real Part of Complex Compliance Function Versus Frequency for Neoprene Sample Under Compression Loading at Peak-to-Peak Amplitude of 0.0015 in. (0.038 mm)
24	Imaginary Part of Complex Compliance Function Versus Frequency for Neoprene Sample Under Compression Loading at Peak-to-Peak Amplitude of 0.0015 in. (0.038 mm)
25	Qualitative Sketeches of G_1 and G_2 According to Equation (32)
26	Comparison of the Correlated and Measured G_1 Functions for Urethane Sample Under Shear Loading at 0.001 in. (0.025 mm) Amplitude and No Preload
27	Comparison of the Correlated and Measured G_2 Functions for Urethane Sample Under Shear Loading at 0.001 in. (0.025 mm) Amplitude and No Preload
28	Comparison of the Correlated and Measured G_1 Functions for Urethane Sample Under Shear Loading at 0.001 in. (0.025 mm) Amplitude and 5% Preload
29	Comparison of the Correlated and Measured G_2 Functions for Urethane Sample Under Shear Loading at 0.001 in. (0.025 mm) Amplitude and 5% Preload
30	Comparison of the Correlated and Measured G_1 Functions for Urethane Sample Under Shear Loading at 0.001 in. (0.025 mm) Amplitude and 10% Preload
31	Comparison of the Correlated and Measured G_2 Functions for Urethane Sample Under Shear Loading at 0.001 in. (0.025 mm) Amplitude and 10% Preload
32	Comparison of the Correlated and Measured G_1 Functions for Neoprene Sample Under Shear Loading at 0.001 in. (0.025 mm) Amplitude and No Preload
33	Comparison of the Correlated and Measured G_2 Functions for Neoprene Sample Under Shear Loading at 0.001 in. (0.025 mm) Amplitude and No Preload

LIST OF FIGURES (concluded)

Figure Number	
34	Comparison of the Correlated and Measured G_1 Functions for Neoprene Sample Under Shear Loading at 0.003 in. (0.076 mm) Amplitude and No Preload
35	Comparison of the Correlated and Measured G_2 Functions for Neoprene Sample Under Shear Loading at 0.003 in. (0.076 mm) Amplitude and No Preload
36	Comparison of the Correlated and Measured G_1 Functions for Noeprene Sample Under Shear Loading at 0.003 in. (0.076 mm) Amplitude and 5% Preload
37	Comparison of the Correlated and Measured G_2 Functions for Neoprene Sample Under Shear Loading at 0.003 in. (0.076 mm) Amplitude and 5% Preload
38	Comparison of the Correlated and Measured G_1 Functions for Noeprene Sample Under Compression Loading at 0.001 in. (0.025 mm) Amplicude and No Preload
39	Comparison of the Correlated and Measured G_2 Functions for Neoprene Sample Under Compression Loading at 0.001 in. (0.025 mm) Amplitude and No Preload
40	Comparison of the Correlated and Measured G_1 Functions for Neoprene Sample Under Compression Loading at 0.001 in. (0.025 mm) Amplitude and 5% Preload
41	Comparison of the Correlated and Measured G_2 Functions for Neoprene Sample Under Compression Loading at 0.001 in. (0.025 mm) Amplitude and 5% Preload
42	Comparison of the Correlated and Measured G_1 Functions for Neoprene Sample Under Compression Loading at 0.0015 in. (0.038 mm) Amplitude and No Preload
43	Comparison of the Correlated and Measured G_2 Functions for Neoprene Sample Under Compression Loading at 0.0015 in. (0.038 mm) Amplitude and No Preload

SUMMARY

The objectives of this program are to catalog elastomer dynamic properties (stiffness and damping) in terms of viscoelastic model constants and to establish practical, designer-oriented procedures whereby these constants may be used to predict the dynamic properties for other elastomer shapes and operating conditions. Achievement of these objectives will permit the application of elastomers, on a firm engineering basis, as energy storage and/or energy dissipation devices for the control of vibrations in a broad variety of applications.

The work reported herein was undertaken to verify the basic methods for obtaining the viscoelastic model constants for elastomers. In this work, a survey of published literature was performed. This survey indicated that basic elastomer dynamic property data is rather sparse in terms of the parameter ranges covered. On the other hand, large volumes of test data are available for specific elastomer devices. Viscoelastic analytical procedures for predicting dynamic properties for general elastomer shapes and operating conditions are not found in the literature because of the level of difficulty of obtaining general solutions to the governing equations.

No test apparatus was available for obtaining, over the range of frequencies, amplitudes, and preloads expected to be encountered in typical engineering applications, elastomer dynamic test data which could be used to generate the material constants. Consequently, a test rig which utilizes the base-excitation, resonant-mass approach was designed, built, and successfully used to obtain test data. This test rig is able to perform uniaxial tests on elastomer samples of a variety of sizes and shapes (test specimen cavity is a cylinder 5 in. (12.7 cm) high by 5 in. (12.7 cm) in diameter) over a frequency range from about 20-30 Hz to over 1000 Hz. Variable resonance mass, which may be selected to match test elastomer properties, permits tests at virtually any reasonable dynamic amplitude at the resonance points, with correspondingly lower amplitudes at off-resonance conditions. Test amplitudes are limited primarily by elastomer properties (and of course shaker power) rather than by the test rig itself. The test rig, which may be driven by any shaker, permits vibration tests to be conducted with force preloads of up to

4100 pounds (18,200 n) applied to the test specimens, and can be readily adapted for constant temperature tests up to about 400°F (205°C).

During the conduct of the work reported herein, tests were conducted on urethane and neoprene elastomer samples in the compression, shear, and combined compression/shear modes. Each sample was composed of two parallel-mounted circular discs, each two inches (5 cm) in diameter by one-half-inch (1.27 cm) high. Tests were conducted at room temperature at a number of frequencies between about 25 and 1000 Hz, at amplitudes of up to 0.005 inch (0.127 mm) (peak-to-peak), and with compressive preloads of zero, five percent, and ten percent of free length. Elastomer and elastomer mount temperatures were recorded during the tests.

Measured amplitudes and phase angles obtained during the tests were used to calculate complex compliances at the test points. This data was then processed via curve-fitting and a selected three-element elastomer analytical model, to obtain the viscoelastic model constants. Through the use of these constants, measured test data could be reproduced, analytically, over wide frequency ranges for a number of test configurations.

It is concluded that the results obtained confirm the validity of the basic approach of the program and the mechanics of cataloging viscoelastic model constants. Immediate attention may therefore be turned to: (1) refining the test rig and measurement system, including the addition of the capability of performing constant-temperature tests over a range of temperature levels; (2) evaluation of several other potentially useful elastomer analytical models; and (3) performance of elastomer dynamic tests at controlled temperatures. Final program efforts should then be directed at: (1) developing and verifying through tests, practical, designer-oriented methods for calculating elastomer dynamic properties for general shapes and operating conditions using the viscoelastic model constants; and (2) development of catalogs of viscoelastic model constants for commonly-used elastomers. It may also prove beneficial to reduce the number of groups of viscoelastic model constants which must be cataloged through development of functional relationships with operating parameters (e.g., temperature) or through corresponding increases in the number of viscoelastic model constants.

INTRODUCTION

General Background

Accurate knowledge of elastomer dynamic properties (stiffness and damping) is becoming increasingly important as elastomers are considered for use in increasingly difficult applications. Many such applications are costly to design and build, and rely heavily upon the properties of the elastomer elements. For instance, machinery rotors are being designed for higher and higher operating speeds, and are becoming lighter and more slender as engine weights and sizes decrease. The major result of these trends is that rotor operation is increasingly at speeds which lie above one or more rotor-bearing bending critical speeds. While good balancing is the key to overall good rotor behavior under such conditions, energy removal, via the use of materials such as elastomers, is required for control of vibration amplitudes in the vicinity of the critical speeds. Critical speeds may also be modified at the same time by the stiffness properties of the elastomer.

A further example of the need for well-understood elastomer dynamic properties is that associated with the control of vibrations in power-transmission shafting, typified by helicopter main rotor synchronization and tail-rotor drive shafts. In both of these cases, the shaft operating speeds would be above many bending critical speeds if the shafts could be supported by a single bearing at each end, incorporating elastomer damping elements. While the dynamic performance of such advanced designs cannot now be predicted analytically or optimized during design, their ultimate achievement would mean significant reductions in numbers of bearings, with accompanying savings in system cost and weight, and certainly increased reliability. Availability of practical and effective elastomer damper designs for use in vibration energy removal, together with a practical and effective shaft balancing procedure, will greatly assist designers in progressing toward this goal.

In addition to these examples, which are concerned primarily with rotating machinery, there are many other elastomer applications in which specified dynamic properties may be required. These include for example: structural dampers, for use in reducing either stress levels for fatigue life purposes or amplitude levels for noise and comfort considerations; isolators, for use in packaging or in

separating fragile equipment from harmful vibration or shock environments; and sandwich constructions in which the elastomer element may replace oscillatory-motion bearings. There are, of course, many additional applications.

In the above examples, effective and efficient design of the mechanical systems requires that the elastomer dynamic properties be available to the designer in analytical form such that he can select or design the proper elastomer configuration required in the particular application.

Program Objectives

Certain elastomer properties, such as bondability, resistance to abrasion and impact, and chemical reaction to various environments, are generally well understood with regard to engineering uses of elastomers. On the other hand, the capability does not presently exist for analytically designing an elastomer element to provide stiffness and damping which is of the accuracy required in many applications. Development of practical, designer-oriented techniques sufficient for this purpose is the major objective of this program.

Although dynamic properties of sample elastomers may be found in various polymer and rubber journals in the literature, this data is somewhat sparse in that the desired properties are not always readily available to mechanical designers for the particular configuration, size, or operating condition desired. This is because of the extreme variability of the dynamic properties with many of the design parameters, such as geometric configuration, loading, vibration frequency and temperature. Furthermore, existing elastomer test apparatuses are generally not fully suited for testing over all desired parameter combinations, particularly at high frequencies and amplitudes. Moreover, at the present time there is apparently no technical body, or combination of technical bodies charged with the generation and publication, in useful engineering form, of elastomer dynamic property data for newer elastomers on a standard basis.

In current engineering practice, a trial-and-error approach to the design of elastomer elements is often taken. This approach commonly involves best estimates based on other designs, and often the building of a demonstration installation using several candidate elastomers in various configurations. Although such a

trial-and-error process often gives useful results, these may be costly and time-consuming to obtain, and may not always be the optimum design in each application. Successful and economically feasible use of elastomers in future engineering applications will require that elastomer dynamics technology be readily available in a form which is practical and readily usable. Achievement of this result is the ultimate goal of the present program, of which the efforts reported herein are an integral part.

Engineering Configurations of Elastomers

A great deal of published elastomer dynamic property data (stiffness and damping) has been obtained through tests of elastomer samples in the configurations shown below:

(a) (b)

Configuration (a) is most appropriate for obtaining compression-tension data, while (b) is most appropriate for obtaining shear data.

On the other hand, elastomers are often used in engineering applications in rotating machinery hardware in the following configurations:

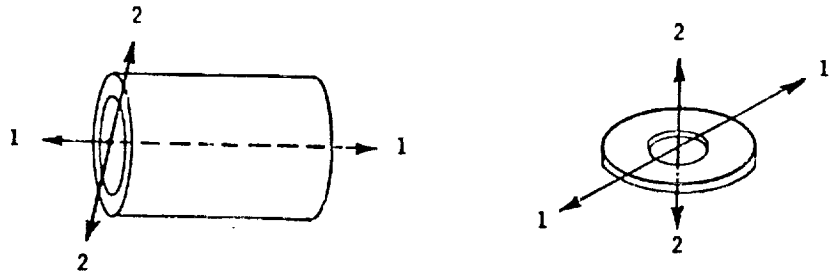

(c) (d)

Configuration (c) is often used in conjunction with bearing supports or in a distributed damping configuration, with loading along a diameter of the elastomer cylinder (the 2-2 axis). Configuration (d) is often used in power-transmission shaft dampers, mounted external to the shaft, with one face of the elastomer disc

fixed and shear loading applied along the other face (the 1-1 axis). Loading of configuration (d) along the 2-2 axis is also common in isolator applications of elastomers. In all cases, the application dynamic conditions involve generally more complex shapes, stresses, amplitudes, and temperature distributions than those existing in test samples such as (a) and (b) from which measured dynamic properties were obtained. Relating the two sets of configurations has proven to be an extremely difficult task, and one which has not yet been satisfactorily solved on a practical, engineering level.

On the one hand, the applied mechanician may advocate a purely analytical treatment of the problem, based upon viscoelasticity theory. This approach, while most rigorous, may become bogged down in details of stress distribution and those resulting difficulties associated with relating stresses to overall body dynamic behavior by integration of unit volume dynamic properties throughout the elastomer body. While this approach has not yet reached the design-engineer level of practicality, it possesses the greatest long-term potential.

On the other hand, the elastomer user who must cope with existing vibration problems without benefit of detailed viscoelastic theory has resorted to the expedient of measuring stiffness and damping of particular elastomers as functions of all pertinent parameters. Unfortunately, there are many such parameters, and while the catalog of dynamic properties thus obtained becomes almost endless, it never seems to contain data immediately applicable to the particular application at hand.

What is required, and what has in fact been undertaken in the program described herein, is the development of an elastomer dynamics technology bridge between these two extreme positions. This bridge accounts for the variability of the dynamic properties with design and operating parameters on the one hand, and contains within it the mechanisms for moving toward the rigorous viscoelasticity solution in the future.

Basic viscoelastic model constants were selected as quantifiable entities which could be obtained through simple tests and cataloged for ranges of operating parameters. These constants will be shown to be invariant with respect to frequency. However, they do depend on parameters such as temperature, preload and elastomer configuration.

This report describes efforts directed at the verification of methods selected for obtaining the elastomer viscoelastic model constants. These efforts involved experimental measurement of elastomer dynamic characteristics through tests of elastomer samples of various configurations, the calculation of the viscoelastic model constants from these dynamic properties, and comparisons between measured dynamic characteristics and those calculated using the derived viscoelastic model constants.

In the program, a test rig was designed, fabricated and assembled for testing elastomer specimens in order to obtain their mechanical dynamic properties. This elastomer test rig, which is described in detail in a later section, utilizes the base-excitation resonance-mass approach and was designed to be mounted on an electrodynamic shaker which provides the input oscillations. The elastomer specimens tested were epoxied to a steel plate which was secured to the shake table. To the other side of the elastomer was epoxied a holder to which a resonant mass was attached. The size of this resonant mass was adjustable, and was selected based upon the frequency range at which the data were to be taken. Generally, data were taken at frequencies somewhat higher than the natural frequency of the elastomer-resonance mass system. The resonant mass was variable between a minimum of 1.7 pounds (0.77 kg) and a maximum of approximately 485 pounds (220 kg). Force preload on elastomer specimens could be changed as desired by adjusting air pressure in loading cylinders on the test rig. Test amplitudes were limited only by elastomer failure limits (and shaker power) rather than by the test rig itself.

Two elastomers, urethane and neoprene, were selected for test from among the many available. Six (6) samples, each composed of two discs 2 in. (5 cm) in diameter and 0.50 in. (1.27 cm) thick, were prepared and tested. These samples are denoted in following sections as the urethane compression sample, the urethane shear sample, the urethane compression/shear combination sample, the neoprene compression sample, the neoprene shear sample, and the neoprene compression/shear combination sample. Tests were performed over the frequency range of about 20-30 to 1000 Hz, with force preloads which produced compression of zero, five percent and ten percent of free length, and with peak-to-peak amplitudes up to 0.005 in. (0.127 mm). Much higher vibration amplitudes were applied during preliminary

testing of the urethane compression-tension sample. These amplitudes, on the order of 0.015 to 0.020 in. (0.3 mm to 0.5 mm) peak-to-peak at up to 1000 Hz, resulted in extreme temperature gradients within the samples, and rapid sample failure.

At each of approximately 570 data points, vibration amplitudes and phase angles were recorded. From this data, elastomer stiffness and damping coefficients, and finally the complex compliance functions, were calculated. The complex compliance functions were thus obtained for all test samples (except of course the urethane compression sample which failed), and were plotted versus frequency with force preload and vibration amplitude as parameters. Good complex compliance data (smooth curves and reasonable trends) were obtained for the urethane and neoprene shear samples, and for the neoprene compression sample. The complex compliance functions for both urethane and neoprene combined compression/shear samples, however, showed considerable and apparently inconsistent variations with frequency over portions of the frequency range of interest. While some of this data, particularly in the frequency range between about 100-200 Hz and 500-600 Hz, appear satisfactory, the functions were not considered to be complete enough for use in determining the viscoelastic model constants which are valid for the entire frequency range. Consequently, further reduction and curve fitting to obtain material property constants was not performed for these two sets of data.

The viscoelastic model constants were obtained by curve-fitting the experimental data for the urethane and neoprene shear samples, and for the neoprene compression sample by means of a three-element viscoelastic model. Satisfactory correlation between measured complex compliance functions and those calculated using the derived viscoelastic model constants was obtained over the entire frequency range for many of the reduced data cases, while less satisfactory correlation (in the case of the dissipation function) was obtained in other cases.

LITERATURE SEARCH

A considerable amount of research work has been done on elastomers at both the basic and applied levels, resulting in many papers and publications, and several textbooks. This work ranges from studies of the effects of elastomer composition and manufacturing procedures on properties, to development of several varieties of test rigs for experimentally determining the properties of various sample shapes and configurations under a number of operating conditions, and to development and proof-testing of elastomer components for engineering use in specific problem situations. In order that maximum attention might be paid to previously published work, and that existing experience be brought to the program wherever possible and appropriate, an effort was undertaken at the start of the herein-reported efforts to survey the existing literature.

Further, efforts were made to identify, through use of NASA and other information retrieval systems, other recent and current Government-supported elastomer dynamics research efforts. This portion of the literature survey led thus to contacts with, among others, personnel of the Strength and Dynamics Branch, Metals and Ceramics Division, Air Force Materiels Laboratory (AFSC), Wright-Patterson Air Force Base, Ohio, who are concerned with the use of elastomer materials for the control of structural component vibration levels. Detailed discussions with these individuals indicated that the planned efforts would, as expected, provide very useful information to the Government provided proper coordination was made with other Government-sponsored efforts. Such coordination was effected through provision of regular reports to interested individuals and agencies, and discussion of program directions and results with these individuals as appropriate.

Elastomer properties such as hardness, resilience, strength, bondability, and resistance to cold flow, tear, wear, and impact may vary widely depending upon the particular elastomer, its components, and the way it is processed. Literally thousands of combinations of properties may be achieved from the many natural and synthetic-base materials which are available (Refs. 1 through 6 for instance).

Elastomer dynamic properties (stiffness and damping) vary not only with respect

to component elements and processing procedures, but also with respect to the operating conditions to which they are exposed. Thus, mounting configuration, vibration frequency and amplitude, and above all temperature and temperature gradient all are quantities which influence the dynamic properties. The net result of this large number of parameters is that dynamic properties have had to be determined through testing under conditions reasonably similar to those in which the elastomer element will actually be used. This has resulted in the development of various types of test apparatus, each of which has advantages and disadvantages. Several of the more common types are discussed below.

The torsion pendulum is a simple apparatus which utilizes the principle of decay of free vibration amplitude to measure the shear modulus and damping of an elastomer sample. In this test method, one end of the specimen is rigidly clamped.The other end of the specimen is attached to a member having known moment of inertia and which is free to oscillate. The pendulum is given an intial motion and allowed to oscillate freely. From recorded values of oscillation frequency and the decrease in amplitude with time, the shear modulus and damping can be calculated (Refs. 7 and 8). This method is restricted to low-frequencies (0.01 to 10Hz).

The vibrating reed method (Refs. 9, 10 and 11) is a forced-vibration, resonance test apparatus. The test specimen is attached to a strip or reed which is clamped at one end and forced to vibrate transversely. As the frequency of the vibrations is changed, the amplitude of the free end of the reed will go through a maximum at the natural frequency of the reed. From the measured amplitude-frequency curve near the natural frequency, the dynamic moduli of the elastomer specimen can be computed. This apparatus covers the frequency range of 10 to 1000 Hz, but it is not suitable for high-damping elastomers.

The forced-vibration method, utilizing both resonance and nonresonance operation, is the most satisfactory means for determining dynamic properties over a wide frequency range at constant temperature. The input in this method is forced sinusoidal oscillation of the elastomer support element. The resulting motion of the mass supported across the elastomer (in terms of displacement, velocity, or acceleration) is measured at the respective frequency. From the measured

input and output signals and their relative phase, and known properties of the test hardware (mass, etc.), the dynamic properties can be calculated. Although the calculation required to obtain the dynamic properties is relatively more complicated than other methods, it can readily be done by computer The important thing is that the test is not critically dependent upon the resonant frequency of the system, although resonance may be required to achieve relatively high amplitudes. Therefore, the frequency of measurement can be changed over a range without major changes in the apparatus. For these reasons the test rig designed under this program and described below employed this method

For elastomer dynamic property tests above about 10,000 Hz, the wave propagation method can be used (Refs. 1, 12 and 38) In this method, the dynamic moduli are calculated from the measured velocity and attenuation of sound waves propagating inside a specimen

Elastomer dynamic properties, obtained by various test methods for specified parameter ranges, are reported by many authors in the literature (Refs. 12 through 32). A brief summary of elastomer elastic and damping properties, together with a collection of references, are included in Reference 35 (pages 241-245). Nolle (Ref. 12), Hopkins (Ref. 14), Painter (Ref. 15), Philippoff (Ref. 16), Fitzgerald, et al (Ref. 17), Kurath, et al (Ref. 25), and Yin and Pariser (Ref. 28 and 30) have tested a number of elastomers including natural rubber, butyl, hypalon, neoprene, polyvinylchloride, and polyisobutylene. Effects of frequency, temperature, preload, amplitude, and shape of test specimen on the dynamic properties were reported for limited parameter ranges. The equivalence of temperature and frequency on the dynamic moduli was reported in, among others, References 13 and 17. It was not until 1954 that the method of reduced variables was developed by Williams and Ferry (Ref 20). By this method, the dynamic moduli over a wide frequency range at some reference temperature can be used to determine the moduli at other temperatures. The effects of preload on dynamic moduli were studied by Nolle (Ref. 13). It was reported that the effect cannot generally be described in terms of any simple systematic shift of the modulus-frequency curve or the modulus-temperature curve. Considerable amplitude dependence of the dynamic moduli of carbon-black filled natural rubber vulcanized was reported in Reference 18. This amplitude dependence does not increase at

low temperatures. The large dynamic strain amplitude effect of a BTR elastomer, as reported by Painter (Ref. 22), is to decrease the dynamic elastic moduli; this effect is more profound at high frequency.

The shape factor, which describes the discrepancy between the elastic modulus of an elastomer and the effective elastic modulus of a particular test specimen, was described in References 5, 6, 36 and 27. For a shear specimen, the shape factor is important only for thick specimens in which bending may occur in addition to simple shear deformation.

DESCRIPTION OF ELASTOMER TEST RIG

The elastomer tests described in this report were conducted in a test apparatus designed and built under this contract. This test rig was designed to impose precisely measured uniaxial vibration amplitudes upon a selected elastomer sample at desired test frequencies and under selected force preloads. The rig is capabl of testing, through the base-excitation resonance-mass technique, elastomer sampl of virtually any size and shape (test sample cavity is a cylinder approximately 5 in. (12.7 cm) high by 5 in. (12.7 cm) in diameter) over a wide frequency range. Selection of the resonance mass to match elastomer sample properties permits testing at very high amplitudes at resonance, with correspondingly lower amplitud at off-resonance conditions. Test amplitudes are limited by elastomer capabiliti and shaker input power rather than by the test rig itself. In the tests describe below, for instance, elastomer samples consisting of two cylinders, each 0.50 in. (1.27 cm) thick by 2 in. (5 cm) in diameter were tested at maximum amplitudes of about 0.006 in. (0.152 mm) peak-to-peak at 1000 Hz, the equivalent of about 600 g on the resonance mass. Double amplitudes of up to about 0.020 in. (0.5 mm) were measured at lower frequencies.

The test rig, which may be driven by any shaker device, permits force preloading of the elastomer samples and has been designed for future incorporation of variable test temperature hardware. The vibration input to the test rig in the tests described below was obtained from a commercially-available electromagnetic shaker system capable of delivering 15,000 lb (66,700 newton) force in the sinusoidal mode of vibration.

Test Apparatus Requirements

The elastomer test rig had to meet five functional requirements:

1. Very low residual damping.
2. A provision for holding the elastomer test material sample for tests in compression, shear, or any combination of the two conditions.
3. A means for providing force preloading to the elastomer test sample in order to perform high preload vibration tests at high (resonance) frequencies.

4. An inertia mass loading of the elastomer test sample with weights ranging from 1.5 to 500 lb (0.68 to 227 kg) such that high amplitude tests could be conducted at resonance between about 30 Hz and 1000 Hz.

5. A means for removing mass preload from the elastomer test sample in order to perform low preload vibration tests at low (resonance) frequencies.

Achievement of these requirements was met through a test rig concept based upon a unidirectional vibrating mass-spring system, with the elastomer specimen represented as an equivalent spring and damper system, with dynamic properties which change with test conditions.

A schematic of the elastomer test rig is shown in Fig. 1 and a layout drawing of the same rig in Fig. 2. Figure 3 shows the complete rig mounted on the shake table. The amount of mass bonded to the elastomer specimen was varied to achieve near-resonant conditions of the spring-mass system such that useful test data could be obtained for frequencies ranging between 30 and 1000 Hz. More precisely, system resonant frequencies between 10 and 750 Hz were desired, because useful test data can generally be obtained in the frequency range of 1.2 to 3 times the system resonant frequency. For the spring stiffness values of the particular test materials considered for evaluation, together with the minimum practical mass (consisting of the top part of the test sample holder and the preload piston), a test specimen consisting of two discs each 2 in. (5 cm) in diameter and 0.50 in. (1.27 cm) thick was predicted to produce a spring-mass system with a resonant frequency of about 750 Hz. A mass of 500 lb (227 kg) was then required to produce the desired lower resonant frequencies between 10 and 30 Hz (mass-resonant frequency relationships for various stiffnesses of elastomer specimens will be discussed below under Description of Tests).

Vibration system power capacity limited the vibration input amplitudes to the spring-mass system at the high frequencies. For high frequency testing the moving part of the test fixture, consisting of specimen holder, preload cylinder and resonant mass, weighed approximately 55 lb (25 kg). Since the vibration table was capable of imparting an 85g acceleration to that mass, vibration input amplitudes (peak-to-peak) of slightly over 0.0015 in. (0.038 mm) could be obtained at 1000 Hz, increasing to 0.003 in. (0.076 mm) for frequencies below 725 Hz. It should be noted here, however, that vibration table input amplitude was not the

test parameter which was specified for the tests. Amplitude across the elastomer (relative amplitude between vibration table and resonance mass) was the parameter controlled during the tests, which were conducted for relative amplitudes of 0.001 (0.25), 0.0015 (0.038), 0.003 (0.076) and occasionally 0.005 in. (0.127 mm). Both the mass required for resonance and the achievable table amplitude increased proportionally to the inverse of the square of the desired test frequency. Since very large vibration table amplitudes were not required at lower frequencies, excess shake table capacity existed at the lower and medium test frequencies.

Test Rig Mechanical Details

The elastomer test discs were bonded to the support fixture surfaces. The urethane compression test specimens were bonded with CONAP AD1152* cured at 130°F (54°C) for three minutes, while the remaining urethane specimens and all of the neoprene specimens were bonded with HYSOL AS7-4323** cured for one-half hour at 140°F (60°C) plus 15 minutes at 325 F (162°C). The bonding material was changed after softening was noted in the high-amplitude, high preload tests of the urethane shear sample. On the vibration table input side, the test specimens were bonded to steel and on the mass side to titanium. The bond failures referred to above, occurred only at the titanium side, which may simply have been a consequence of the generally higher temperatures prevailing in the titanium due to its lower heat transfer capacities. The mounting configurations for all test specimens are shown in Figures 2 and 4.

Test specimen preloading was achieved via an air cylinder located directly above the elastomer and designed such that no external loading would be applied to the test rig frame. The titanium piston was screwed to the upper-specimen holding-plate and sealed in the cylinder with two rolling diaphragm seals (Bellofram 3C-600-37-FPJ and 3-119-119-CBJ). The air cylinder inlet hole was 0.030 in. (0.762 mm) in diameter, making the cylinder essentially a "closed" cavity under vibration conditions. Preload on the test specimen was maintained through regulation of air

*CONAP Incorporated, Allegheny, New York

**Hysol Division, the Dexter Corporation.

pressure in the cylinder. The preload provided was therefore of the constant load type. The elastomer deflections at five and ten percent preloads (0.025 in. (0.63 mm) and 0.050 in. (1.27 mm) deflection) were obtained at ambient room temperature.

Under vibration conditions, the compressibility of the air in the cylinder added a small but measurable stiffness to the system. This stiffness was included in later calculations of elastomer properties.

The resonance mass bonded to the top of the elastomer specimens was comprised of a number of elements. For high frequency tests, in which only a minimum of mass was required, the resonance mass could be reduced to the top plate of the specimen holder and the preload piston. Both pieces were made out of titanium for minimum weight. Requirements for increased mass for medium or low frequency testing were met through addition of a long rod rigidly coupled to the top of the preload piston, and of steel weights. The weights were centered by the rod and were axially restrained by spacers of various lengths and a locknut near the upper rod end.

The rod itself received radial support from two frictionless guide bearings (Figure 5 shows one of the dismounted bearings), each of which consisted of a hub and 12 steel spokes. The hub fitted over the end of the rod and was axially clamped to it. This kind of bearing arrangement provides good radial stiffness for reasonably high spoke tension, but provides only limited freedom for motion if overstressing of the spokes is to be avoided. Consequently, preloading of the elastomer test specimen by the air cylinder required that the outer frame (to which the guide bearings were attached) be lowered. An adjustment of the position of the outer frame was also necessary when there was a change in the air pressure in the upper cylinder, which was used to remove dead weight from the elastomer when the rig was set up to perform low frequency resonance tests. Such adjustments to the outer frame may be avoided in future tests by testing with the spokes more highly stressed. This may require stronger spokes if large preloads are to be imposed.

The function of the upper air cylinder (whose piston was attached to the inertia mass) was to keep the mass from resting on the elastomer test specimen and thus

loading it in compression or shear. When preloading of the test specimen was desired, air pressure in the upper cylinder was reduced until the specified preloa was obtained. If the air pressure in the upper cylinder had already been reduced to ambient (the full weight of the mass was supported by the test specimen), additional preload could then be supplied by the lower air cylinder.

The compressibility of the air in the upper cylinder added to the system another small stiffness of nearly the same magnitude as that provided by the lower cylinder. The two guide bearings (spoke planes), which were always operated at approximately their neutral (unstressed) axial position, contributed a third small spring stiffness which was considered in later calculations.

Instrumentation

The measurement requirements associated with the experimental investigation of the elastomer dynamic properties were as follows:

(1) Displacement measurement of elastomer support plate attached to vibration table, relative to ground;

(2) Displacement measurement of elastomer support plate attached to resonance mass, relative to ground;

(3) Phase angle measurement between displacement measurements (1) and (2) above;

(4) Displacement measurement between two elastomer support plates, relative amplitude across the elastomer;

(5) Vibration frequency;

(6) Temperature of elastomer and elastomer support plates.

For convenience, the displacement measurements were made relative to the massive shaker body frame, which was supported relative to the shaker base by springs. The very low level of motion of the shaker body frame was measured by accelerometer.

At medium or high vibration frequencies (above 300 Hz) displacement measurements were replaced by acceleration measurements. Resonances of the displacement probe

supports, together with elastomer thickness changes due to thermal expansion caused by changing temperatures in the test specimen, prompted the substitution. At low frequencies, displacement measurements were required because of the hum and noise in the shaker (0.1 g or less according to manufacturer's specifications). At these low frequencies, with the low g-levels required for testing, this hum and noise resulted in too much acceleration signal distortion. The phase angle measurements were of course not affected by the use of accelerometers at the higher frequencies.

The measurements of the relative displacement amplitude between the vibration input and mass response could also be made either as displacement or acceleration measurements. In the latter case, conversion of the signal to displacement form would have been required during the tests, since the analytical evaluation of the experimental data required the relative displacement amplitude to be a constant parameter. It was thus measured directly by using a displacement probe mounted to and vibrating with the shaker table. Noncontacting displacement probes of the capacitance-measurement type were employed for this purpose, as well as all other displacement measurements in this program.

Temperature at the center of each elastomer test specimen was judged to be an important test parameter, together with temperatures at several locations immediately adjacent to the sample. This was because the dynamic properties of elastomers are known to be very strongly dependent upon temperature. In order to make the former measurement, a thermocouple was located in the first (urethane compression) sample at the geometric center of one of the two test specimens. While test temperatures were successfully recorded for a time, the hole through which the thermocouple was inserted (along the axis of the cylindrical sample) appeared to act as a local stress raiser, causing what was apparently a fatigue-type shear failure to propagate radially outward over a large sector of the specimen. This failure appeared as a circumferential cut on the side of the disc (see Fig. 6). While early failure of the urethane compression sample limited the amount of data which could be obtained from this particular sample, and forced the abandonment of this type of temperature measurement for future samples, it nonetheless demonstrated clearly the ability of the test rig to apply high amplitude, high frequency vibrations to very large samples.

Subsequent temperature measurements were made at a point directly under the center of the elastomer disc in the steel support plate (vibration table input side) at a distance of approximately 1/16 in. (1.6 mm) from the surface, and directly above this point on the other side of the elastomer disc in the titanium holding plate (mass side). In the titanium plate the thermocouple was located about 1/8 in. (3.2 mm) from the surface bonded to the elastomer. Chromel-Alumel thermocouples were used.

Data Acquisition System

A schematic of the data acquisition system used for the experimental investigations reported herein is shown in Fig. 7. Displacement signals from noncontacting capacitance type probes and Wayne-Kerr amplifiers, or acceleration signals from crystal accelerometers and Kistler charge amplifiers, were sequentially switched by an analog scanner (Monsanto 508P) into a two-channel tracking filter (Vibration Instruments Company, Model 235D). The tracking filter provided a visual readout of vibration frequency and of two filtered amplitude signals. The mass amplitude signal (displacement or acceleration) was fed at all times into one of the two channels of the tracking filter and from there into the phase meter (Vibration Instruments Company, Model 933A) where it served as a reference signal for the measurement of the phase angle relative to the vibration table amplitude signal (displacement or acceleration, respectively). The d-c values proportionate to phase angle and amplitudes from the phase meter and the tracking filter were then converted into binary form in two digital voltmeters (Monsanto, Model 200A) and printed on paper by a 21-line printer (Monsanto, Model 511A) at a rate of approximately three lines per second. (See Fig. 8 for a sample data printout, and Fig. 9 for a photograph of the Monsanto and Vibration Instruments' instrumentation.)

Temperature values were obtained and read from a thermocouple bridge (Technique Assoc., Model 9B) after manual switching between thermocouples in a special thermocouple switch (Wheelco Instrument Division).

During testing, the wave forms of all amplitude signals were monitored on oscilloscopes. The relative amplitude signal was also monitored on an a-c voltmeter (two such signals were recorded for the compression and combined compression-shear

test specimens, one on each side, in order to obtain estimates of the amount of side-to-side resonance mass motion during tests without external resonance mass connection; one such measurement was made for the shear test specimens). These signals indicated deflection across the elastomer test specimen ($x_2 - x_1$).

Vibration test frequency was set and adjusted at high frequencies according to the readout of the tracking filter and at low frequencies according to the frequency meter on the shaker control console, which was equipped with a logarithmic scale frequency meter for higher accuracy and resolution at low frequencies.

DESCRIPTION OF TESTS

Selection of Elastomers for Testing

It was considered that, as a basic requirement, the elastomers used for this test program should have not only good bonding capability with metals, but also measurable damping. Based on these criteria, four elastomers were chosen from among the many available for possible use; they are Buna N, Hypalon, Neoprene and Urethane. One 6 in. by 6 in. by 0.50 in. (15.2 cm by 15.2 cm x 1.27 cm) sample of each of the above four elastomers was obtained for possible use in the tests, through the courtesy of the Nichols Engineering Company of Shelton, Connecticut. The Nichols Engineering Compound Numbers of the four elastomers are, Buna N: NE-1035; Hypalon: NE X-193; Neoprene: NE-1096; Urethane: NE-854AK.

One of the major features of the current test program is the performance of the scheduled tests at near-resonance conditions in order to achieve amplitude requirements. If resonance cannot be reached at the desired test frequency because of either low test sample elastomer stiffness or high resonance mass (particularly at higher frequencies) tests may be conducted such that the test frequency is higher than the resonant frequency. The resonance frequency is defined as

$$f_n = \frac{1}{2\pi} \frac{k}{W/g}$$

where k is the total stiffness of the elastomer sample and W is the weight of the total resonant mass attached to the elastomer sample. The resonance mass may be adjusted in discrete steps, depending on the weight attachments designed for the test rig. The elastomer stiffness k for the compression mode is determined by

$$k = 2 E_e A/L$$

where E_e is the effective Young's modulus of elastomer; A is the cross-sectional area of elastomer specimen; and L is the thickness of elastomer specimen.

The factor of 2 in the stiffness formula accounts for two elastomer specimens connected in parallel in each elastomer sample in the test rig. The configuration of each elastomer specimen is a disc 0.50 in. (1.27 cm) thick and 2 in. (5 cm) in diameter. Thus, according to the shape factor data of Ref. 36, the effective Young's modulus E_e is approximately 2.5 times the actual Young's modulus E for the particular material. The stiffness for the shear mode can be determined by the same formula with E_e replaced by the effective shear modulus.

The Young's moduli of the four elastomers supplied by Nichols Engineering Company were not available. However, such information is required in order to determine the compatibility of the elastomer test samples with the designed test rig. Simple compression stiffness tests were therefore carried out to determine the Young's modulus. In these tests, cubes of the candidate elastomers, 0.50 in. (1.27 cm) on a side were cut from the sample slabs and loaded statically on the same axis along which the samples were later to be tested. The elastomer cubes were loaded between plates without epoxy. The results were as follows:

Elastomer	Statically Measured Young's Modulus For Elastomer Cube [0.50 in.(1.27 cm)] lb/in.^{2} (n/m^2)	Calculated Elastomer Stiffness for Two Circular Test Samples [2 in. (5 cm) Dia. By 0.50 in. (1.27 cm) Long] lb/in. (n/m)
Buna N (NE-1035)	10,500 (7.25 x 10^7)	330,000 (5.77 x 10^7)
Hypalon (NE X-193)	1,110 (7.65 x 10^6)	34,500 (5.95 x 10^6)
Neoprene (NE-1096)	3,600 (2.49 x 10^7)	113,000 (1.98 x 10^7)
Urethane (NE-854AK)	2,260 (1.56 x 10^7)	71,000 (1.25 x 10^6)

These results should be interpreted as estimates only of the stiffnesses which would be obtained under actual tests. Since the shear modulus is approximately 1/3 of the Young's modulus for this type of material, the expected shear stiffness value is about 1/(3 x 2.5) times the compression stiffness.

Neoprene and urethane were selected as the two test elastomers. Their stiffnesses are midway in the range between the low value obtained for hypalon and the high value obtained for Buna N in the available sample materials. Also the ratio of the stiffnesses of neoprene and urethane is only 1.59. Thus, near-resonance tests may be performed on two different elastomers without drastic changes to the test rig resonance masses, which would be required if the stiffnesses were very dissimilar.

The masses that can be utilized for resonance in the current test rig design are: 1.5, 3, 5, 15, 25, 35, 65, 125, 185, 245, 305, 365, 425, and 485 lbs (0.7, 1.4, 2.3, 6.8, 11.3, 15.9, 29.5, 56.7, 81.9, 111.1, 138.3, 165.6, 192.8, and 220 kg). Therefore, for urethane, the range of resonant frequencies is from about 38 Hz to about 680 Hz for tests in compression, and from about 14 Hz to about 250 Hz for tests in shear. For neoprene, the range of resonant frequencies is from about

48 Hz to about 860 Hz for tests in compression and from about 17 Hz to 310 Hz for tests in shear. These ranges are illustrated on the resonant frequency plot, shown in Fig. 10, with U-C and U-S denoting urethane compression and shear respectively, and N-C and N-S denoting neoprene compression and shear respectively.

Description of Tests Conducted

Two elastomers, urethane and neoprene, were tested in this program, each in three loading configurations: compression, shear and combined compression-shear

Urethane in compression was tested first. In an attempt to measure the temperature at the center of the elastomer, during the tests, a small hole 0.030 in. (0.76 mm) in diameter was drilled along the axis of one of the two elastomer discs. A thermocouple was lodged in this small hole. The urethane compression sample was subsequently tested in the high frequency range (300 to 1000 Hz) and with peak-to-peak amplitudes ranging from 0.001 in. (0.025 mm) to approximately 0.009 in. (0.228 mm) at each frequency. After approximately three to four hours of high frequency testing, the elastomer disc that contained the thermocouple failed. A crack had developed near the midplane perpendicular to the axial direction of the disc. The failure was apparently due to repeated stress reversals and the stress concentration effect at the end of the small hole. Tests on this sample were discontinued subsequent to the failure. Approximately 30-35 percent of the data scheduled to be taken for this sample had been obtained Much of the recorded data had to be discarded, however, because careful examination indicated data "contamination" due to the gradual propagation of the crack during the data taking.

No thermocouple holes were drilled in the remaining test samples in the elastomer discs. While this limited the amount of temperature data which could be obtained, it also prevented the reoccurrence of fatigue failures due to stress concentration.

The procedure used to obtain the test data was developed in the course of the initial tests on the urethane compression sample. In subsequent tests, limitations in the engineering properties of the elastomer materials were treated conservatively. Test rig amplitudes were held below maximum capacity and test

duration at high frequencies and high amplitudes was limited to the time required for machine adjustment and data taking.

Levels of dissipative heating in the elastomer test samples varied depending upon vibration frequency, specimen deflection amplitude and time. At low frequencies, the heat generated in the elastomer caused only a small (1-2°F; ca 1°C) temperature rise in the bonded metal plates at all test amplitudes. At higher vibration frequencies the elastomer temperature rose rapidly by as much as 50°F (28°C). The test rig in its current configuration did not have specimen ambient temperature control capabilities.

Attempts to obtain "transient" data (elastomer deflection data at less than steady state elastomer temperature for the particular vibration frequency under test) proved to be unsuccessful due to limitations inherent in the electromagnetic shaker system, in which rapid changes in power output are not tolerated at high power levels.

Data Taking Procedure

1. Shaker system vibration frequency was set. The initial test was found by scanning upward in frequency until an operating frequency just above the critical frequency of the elastomer-mass system was reached.
2. Shake table power input was then adjusted until the desired deflection across the elastomer ($x_2 - x_1$) had been read on an a-c voltmeter.
3. When all signals appeared acceptable in amplitude and wave form, the data printout command was given.
4. Data signals were printed. Frequency and calibration factors from the tracking analyzer were recorded.
5. Simultaneously with (4), temperature was recorded (manually).
6. After advancement to the next test frequency, steps (2) through (5) were repeated. The maximum test frequency was generally reached at 3 to 3.5 times the critical frequency of the elastomer-mass system. Above that point generally excessive power input to the shaker was required to maintain deflection amplitude across the elastomer, and the phase angle between table input and mass response changed only minutely.

7. Steps (1) through (6) were repeated for each higher deflection amplitude across the elastomer.

8. Steps (1) through (7) were repeated first for the five percent and then for the ten percent preload values.

DEVELOPMENT OF ANALYTICAL METHODS

Dynamic Model Nomenclature

The test rig designed, built, and successfully used for the determination of dynamic elastomer properties as reported here is based on the base-excitation, resonance-mass method. A schematic diagram of the test rig is shown in Fig. 1. The test specimens were epoxied onto a holder which was fastened securely to the shake table. The other side of the elastomer holder was connected to the resonant mass. The vibrational motion was therefore transmitted from the shake table through the elastomer to the resonant mass. This is shown diagramatically in Fig. 11, in which the motions of the shake table and the resonant mass are represented by x_1 and x_2 respectively. Because of the electromechanical forces (denoted by F) which act between the shaker body and the shake table, the shaker body may experience vibratory motion. Although this motion, denoted by x_f, is expected to be small under normal operating conditions, it is included in the analysis for generality.

The elastomer specimen, when installed in place, provides the major dynamic link between the shake table and the resonant mass. Under dynamic conditions, the elastomer can be represented by equivalent stiffness and damping coefficients, k_e and c_e respectively. Both k_e and c_e are frequency dependent. There are also two air cylinders in the test rig. The lower one is for the purpose of preloading the elastomer, and the upper one is to unload the deadweight of the resonant mass. Their stiffness and damping properties are represented by k_ℓ, c_ℓ and k_u, c_u respectively. There are also two spoke systems to restrict the resonant mass to vertical movement. Each spoke system has stiffness k_s and damping c_s. These stiffness and damping elements, all of which are shown in Fig. 11, are all very small numerically compared to the elastomer properties. This relative sizing has been done deliberately in order to decrease the effect of each of these required elements upon the accuracy with which the elastomer properties may be calculated.

Equations of Motion

The equation of motion for the resonant mass m can be written as follows:

$$m\ddot{x}_2 + (c_\ell + c_e)(\dot{x}_2 - \dot{x}_1) + (c_u + 2c_s)(\dot{x}_2 - \dot{x}_f) + (k_\ell + k_e)(x_2 - x_1) + (k_u + 2k_s)(x_2 - x_f) = 0 \quad (1)$$

Denote

$$\left.\begin{aligned} x_{1f} &= x_1 - x_f \\ x_{2f} &= x_2 - x_f \end{aligned}\right] \quad (2)$$

Then

$$x_2 - x_1 = x_{2f} - x_{1f} \text{ and } \dot{x}_2 - \dot{x}_1 = \dot{x}_{2f} - \dot{x}_{1f}$$

Equation (1) takes the form,

$$m\ddot{x}_{2f} + (c_e + c_\ell)(\dot{x}_{2f} - \dot{x}_{1f}) + (c_u + 2c_s)\,\dot{x}_{2f} + (k_e + k_\ell)(x_{2f} - x_{1f}) + (k_u + 2k_s)\,x_{2f} = -m\ddot{x}_f \quad (3)$$

It is noted that if displacement probes are to be used to measure the motions of the mass and the shake table, the probes are mounted with the shaker body as their references. Therefore, x_{1f} and x_{2f} are the measured quantities.

The shaker table motion, which is sinusoidal in time, can be expressed as

$$x_{1f} = X_{1f} \exp i\,(\omega t + \varphi_1) \quad (4)$$

where X_{1f} and φ_1 are respectively the input amplitude and phase angle, and ω is the frequency.

Now, assume that x_{2f} and x_f are also sinusoidal in time (actual measurement verified that such is indeed the case). Thus,

$$\left.\begin{aligned} x_{2f} &= X_{2f} \exp i\,(\omega t + \varphi_2) \\ x_f &= X_f \exp i\,(\omega t + \varphi) \end{aligned}\right] \quad (5)$$

Substitute Eq. (4) and (5) into Eq. (3) and take only the real part:

$$- m\omega^2 X_{2f} \cos(\omega t + \varphi_2) + k'_e [X_{2f} \cos(\omega t + \varphi_2) - X_{1f} \cos(\omega t + \varphi_1)] + k'_u X_{2f} \cos(\omega t + \varphi_2) - c'_e \omega [X_{2f} \sin(\omega t + \varphi_2) - X_{1f} \sin(\omega t + \varphi_1)] - c'_u \omega X_{2f} \sin(\omega t + \varphi_2) = m\omega^2 X_f \cos(\omega t + \varphi) \quad (6)$$

where $k'_e = k_e + k_\ell$; $c'_e = c_e + c_\ell$ (7)

$k'_u = k_u + 2K_s$; $c'_u = c_u + 2c_s$ (8)

Equating the cos ωt terms in Eq. (6), we have

$$- m\omega^2 X_{2f} \cos\varphi_2 + k'_e [X_{2f} \cos\varphi_2 - X_{1f} \cos\varphi_1] + k'_u X_{2f} \cos\varphi_2 - c'_e \omega [X_{2f} \sin\varphi_2 - X_{1f} \sin\varphi_1] - c'_u \omega X_{2f} \sin\varphi_2 = m\omega^2 X_f \cos\varphi \quad (9)$$

Equating the sin ωt terms in Eq. (6), we have

$$m\omega^2 X_{2f} \sin\varphi_2 + k'_e [- X_{2f} \sin\varphi_2 + X_{1f} \sin\varphi_1] - k'_u X_{2f} \sin\varphi_2 - c'_e \omega [X_{2f} \cos\varphi_2 - X_{1f} \cos\varphi_1] - c'_u \omega X_{2f} \cos\varphi_2 = - m\omega^2 X_f \sin\varphi \quad (10)$$

Rewrite Eqs. (9) and (10) in the following form:

$$a_{11} k'_e + a_{12} c'_e = d_1 \quad (11)$$

$$a_{21} k'_e + a_{22} c'_e = d_2 \quad (12)$$

where

$$\left.\begin{aligned} a_{11} &= X_{2f}\cos\varphi_2 - X_{1f}\cos\varphi_1 \\ a_{12} &= -\omega\,(X_{2f}\sin\varphi_2 - X_{1f}\sin\varphi_1) \\ a_{21} &= a_{12}/\omega \\ a_{22} &= -\omega\, a_{11} \\ d_1 &= m\omega^2\,(X_{2f}\cos\varphi_2 + X_f\cos\varphi) - k'_u\, X_{2f}\cos\varphi_2 \\ &\quad + c'_u\,\omega\, X_{2f}\sin\varphi_2 \\ d_2 &= -m\omega^2\,(X_{2f}\sin\varphi_2 + X_f\sin\varphi) - k'_u\, X_{2f}\sin\varphi_2 \\ &\quad + c'_u\,\omega\, X_{2f}\cos\varphi_2 \end{aligned}\right\} \qquad (13)$$

Note that quantities in Eq. (13) are either known or measured in the experiment. For example, the frequency ω, the displacement amplitudes X_{1f}, X_{2f} and X_f, and the phase angles are measured quantities in the dynamic testing, and k'_u and c'_u are known quantities (by prior measurement). Thus, k'_e and c'_e can be solved from Eqs. (11) and (12). The results are:

$$\left.\begin{aligned} k'_e &= \frac{d_1\, a_{22} - d_2\, a_{12}}{a_{11}\, a_{22} - a_{12}\, a_{21}} \\ c'_e &= \frac{d_2\, a_{11} - d_1\, a_{21}}{a_{11}\, a_{22} - a_{12}\, a_{21}} \end{aligned}\right\} \qquad (14)$$

from which k_e and c_e can be readily calculated, using Eq. (7),

$$k_e = k'_e - k_\ell \quad \text{and} \quad c_e = c'_e - c_\ell \qquad (15)$$

Therefore, from each set of dynamic test data (amplitudes, phase angles, frequency, etc.) one pair of elastomer specimen dynamic stiffness and damping values can be calculated.

The above approach has been prepared for the case in which the motions are measured by displacement probes. A slight modification is required when the motions are measured by accelerometers instead. This is necessary because the displacement

probes give readings with respect to a specific reference body (in this case, the shaker body), whereas an accelerometer gives an absolute reading. In the case of accelerometer input data, the analysis should begin with Eq. (1).

Let the displacements be represented by:

$$\begin{aligned} x_1 &= X_1 \exp i\,(\omega t + \varphi_1) = X_1 \cos\,(\omega t + \varphi_1) \\ x_2 &= X_2 \exp i\,(\omega t + \varphi_2) = X_2 \cos\,(\omega t + \varphi_2) \\ x_f &= X_f \exp i\,(\omega t + \varphi) = X_f \cos\,(\omega t + \varphi) \end{aligned} \tag{16}$$

in which only the real parts are taken.

The respective accelerations A_1, A_2 and A_f are readily obtained by differentiating twice with respect to time:

$$\left.\begin{aligned} A_1 &= -\omega^2 X_1 \cos\,(\omega t + \varphi_1) = \omega^2 X_1 \cos\,(\omega t + \varphi_1 + 180^o) \\ A_2 &= -\omega^2 X_2 \cos\,(\omega t + \varphi_2) = \omega^2 X_2 \cos\,(\omega t + \varphi_2 + 180^o) \\ A_f &= -\omega^2 X_f \cos\,(\omega t + \varphi) = \omega^2 X_f \cos\,(\omega t + \varphi + 180^o) \end{aligned}\right] \tag{17}$$

Therefore, it is seen that for sinusoidal motions the relative phase between the displacements is preserved in the accelerations. In other words, the relative phase between x_1 and x_2 is the same as the relative phase between A_1 and A_2. Thus, the measured phase angles of the acceleration signals may be used directly. With the accelerations as the measured quantities, their amplitudes may be divided by the square of the test frequency to obtain th respective displacement amplitudes. It should be noted that if the measured quantities are mixed, for example, x_1 and A_2, then in order to be consistent, one of the phase angles has to be increased by 180 degrees for proper interpretation of results.

Substituting Eq. (16) into Eq. (1) and following the same procedure as in the derivation of Eqs. (6) through (12), Eqs. (11) and (12) are again obtained. The elastomer stiffness and damping can be calculated from Eqs. (14) and (15) as before. But instead of through Eq. (13), the coefficients a_{11}, a_{12}, etc. should be computed from the following equation:

$$
\begin{aligned}
a_{11} &= X_2 \cos \varphi_2 - X_1 \cos \varphi_1 \\
a_{12} &= -\omega (X_2 \sin \varphi_2 - X_1 \sin \varphi_1) \\
a_{21} &= a_{12}/\omega \\
a_{22} &= -\omega\, a_{11} \\
d_1 &= m \omega^2 X_2 \cos \varphi_2 - c'_u \omega (X_f \sin \varphi - X_2 \sin \varphi_2) \\
&\quad + k'_u (X_f \cos \varphi - X_2 \cos \varphi_2) \\
d_2 &= -m \omega^2 X_2 \sin \varphi_2 - c'_u (X_f \cos \varphi - X_2 \cos \varphi_2) \\
&\quad - k'_u (X_f \sin \varphi - X_2 \sin \varphi_2)
\end{aligned}
\qquad (18)
$$

where
$$
\begin{aligned}
&X_1 = \bar{A}_1/\omega^2;\ X_2 = \bar{A}_2/\omega^2 \\
&X_f = \bar{A}_f/\omega^2 \\
&\bar{A}_1,\ \bar{A}_2 \text{ and } \bar{A}_f \text{ are amplitudes of accelerations}
\end{aligned}
\qquad (19)
$$

In summary, the elastomer stiffness and damping quantities can be calculated from Eqs. (14) and (15). If the motions are measured by displacement probes, then the coefficients a_{11}, a_{12}, a_{21}, a_{22}, d_1, and d_2 should be calculated from Eq. (13). But, if accelerometers are used to measure the motions, Eqs. (18) and (19) should be used for the coefficients.

Mechanical Impedance and Compliance

The complex mechanical impedence of an elastomer is given in terms of the stiffness and damping as follows:

$$Z_e = k_e + i \omega c_e \qquad (20)$$

A complex compliance function can be defined as the inverse of Z_e:

$$G = G_1 - i G_2 = \frac{1}{Z_e} = \frac{1}{k_e + i \omega c_e} \qquad (21)$$

Thus,

$$\left.\begin{aligned} G_1 &= \frac{k_e}{k_e^2 + \omega^2 c_e^2} \\ G_2 &= \frac{\omega c_e}{k_e^2 + \omega^2 c_e^2} \end{aligned}\right] \qquad (22)$$

In the foregoing sections, a procedure has been described whereby elastomer stiffness and damping coefficients, or the complex compliance function, can be calculated from measured motions of the shake table and the resonant mass. In the following section, a relationship between the elastomer complex compliance function and a set of constants based on a viscoelastic model, will be derived.

In an elastic material, a simple linear relationship commonly known as Hooke's Law, exists between stress and strain. In an elastomer, or a viscoelastic material, the time rates of change of stress or strain, or both, must also be considered in the stress-strain relationship. The precise form of the relationship depends on what viscoelastic model is used in the formulation.

One elastomer viscoelastic model is the three-element model shown in Fig. 12. This model, consisting of one linear spring in series with a linear parallel-connected spring and damper, (one of many such arrangements - see Ref. 35, for instance) has provided reasonably good qualitative descriptions of elastomer behavior.

In Fig. 12, suppose that the elastomer is acted upon as shown by a sinusoidally varying force F, producing displacement ϵ. Denote the displacement of the movable end of spring K_2 by ϵ'. By applying a force balance at the junction of the spring K_2 and the spring-damper element:

$$K_2\epsilon' = K_1(\epsilon - \epsilon') + C(\dot{\epsilon} - \dot{\epsilon}') \qquad (23)$$

Also, the force in the spring K_2 must be equal to F. Thus,

$$F = K_2\epsilon' \qquad (24)$$

By eliminating ϵ' from the above two equations, we have

$$F + \frac{C}{K_1 + K_2} \dot{F} = \frac{K_1 K_2}{K_1 + K_2} \epsilon + \frac{C K_2}{K_1 + K_2} \dot{\epsilon} \tag{25}$$

or

$$F + a_1 \dot{F} = a_2 \epsilon + a_3 \dot{\epsilon} \tag{26}$$

where a_1, a_2 and a_3 are the viscoelastic model constants,

$$\left.\begin{aligned} a_1 &= \frac{C}{K_1 + K_2} \\ a_2 &= \frac{K_1 K_2}{K_1 + K_2} \\ a_3 &= \frac{C K_2}{K_1 + K_2} \end{aligned}\right] \tag{27}$$

The displacement ϵ and the force F are related by the complex compliance function G:

$$\epsilon = G F \tag{28}$$

Since F is sinusoidal in time,

$$F = F_o \exp i \omega t \tag{29}$$

Thus,

$$\epsilon = (G_1 - i G_2) F_o \exp i \omega t \tag{30}$$

Substituting Eqs. (29) and (30) into Eq. (26),

$$1 + i \omega a_1 = a_2 (G_1 - i G_2) + a_3 i \omega (G_1 - i G_2) \tag{31}$$

Equating the real parts and the imaginary parts separately, we have

$$\left.\begin{aligned} G_1 &= \frac{a_2 + a_1 a_3 \omega^2}{a_2^2 + a_3^3 \omega^2} \\ G_2 &= \frac{(a_3 - a_1 a_2)\,\omega}{a_2^2 + a_3^3 \omega^2} \end{aligned}\right] \qquad (32)$$

From a set of experimental data, the elastomer stiffness and damping coefficients, and subsequently the complex compliance function, can be calculated as indicated earlier in Eqs. (14), (15) and (22). Thus, plots of G_1 and G_2 versus frequency can be generated. Now, from Eq.(32), a given set of values for the viscoelastic model constants a_1, a_2 and a_3 would specify G_1 and G_2 as functions of frequency. If a particular set of a_1, a_2 and a_3 can be found which provide G_1 and G_2 functions, then, a good correlation has been obtained by means of the selected three-element model. The analysis and reduction of experimental data to find such sets of a_1, a_2, and a_3 are discussed in a later section.

DATA REDUCTION AND CORRELATION

Data taken during the efforts reported herein is summarized in Table 1.

Data Reduction

The analysis and reduction of the recorded data are illustrated by considering the data obtained through use of the urethane shear sample with no preload, at a frequency of 200 Hz, and with amplitude of 0.001 in. (0.025 mm) peak-to-peak. The absolute motions are measured by accelerometers whereas the relative motion across the elastomer was obtained by a displacement probe. This probe yielded a reading of 0.17 volt, which corresponds to a peak displacement amplitude of 0.0005 in. (0.0127 mm). The accelerometer readings of the shake table and the resonant mass were 0.152 volt and 0.0231 volt, respectively. The motion of the foundation was negligibly small. The calibration factor of both accelerometers is 0.071 volt/g. Therefore,

$$\bar{A}_1 = 0.152/0.071 = 2.14 \text{ g} = 825 \text{ in./sec}^2 \ (21.0 \text{ m/sec}^2)$$

$$\bar{A}_2 = 0.0231/0.071 = 0.326 \text{ g} = 126 \text{ in./sec}^2 \ (3.2 \text{ m/sec}^2)$$

The recorded phase angles were $\varphi_1 = 169.1^\circ$ and $\varphi_2 = 0$ (the resonance mass motion was used as a reference in measuring the phase angles). The weight of the total resonant mass on top of the elastomer specimen was 69 lb (31.3 kg). The stiffness of each spoke assembly as measured was $k_s = 140$ lb/in. (2.45×10^4 n/m). From recorded air pressures, air cylinder stiffnesses were determined to be $k_u = 1000$ lb/in. (1.75×10^5 n/m) and $k_\ell = 830$ lb/in. (1.45×10^5 n/m), see Appendix I. The damping coefficients of the air cylinder assemblies and the spoke assemblies are small; they were estimated, on the basis of log decrement measurements in vibration decay tests, to be $c_u = c_\ell = 0.5$ lb-sec/in. (87.5 n-sec/m), and $c_s = 0$.

With the above input data, the elastomer stiffness and damping coefficient at 200 Hz is calculated from Eqs. (14), (15) and (18):

TABLE 1a SUMMARY OF URETHANE EXPERIMENTAL DATA

Test Condition	Preload	Amplitudes in.x10^{-3}(mm)	Frequency Range (Hz) 15	20	25	30	40	50	70	100	150	200	250	300	350	400	450	500	600	650	700	800	850	900	1000	1100	1200
Compression	0%	1.0 (0.025)								a				a		a		a			a			a			
		1.5 (0.038)								a				a		a		a			a			a			
		3.0 (0.076)								a				a		a		a			a			a			
		5.0 (0.127)												a		a		a			a			a			
	5%	1.0 (0.025)																			a			a			
		1.5 (0.038)																			a			a			
		3.0 (0.076)						SPECIMEN FAILURE													a			a			
		5.0 (0.127)																			a			a			
	10%	SPECIMEN FAILURE																									
Shear	0%	1.0 (0.025)			*	*	*	*	*	*	*	*		*				*			*			*			
		1.5 (0.038)			a	*	*	*	*	*	*	*	*	*				*			*			*			
		3.0 (0.076)			a	a	a	a	a	a	a	a		*				*			*			*			
		5.0 (0.127)			a	a	a	a	a	a	a	a															
	5%	1.0 (0.025)			a	*	*	*	a	*	a	*		*				*			*			*			
		1.5 (0.038)			a	a	a	a	a	a	a	a		*				*			*			*			
		3.0 (0.076)			a	a	a	a	a	a	a	a		a				a			a			a			
		5.0 (0.127)			a	a	a	a	a	a	a	a															
	10%	1.0 (0.025)			a	*	*	*	*	*	*	*		*	a			*			*			*			
		1.5 (0.038)			a	*	*	*	*	*	a	a				a		*			*						
		3.0 (0.076)			a	a	a	a	a	a					a	a		a									
		5.0 (0.127)			a	a	a	a	a	a						a		a			a						
Combined Compression And Shear	0%	1.0 (0.025)						*	*	*		*	a	*		*		*	*		*				*		
		1.5 (0.038)						a	a	a			a	a		a		a									
		3.0 (0.076)						*	*	*		*	a	*		*		*			*						
		5.0 (0.127)						a	a	a		a	a	a		a		a									
	5%	1.0 (0.025)						*	*	*			a	*		*		*	*		*				*		
		1.5 (0.038)						a	a	a			a	a		a		a			a				a		
		3.0 (0.076)						*	*	*			a	*		*		*	*		*				*		
		5.0 (0.127)																									
	10%	1.0 (0.025)						*	*	*			a	*		*		*	*		*				*		
		1.5 (0.038)						a	a	a			a	a		a		a	a		a						
		3.0 (0.076)						*	*	*			a	*		*		*	*		*						
		5.0 (0.127)						a	a	a			a	a		a		a									

a = data taken
* = data taken and stiffness and damping calculated

TABLE 1b SUMMARY OF NEOPRENE EXPERIMENTAL DATA

Test Condition	Preload	Amplitudes in.x10^{-3}(mm)	Frequency Range (Hz) 15	20	25	30	40	50	70	100	150	200	250	300	350	400	450	500	600	650	700	800	850	900	1000	1100	1200
Compression	0%	1.0 (0.025)							a	*	*	*		*		*		*	*		*	*			*		
		1.5 (0.038)							a	*	*	*	*	*		*		*	*				*		a		
		3.0 (0.076)							a	a	a	a	a	a		a		a		a							
		5.0 (0.127)								a	a	a	a	a		a		a									
	5%	1.0 (0.025)							*	*	*	a		*		*		*	*		*				*		
		1.5 (0.038)							*	*	*	a					*	*		*					*	a	a
		3.0 (0.076)							a	a	a	a															
		5.0 (0.127)							a	a	a																
	10%	1.0 (0.025)							a	a	a																
		1.5 (0.038)							a	a	a																
		3.0 (0.076)							a	a	a																
		5.0 (0.127)							a	a	a																
Shear	0%	1.0 (0.025)			a	*	*	a	*	*	a	*		*				*			*			*	a		
		1.5 (0.038)	a	a	a	a	a	a	a	a	a	a		a				a			a			a			
		3.0 (0.076)			a	*	*	*	*	*	a	*		*				*			*			*			
		5.0 (0.127)			a	a	a	a	a	a	a	a		a				a			a						
	5%	1.0 (0.025)			a	*	*	*	*	*	a	*		*				*			*				*		
		1.5 (0.038)			a	a	a	a	a	a	a	a		a				a			a				a		
		3.0 (0.076)	a	a	a	*	*	*	*	*	a	*		*			*				*			*			
		5.0 (0.127)			a	a	a	a	a	a	a	a		a			a				a						
	10%	1.0 (0.025)	a	a	a	*	*	*	*	*	a	*		*				*			*				*		
		1.5 (0.038)			a	a	a	a	a	a	a	a		a			a				a				a		
		3.0 (0.076)			a	*	*	*	*	*	a	*		*													
		5.0 (0.127)				a	a	a	a	a	a	a		a													
Combined Compression And Shear	0%	1.0 (0.025)					*	*	*					*		*		*			*				*		
		1.5 (0.038)					a	a	a	a				a		a		a			a				a		
		3.0 (0.076)					*	*	*	*				*		*		*			*						
		5.0 (0.127)					a	a	a	a				a		a		a									
	5%	1.0 (0.025)						*	*	*				*		*		*			*				*		
		1.5 (0.038)						a	a	a				a		a		a			a				a		
		3.0 (0.076)						*	*	*				*		*		*			*						
		5.0 (0.127)						a	a	a				a		a		a									
	10%	1.0 (0.025)						*	*	*				*		*					*				*		
		1.5 (0.038)						a	a	a				a		a					a				a		
		3.0 (0.076)						*	*	*				*		*					*				a		
		5.0 (0.127)						a	a	a				a		a											

a = data taken
* = data taken and stiffness and damping calculated

k_e = 36,000 lb/in. (6.3×10^6 n/m)

c_e = 4.3 lb-sec/in. (7.53×10^2 n-sec/m)

Then, from Eq. (22)

G_1 = 2.73×10^{-5} in./lb (1.56×10^{-7} m/n)

G_2 = 4.12×10^{-6} in./lb (2.35×10^{-8} m/n).

By following the same procedure, the values of G_1 and G_2 at other frequencies and preloads are calculated and plotted. In Figs. 13 and 14, the real and imaginary parts of the complex compliance function are respectively plotted for the urethane shear sample at a peak-to-peak amplitude of 0.001 in. (0.025 mm). Various curves are shown for different values of the preload. Figures 15 and 16 show, respectively, the G_1 and G_2 plots obtained for the urethane shear sample at a peak-to-peak amplitude of 0.0015 in. (0.038 mm). Preloading appears to have the effect of decreasing the frequency dependence of the G_1 and G_2 functions. As the frequency increases, the G_1 function decreases, corresponding to an increase in stiffness. This is in agreement with elastomer data reported in the literature. The three-element viscoelastic model shown in Fig. 12 also predicts the same general behavior for G_1.

Figures 17 to 20 show the G_1 and G_2 curves for the neoprene shear sample at peak-to-peak amplitudes of 0.001 in. (0.025 mm) and 0.003 in. (0.076 mm). It is seen in Fig. 17 that G_1 appears to increase with frequency in the 50 to 70 Hz range for both the no preload and five percent preload cases. This is in contrast to what is generally believed to be normal elastomer behavior although such reverse trends are reported in the literature (Ref. 31). It should be noted that no such reversal was found in the case of the urethane shear sample (Figs 13 and 15), which was tested in the same manner and under similar conditions. One possible explanation might be a low-frequency test rig resonance. Several additional tests, with additional accelerometers, would be required to fully explain this apparent anomaly.

Figures 21 and 22 are, respectively, the G_1 and G_2 curves for neoprene under compression dynamic loading at a peak-to-peak amplitude of 0.001 in. (0.025 mm);

whereas Figs. 23 and 24 are those for the same sample at peak-to-peak amplitude of 0.0015 in. (0.038 mm). Since the compression specimen is considerably stiffer than the shear specimen, the natural frequency, even with all the weights installed in place, is still too high (in the 120 Hz range) to obtain good data below about 100 Hz. It may be noted that G_1 again exhibits a reverse trend in the 100-150 Hz frequency range.

The data of the combined compression-shear samples of both urethane and neoprene were also analyzed. The resulting G_1 and G_2 functions show considerable and apparently inconsistent variations with frequency over portions of the frequency range of interest. While portions of the curves (in the middle frequency range) appear satisfactory, the results of the tests are considered to be unsatisfactory from the standpoint of determining dynamic coefficients which would be usable over the entire frequency range. Further reduction of this data has, thus, not been attempted.

The variations in G_1 and G_2 may be traced back to the order in which these tests were conducted. Tests of the previous four samples were conducted with frequency as the first variable and amplitude as the second. For the last two samples (the combined samples) the order was reversed, with amplitude varied first at constant frequency and test frequency as the second variable. The resulting temperature history of each sample was thereby apparently confused because of the higher heat levels generated at the higher amplitudes. This problem area is discussed in more detail under the Discussion of Results section.

Correlation of Data with Viscoelastic Model

In the last section, the reduction of experimental data was described. This data was expressed in the form of G_1 and G_2 versus frequency with preloading and amplitude as parameters. This reduced data is next correlated with calculated results through use of the selected three-element viscoelastic model shown in Fig. 12. It may be recalled that the quantities G_1 and G_2 were derived in Eq. (32) in terms of a_1, a_2, and a_3, the viscoelastic model constants. The correlation efforts may be described as the obtaining, from the experimental results, of a particular set of values for a_1, a_2, and a_3, which by means of Eq. (32) may be used to calculate G_1 and G_2 functions which compare satisfactorily with a particular pair of measured G_1 and G_2 curves.

Before discussing the correlation of the data obtainable through the selected three-element model, it is appropriate to discuss the functional behavior of the complex compliance function as expressed in Eq. (32). First, the viscoelastic model constants a_1, a_2, and a_3 must be positive, as can be seen from Eq. (27). Since the elastomer stiffness and damping coefficients are positive quantities, it immediately follows from Eq. (22) that G_1 and G_2 are also positive. Equation (32) then indicates that

$$a_3 - a_1 a_2 > 0 \tag{33}$$

because otherwise G_2, and hence the elastomer damping coefficient c_e, will be negative.

Differentiating Eq. (32) with respect to ω yields

$$\frac{dG_1}{d\omega} = - \frac{2 a_2 a_3 (a_3 - a_1 a_2) \omega}{(a_2^2 + a_3^3 \omega^2)^2} \tag{34}$$

$$\frac{dG_2}{d\omega} = (a_3 - a_1 a_2) \frac{a_2^2 - a_3^3 \omega^2}{(a_2^2 + a_3^2 \omega^2)^2} \tag{35}$$

From Eqs. (33) and (34), it may be seen that $dG_1/d\omega$ is always negative. The slope of G_1 is zero both at $\omega = 0$ and $\omega = \infty$. The largest numerical value of the slope of G_1 can be shown to occur at $\omega_1 = a_2/\sqrt{3}\, a_3$. Qualitatively, the dependence of G_1 and G_2 on frequency is shown in Fig. 25. Note that G_2 first increases with ω in the low frequency region and then decreases in the high frequency region. The maximum of G_2 occurs at $\omega_2 = a_2/a_3$. These facts are extremely helpful in determining the approximate range of a_1, a_2 and a_3 in the correlation study. When the measured G_1 and G_2 curves show sufficient resemblance with the sketches of G_1 and G_2 as functions of frequency as shown in Fig. 25, a good correlation can be expected for the three-element model chosen. The monotonic character of the G_1 curve shown in Fig. 25 appears to suggest that either the reverse trends noted at low frequencies in Figs. 19, 21, and 23 are due to undesirable test rig behavior, or that the three-element model, from which the curves in Fig. 25 are obtained, is not fully adequate for this particular elastomer.

In addition to the curves presented in Fig. 25, a large number of calculated G_1 and G_2 curves were plotted in the frequency range of interest, for many different combinations of a_1, a_2 and a_3. These sets of curves, which are in essence the result of a parameter study of Eq. (32), are henceforth referred to as "master curves." In the process of correlating the test data, the actual G_1 and G_2 curves obtained from the test data for a specific test sample were first compared with the "master curves." This yielded approximate values of the quantities a_1, a_2 and a_3 from which to begin the curve-fitting process. Once the approximate ranges of a_1, a_2 and a_3 were known, a standard curve-fitting computer program was used to select the best possible combination of a_1, a_2 and a_3 which gives the smallest deviation from the measured data.

Data correlation analyses have been performed to obtain the viscoelastic model constants corresponding to the selected three-element model. The term "measured curves" in the plotted results is used to denote those obtained from the reduction of measured data, whereas the correlated curves are those calculated from a given set of a_1, a_2 and a_3.

A correlation analysis was made with the urethane shear data obtained with no preload and at 0.001 in. (0.0254 mm) peak-to-peak amplitude. The viscoelastic model constants are found to be $a_1 = 0.0017$, $a_2 = 19{,}000$ and $a_3 = 70$. Plots of the correlated and measured complex compliance functions are shown in Figs. 26 and 27. It is seen that the correlation in G_1 is good, whereas the correlation in G_2 is not satisfactory. The three-element model chosen is apparently incapable of correlating the measured G_2 curve for this particular test condition.

Similar correlation analyses were made for this test sample for preloads of five percent and ten percent. The results are shown in Figs. 28 to 31. Again, the correlation for G_1 is generally very good for both cases. The correlation for G_2 at five percent preload is fair, while that at ten percent preload is fair to poor.

Attempts were also made to correlate the urethane shear data at a peak-to-peak amplitude of 0.0015 in. (0.038 mm) as shown in Figs. 15 & 16. While the correlation for G_1 was acceptable, that for G_2 was only fair to poor. It may be remarked here that the three-element model selected for use in this program very likely pro-

vides the answer to the disparity between the excellent correlations obtained for the G_1 functions and the fair to fair-to-poor correlations obtained for the G_2 functions. As indicated in Fig. 12, the model possesses two spring elements but only one damping element. A more general four-element model should produce better G_2 results.

Figures 32 to 37 are the correlations obtained for the neoprene shear data at 0.001 in. (0.025 mm) peak-to-peak amplitude, no preload, and at 0.003 in. (0.076) peak-to-peak amplitude, zero percent and five percent preload. It is seen that they all correlate very well, with the exception of the G_2 data in Fig. 33 in the range 150 to 500 Hz. From the results shown in Figs. 32 through 37, it may be concluded that the three-element viscoelastic model is satisfactory in many respects for neoprene in shear. However, the extent of the capability is apparently somewhat limited, judging from the several cases of poor correlation observed.

The neoprene compression data at 0.001 in. (0.025 mm) peak-to-peak amplitude, for zero percent and five percent preload, and at 0.0015 in. (0.038 mm) peak-to-peak amplitude, for zero percent preload were correlated and are shown in Figs. 38 through 43. The correlations are fairly good except the data at 0.001 in. (0.025 mm) peak-to-peak amplitude, five percent preload.

The viscoelastic model constants are summarized in Table 2, from which some preliminary trend of the elastomer constants with various parameters can be drawn. For the urethane shear sample when the preload is increased from 0 to 10 percent, both a_1 and a_3 first decrease and then increase, whereas a_2 first increases and then levels off. In both the neoprene shear sample and the neoprene compression sample, as amplitude increases, both a_1 and a_3 decrease, whereas a_2 remains at practically the same value.

Table 2 Summary of Viscoelastic Model Constants

	Amplitude (peak-to-peak) inch (mm)	Preload (% of Free Length)	a_1	a_2	a_3
Urethane Shear	0.001 (0.025)	0%	0.0017	19,000	70
	0.001 (0.025)	5%	0.00068	23,000	29
	0.001 (0.025)	10%	0.00122	23,000	49
Neoprene Shear	0.001 (0.025)	0%	0.0013	15,000	35
	0.003 (0.075)	0%	0.00075	15,400	19.5
	0.003 (0.075)	5%	0.0006	23,000	20
Neoprene Compression	0.001 (0.025)	0%	0.00048	125,000	76
	0.001 (0.025)	5%	0.00047	100,000	98
	0.0015 (0.038)	0%	0.00035	125,000	65

DISCUSSION OF RESULTS

The efforts reported herein have verified the basic methods selected for obtaining elastomer dynamic property material constants. During these efforts, an elastomer test rig was successfully designed, fabricated, assembled and tested. The test rig utilizes the base-excitation, resonance-mass method, in which the excitation is the motion provided by a shaker. The size of the resonance mass attached to the top of the elastomer sample can be varied in order to achieve desired dynamic test conditions over a wide frequency range.

The test rig is able to perform uniaxial tests on elastomer samples of a variety of sizes and shapes (test specimen envelope is a cylinder five inches high by five inches in diameter) over a frequency range from about 20-30 Hz to over 1000 Hz. Variable resonance mass, which may be selected to match test elastomer properties, permits tests at virtually any reasonable dynamic amplitude at the resonance points, with correspondingly lower amplitudes at off-resonance conditions. Test amplitudes are limited primarily by elastomer properties (and of course shaker power) rather than by the test rig itself. The test rig, which may be driven by any shaker, permits vibration tests to be conducted with force preloads of up to 4100 pounds (18,200 newtons) applied to the test specimens, and can be readily adapted for constant temperature tests up to about 400°F (205°C).

During the conduct of the work reported herein, tests were conducted on urethane and neoprene elastomer samples in the compression, shear, and combined compression/shear modes. Each sample was composed of two parallel-mounted circular discs, each 2 in. (5 cm) in diameter by 1/2 in. (1.27 cm) high. Tests were conducted at room temperature at a number of frequencies between about 25 and 1000 Hz, at amplitudes of up to 0.005 in. (0.127 mm) peak-to-peak, and with compressive preloads of zero, five percent, and ten percent of free length. During dynamic testing, energy is dissipated in the elastomer sample, causing its temperature to rise above the ambient. This heating effect is more pronounced in the high frequency, large amplitude region. Since it is difficult to measure the temperature inside the body of the test elastomer itself, the temperatures in the elastomer mounts adjacent to the bonding surface were measured and recorded during the tests.

Amplitudes and phase angles at various locations in the test rig were measured. From these measured ampltiudes and phase angles, and the frequency, the dynamic complex compliances were calculated at the test points. This data was then processed by a correlation analysis, through the use of curve-fitting and a selected three-element elastomer model, to obtain viscoelastic model constants. These constants were used to calculate the dynamic properties. The results were compared with the measured dynamic properties to determine the quality of the correlation.

For the urethane sample under shear and with no preload, the temperature in the resonance mass elastomer mount was found to be 97°F (36°C) at 0.001 in. (0.025 mm) peak-to-peak amplitude at a frequency of 1000 Hz, and 91°F (33°C) at 100 Hz (the ambient temperature was approximately 90°F (32°C)); at a peak-to-peak amplitude of 0.0015 in. (0.038 mm) this temperature was found to be 105°F (40.5°C) at 1000 Hz and 94°F (34.5°C) at 200 Hz. While elastomer dynamic properties are known to be temperature dependent, provisions for constant temperature testing were not included in this initial effort because of program limitations. It was felt, instead, that the basic methods involved in obtaining the viscoelastic model constants could be verified without precise control of test temperatures, which were expected to fall in the ranges actually encountered. The results obtained fully justify this initial procedure. It must be remembered that the measured elastomer dynamic properties obtained in these efforts have this temperature effect, particularly in the high frequency, high amplitude region.

It should be clearly understood, of course, that viscoelastic model constants destined for use by the engineering designer must be based upon test data which has been obtained under constant temperature conditions. For this reason, maximum flexibility for controlling elastomer test cavity temperature was built into the test rig at the start. Achievement of this capability requires only additional components, rather than extensive modifications.

The urethane shear sample gave generally good dynamic mechanical property data. The correlation in G_1, the real part of the complex compliance function, was good. However, the correlation in G_2, the imaginary part of the complex compliance function was not satisfactory. This was probably because the three-element viscoelastic

model used in the correlation analysis was not sufficient to represent the particular elastomer material.

The data obtained for the neoprene shear sample and the neoprene compression sample were generally satisfactory, except perhaps in some isolated cases where the data showed reverse trends in the low frequency region. While such trends have apparently been reported in the past, they are not generally accepted as valid by elastomer technologists. Reasons for the observed trends need clarification. Most of the neoprene shear data correlated very well using the same three-element model as before. The correlation of the neoprene compression data was also fairly good.

The data obtained from the urethane compression sample were poor because a crack had developed during the data taking. In this sample, one small hole was drilled along the axis of one of the two circular discs to reach the center so that its temperature could be directly measured. The specimen apparently failed due to stress concentration and fatigue. The data was not processed any further after the crack was discovered.

The data obtained from both the urethane and neoprene combined compression-shear samples showed considerable and apparently inconsistent variation with frequency over portions of the frequency range of interest. This is probably due to the test temperature effects mentioned above, which were due primarily to the test sequence followed for these two samples. The sequence of data taking in the shear samples and compression samples (first four samples) started with the lowest amplitude (0.001 in. (0.025 mm) peak-to-peak) with data obtained at various frequency points. Then, data were obtained at the next higher amplitude at various frequencies. Thus, as far as the 0.001 in. (0.025 mm) amplitude data are concerned, the only inherent temperature effect is that due to the difference in frequency. This effect is less than that due to difference in amplitude.

The sequence of data taking in the combined compression-shear samples, however, started with the lowest frequency, at which amplitudes were varied from lowest to highest values (0.001 in. to 0.005 in. (0.025 to 0.127 mm)). Testing then proceeded to the next higher frequency and so on. Thus, the data obtained at

0.001 in. (0.025 mm) amplitude has, in addition to the heating effect due to frequency, the heating effect due to amplitude as well. This test sequence must be avoided in the future unless long temperature stabilization periods are allowed or unless test temperatures are carefully controlled.

From the measured data obtained in this program it is evident that some heating effects are always present during dynamic testing and in actual application of elastomers. If there is no positive control on the ambient temperature, the temperature of the elastomer sample will vary depending upon the test frequency and amplitude. The elastomer dynamic properties obtained from these tests will therefore be the properties at various temperatures. Future tests therefore require refinement of the test rig to include the capability of controlling the ambient temperature over a range of temperature levels.

The test rig described above was designed to exhibit small values of tare damping, primarily in the air cylinders and their diaphragms. While the estimated damping levels present in the rig were reasonably small relative to the values calculated for the urethane and neoprene samples, it is apparent that such may not be the case for other elastomers or sample sizes. Precise measurement of tare stiffness and damping levels in the rig, through use of calibrated spring and viscous damper elements is needed to ensure accurate measurement of the properties of low damping elastomers. Such measurements are best accompanied by calculations designed to show the effect upon measured elastomer properties of errors in the values of the test rig tare stiffness and damping.

With regard to the elastomer three-element viscoelastic model, very good correlation was obtained for some elastomer sample test conditions, while results were less satisfactory for others. It must be recalled that this model, composed of two spring elements and one damping element, was only one of three or four such models which exist. Other models have different arrangements. It is anticipated that a four-element model, with two stiffness and two damping elements, may provide substantially better correlation of the dissipation characteristics while retaining the demonstrated good qualities of the three-element model with regard to stiffness properties. Evaluation of several models, using the same set of test data, will indicate suitability of the various models for different elastomers and different test conditions. It is felt that one model will eventually prove

to be usable over a wide range of materials and conditions. Such a model may eventually permit incorporation of temperature as a parameter through, perhaps, the use of an additional constant.

CONCLUSIONS AND RECOMMENDATIONS

The objectives of this program are to catalog elastomer dynamic properties (stiffness and damping) in terms of a set of viscoelastic model constants, and to establish practical, designer-oriented procedures whereby these constants may be used to predict the dynamic properties for other operating conditions.

The work reported herein was undertaken to verify the basic methods for obtaining the viscoelastic model constants. The results obtained confirm the basic approach of the program and the mechanics of cataloging viscoelastic model constants.

Detailed Conclusions

The following specific conclusions may be drawn as a result of this work:

1. A survey of published literature indicated that while basic elastomer dynamic property data (stiffness and damping) is rather sparse in terms of the parameter ranges covered, large volumes of test data are available for specific elastomer devices. Viscoelastic analytical procedures for predicting dynamic properties for general elastomer shapes and operating conditions are not yet available in the literature. It is concluded that a very real need exists for substantial quantities of the designer-oriented data this program is to provide.

2. No test apparatus was available prior to this effort for obtaining elastomer dynamic test data over the range of frequencies, amplitudes, and preloads expected to be encountered in typical engineering applications. Therefore, a test rig, utilizing the base-excitation, resonance-mass approach, was designed, built and successfully used to obtain elastomer data. Based upon the range of tests conducted, it must be concluded that the test rig which now exists is fully capable of performing uniaxial testing of large elastomer specimens or devices at virtually any desired combination of amplitude, frequency, and preload. However, the success of this programmatic approach rests on the accuracy

and sufficiency of the test data, and hence on the performance of the test rig. It is further concluded, therefore, that several test rig and instrumentation system refinements are required in order that the full capability of the test rig may be utilized.

3. The data reduction and correlation procedures and techniques developed during this effort proved effective in the calculation of stiffness and damping properties from test data, and for the extraction of viscoelastic model constants through curve fitting.

4. With regard to the elastomer dynamic model, it is concluded that the three-element model investigated possesses only limited value for use in cataloging viscoelastic model constants for elastomers. This conclusion is based upon the relative inability of the constants thus obtained to reproduce the energy dissipation (damping) properties of the elastomers studied. It must be noted, however, that the model used yielded reasonably good results for the energy storage (stiffness) properties.

   It is concluded, therefore, that the relatively simple three-element model has served its purpose of assisting in the verification of the basic methods to be used for obtaining viscoelastic model constants, and that a more complete model must be used in the future.

5. Based upon the extreme variability of elastomer dynamic properties with changes in temperature, it is concluded that future evaluation of more complex elastomer models should be conducted in a constant temperature environment, achieved through test rig refinements, and that future tests should be conducted on a material which is relatively insensitive to changes in temperature. It is further concluded that the effects of temperature must ultimately be included in the elastomer analytical model, perhaps through the use of one or more material constants.

Recommendations

The following specific recommendations are made as a result of this work:

1. Existing test data should be used to evaluate the utility of several additional elastomer dynamic models.

2. The test rig and instrumentation system should be refined to permit constant temperature testing. Refinements should include:

   a) Provision for simplification of test startup and shutdown procedures to eliminate possible overstressing of resonance-mass guide spokes due to startup transients;

   b) Provision for insulating and heating of the elastomer test cavity, and for test temperature control;

   c) Provision for precise measurement of test rig tare stiffness and damping;

   d) Calculations of the sensitivity of measured results to errors in test rig inherent stiffness, damping, and mass, and evaluation of the possible need for statistical controls of experimental data.

3. The elastomer mounting arrangements should be modified to permit compression testing of specimens with larger length-to-diameter ratios and to eliminate the possibility of nonaxial motions during high-frequency resonance test conditions in which the guided, external resonance mass is not used.

4. Tests on elastomers which are relatively insensitive to temperature changes should be performed under carefully controlled test temperature conditions to yield high-confidence, elastomer uniaxial dynamic properties.

5. Elastomer uniaxial dynamic properties should be used to develop, practical, designer-oriented prediction techniques for more general dynamic loading conditions. Such techniques should be verified through tests.

6. Catalogs of viscoelastic model constants should be prepared for commonly-used elastomers. It may prove beneficial, further, to reduce the number of groups of material constants which must be cataloged through development of functional relationships with operating parameters or through corresponding increases in the number of material constants.

APPENDIX I

CALCULATION OF AIR CYLINDER STIFFNESS

For an air cylinder of area A and height L, the air volume is V = AL and the force on the piston is

$$F = p A \tag{36}$$

where p is the air pressure (gage).

When the piston is moved in the direction to further compress the air, the pressure inside the cylinder will increase. Consequently, the force F will also increase. This increment of force corresponds to a stiffness of the air cylinder.

If the air inside the cylinder is assumed to be at a constant temperature, then from thermodynamics:

$$p V = \text{constant}$$

Differentiation yields:

$$p\, d V + V\, d p = 0$$

or

$$d p = -\frac{p}{V} d V = -\frac{p}{L} d L \tag{37}$$

From Eqs. (36) and (37),

$$d f = A\, d p = -\frac{A p}{L} d L$$

By definition, the air cylinder stiffness is the force increment per unit decrement of air cylinder height. Thus,

$$k_{air} = \frac{d F}{-d L} = \frac{A p}{L} .$$

SYMBOLS

a_1, a_2, a_3	elastomeric constants
a_{11}, a_{12}, a_{21}, a_{22}	defined in Eq. (13)
A_1	acceleration of shake table, in./sec^2
A_2	acceleration of resonant mass, in./sec^2
A_f	acceleration of foundation, in./sec^2
C	damping coefficient, lb-sec/in.
C_e	elastomer damping coefficient, lb-sec/in.
C'_e	$C_e + C_\ell$
d_1, d_2	defined in Eq. (13)
f	frequency, Hz
F	force, lb
G	complex compliance function, in./lb
G_1, G_2	real and imaginary parts of G, in./lb
k	stiffness, lb/in.
k_e	elastomer stiffness, lb/in.
k'_e	$k_e + k_\ell$
m	mass, lb-sec^2/in.
x	displacement, in.
x_1	displacement of shake table, in.
x_2	displacement of resonant mass, in.
x_f	displacement of foundation, in.
X	amplitude of displacement x, in.
t	time, sec
Z_e	elastomer mechanical impedence = $k_e + i\omega c_e$
ϵ	displacement, in.

φ	phase angle, radians
ω	frequency, radians/sec

Superscripts

$\bar{(\ )}$	denotes amplitude of ( )
$\dot{(\ )}$	denotes time-derivative of ( )

Subscripts

1	shake table
2	resonant mass
e	elastomer specimen
f	shaker body
ℓ	lower air cylinder
u	upper air cylinder

REFERENCES

1. Ferry, J.D., VISCOELASTIC PROPERTIES OF POLYMERS, John Wiley and Sons, Inc., New York, 1961.

2. Bueche, F., PHYSICAL PROPERTIES OF POLYMERS, Interscience Publisher, New York, 1962.

3. Nielsen, L.E., MECHANICAL PROPERTIES OF POLYMERS, VanNostrand Reinhold Company, New York, 1962.

4. Tobolsky, A.U., PROPERTIES AND STRUCTURE OF POLYMERS, John Wiley and Sons, Inc., New York, 1960.

5. Payne, A.R. and Scott, J.R., ENGINEERING DESIGN WITH RUBBER, Interscience Publisher, New York, 1960.

6. Scott, J.R., PHYSICAL TESTING OF RUBBERS, Palmerton Publishing Company, New York, 1965.

7. Illers, K.H., and Jenckel, E., "Dynamic Mechanical Behavior of Polystyrene at Low Temperatures," J. of Polymer Science, Vol. 41, p. 528, 1959.

8. Nielsen, L.E., ASTM Bul. No. 165, 48, April 1950.

9. Newman, S., "A Vibrating Reed Apparatus for Measuring the Dynamic Mechanical Properties of Polymers," J. Applied Polymer Science, Vol. 2, p. 333, 1959.

10. Robinson, D.W., "An Apparatus for the Measurement of Dynamic Mechanical Properties of Polymers over a Wide Temperature Range," J. Scientific Instrument, Vol. 32, p. 2, 1955.

11. Strella, S., "Vibrating Reed Tests for Plastics," ASTM Bul., No. 214, p. 47, 1956.

12. Nolle, A.W., "Methods for Measuring Dynamic Mechanical Properties of Rubberlike Materials," J. of Applied Physics, Vol. 19, pp. 753-774, August 1948.

13. Nolle, A.W., Dynamic Mechanical Properties of Rubberlike Materials," J. of Polymer Science, Vol. 5, No. 1, pp. 1-54, 1950.

14. Hopkins, I.L., "Dynamic Shear Properties of Rubberlike Polymers," Trans. ASME, pp. 195-204, February 1951.

15. Painter, G.W., "Dynamic Characteristics of Silicone Rubber," Trans. ASME, pp. 1131-1135, October 1954.

16. Philippoff, W., "Mechanical Investigations of Elastomers in a Wide Range of Frequencies," J. of Applied Physics, Vol. 24, No. 6, pp. 685-689, June 1953.

17. Fitzgerald, E.R., Grandine, L.D., and Ferry, J.D., "Dynamic Mechanical Properties of Polyisobutylene," J. of Applied Physics, Vol. 24, No. 5, pp. 650-655, May 1953.

18. Fletcher, W.P. and Gent, A.N., "Nonlinearity of the Dynamic Properties of Vulcanized Rubber Compounds," Trans. Inst. Rubber Ind., Vol. 29, pp. 255-280, 1953.

19. Hutton, A.Q. and Nolle, A.W., "Experimental Study of Low-Frequency Effects on the Dynamic Modulus of a Buna-N Rubber," J. of Applied Physics, Vol. 25, No. 3, pp. 350-354, March 1954.

20. Williams, M.L. and Ferry, J.D., "Dynamic Mechanical Properties of Polyvinyl Acetate," J. Colloid Science, Vol. 9, pp. 479-492, 1954.

21. McCallion, H. and Davies, D.M., "Behavior of Rubber in Compression Under Dynamic Conditions," Proc. Inst. of Mech. Eng., Vol. 169, pp. 1125-1132, 1955.

22. Painter, G.W., "Dynamic Properties of BTR Elastomers," presented at the SAE National Aeronautic Meeting, Los Angeles, California, September 1958.

23. Kurath, S.F., Passaglia, E. and Pariser, R., "Dynamic Mechanical Properties of Polyhexene-1," J. of Applied Physics, Vol. 28, No. 4, pp. 499-502, April 1957.

24. Fletcher, W.P. and Gent, A.N., "Dynamic Shear Properties of Some Rubber-like Materials," British J. of Applied Physics, Vol. 8, pp. 194-201, May 1957.

25. Kurath, S.F., Passaglia, E. and Pariser, R., "The Dynamic Mechanical Properties of Hypalon-20 Synthetic Rubber at Small Strains," J. of Applied Polymer Science, Vol. 1, No. 2, pp. 150-157, 1959.

26. Ungar, E.E. and Hatch, D.K., "High Damping Materials," Product Engineering, pp. 44-56, April 17, 1961.

27. Warnaka, G.E., "Dynamic Strain Effects in Elastomers," ASME Paper No. 62-WA-323, presented at the Meeting of the Rubber and Plastics Division, ASME, New York, November 1962.

28. Yin, T.P. and Pariser, R., "Dynamic Mechanical Properties of Neoprene Type W," J. of Applied Polymer Science, Vol. 7, pp. 667-673, 1963.

29. Yin, T.P., "The Dynamic Characterization of Elastomers for Vibration Control Applications," presented at Automobile Week, SAE, Detroit, Michigan, March 1964.

30. Yin, T.P. and Pariser, R., "Dynamic Mechanical Properties of Several Elastomers and Their Potentialities in Vibration Control Applications," J. of Applied Polymer Science, Vol. 8, pp. 2427-2443, 1964.

31. Preiss, D.M. and Skinner, D.W., "Damping Characteristics of Elastomers," Rubber Age, pp. 58-68, August 1965.

32. Snowdon, J.C., "Rubberlike Materials, Their Internal Damping and Role in Vibration Isolation," J. of Sound and Vibration, Vol. 2, No. 2, pp. 175-193, 1965.

33. Henderson, J.P., "Energy Dissipation in a Vibration Damper Utilizing a Viscoelastic Suspension," Shock and Vibration Bulletin 35, Part 7, pp. 213-229, Naval Research Laboratory, Washington, D.C., April 1966.

34. Cannon, C.M., Nashif, A.D. and Jones, D.I.G., "Damping Measurements on Soft Viscoelastic Materials Using a Tuned Damper Technique," Shock and Vibration Bulletin 38, Part 3, pp. 151-163, Naval Research Laboratory, Washington, D.C., November 1968.

35. Lazan, B.J., DAMPING IN MATERIALS AND MEMBERS IN STRUCTURAL MECHANICS, Pergamon Press, New York, 1968.

36. Snowdon, J.C., VIBRATION AND SHOCK IN DAMPED MECHANICAL SYSTEMS, John Wiley and Sons, Inc., New York, 1968.

37. Gent, A.N. and Lindley, P.B., "The Compression of Bonded Rubber Blocks," Proc. Inst. Mech. Engrs., Vol. 173, p. 111, 1959.

38. Auberger, M. and Rinehart, J.S., "Ultrasonic Attenuation of Longitudinal Waves in Plastics," J. of Applied Physics, Vol. 32, p. 219, 1961.

FIGURES

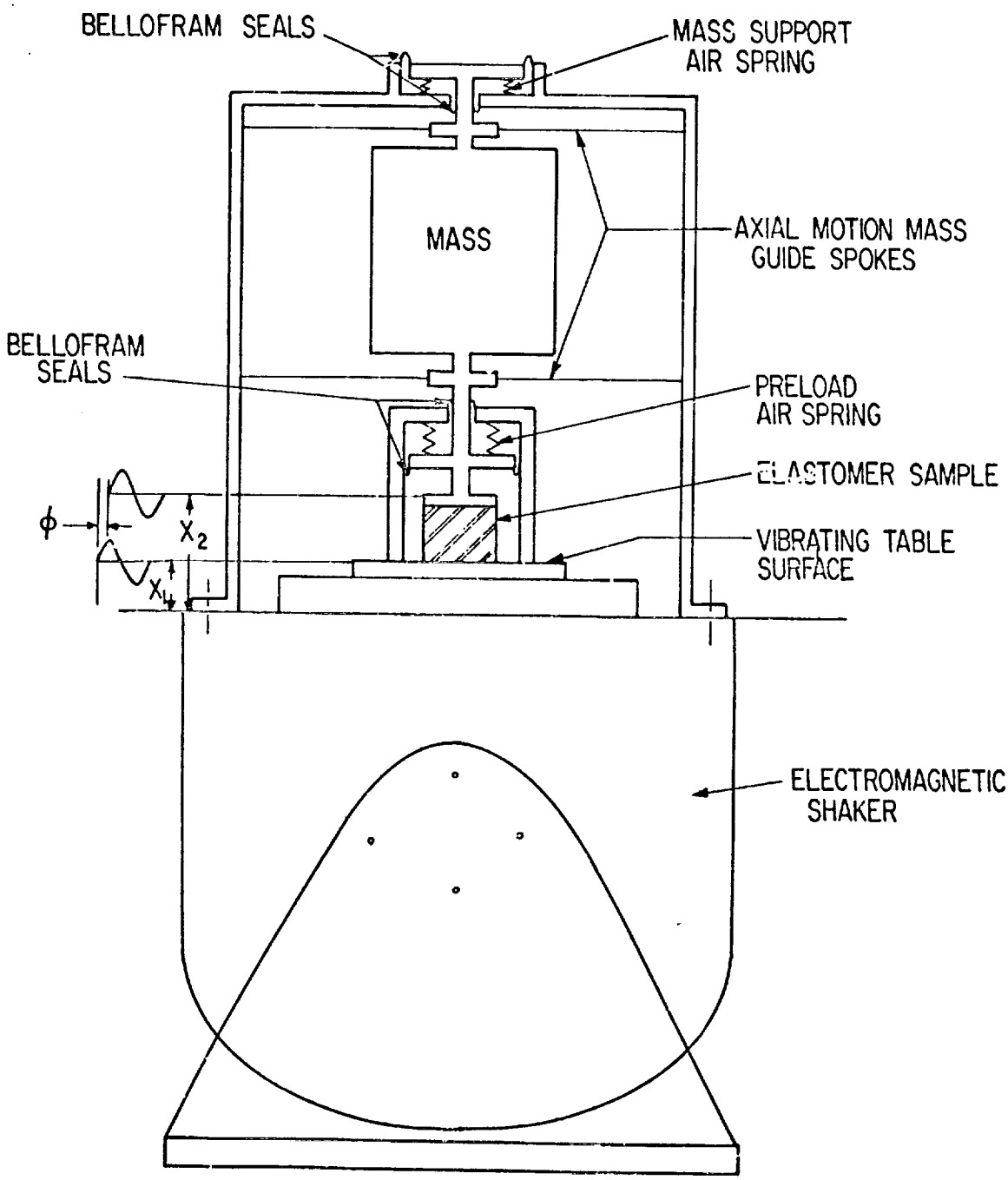

Fig. 1 Schematic of Elastomer Test Rig

MTI-13295

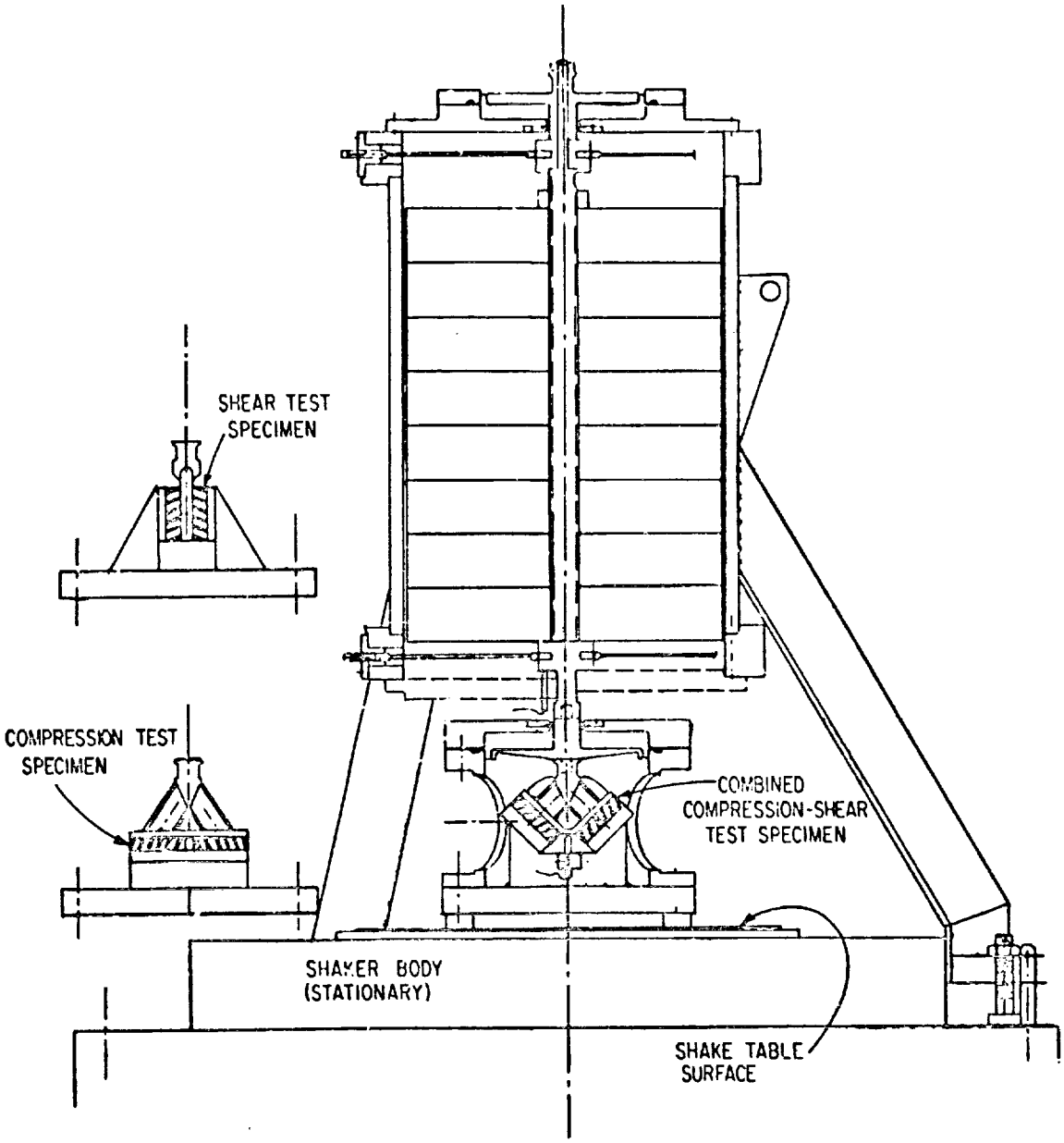

Fig. 2 Elastomer Test Rig Details

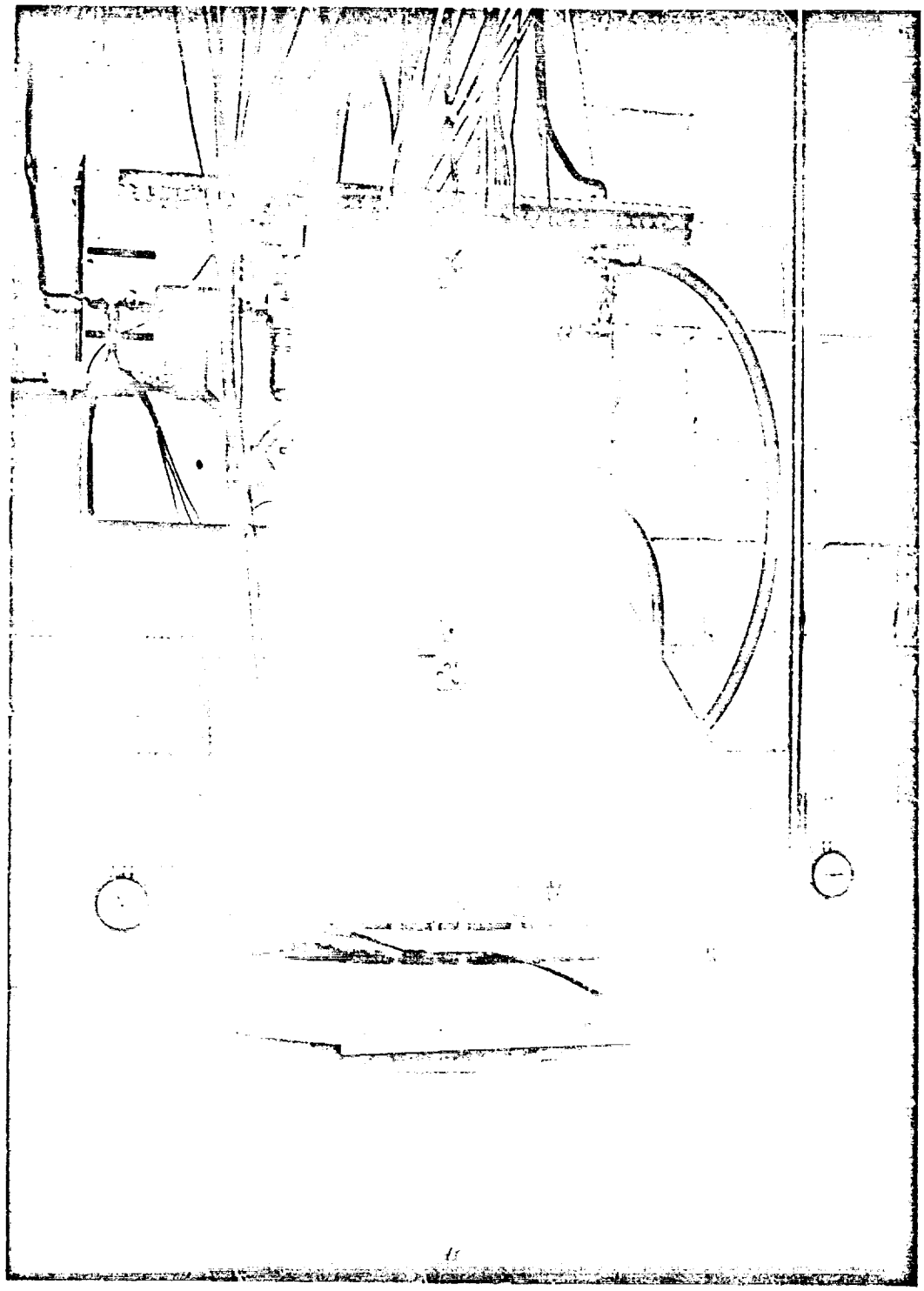

Fig. 3 Elastomer Test Rig Mounted on Vibration Table

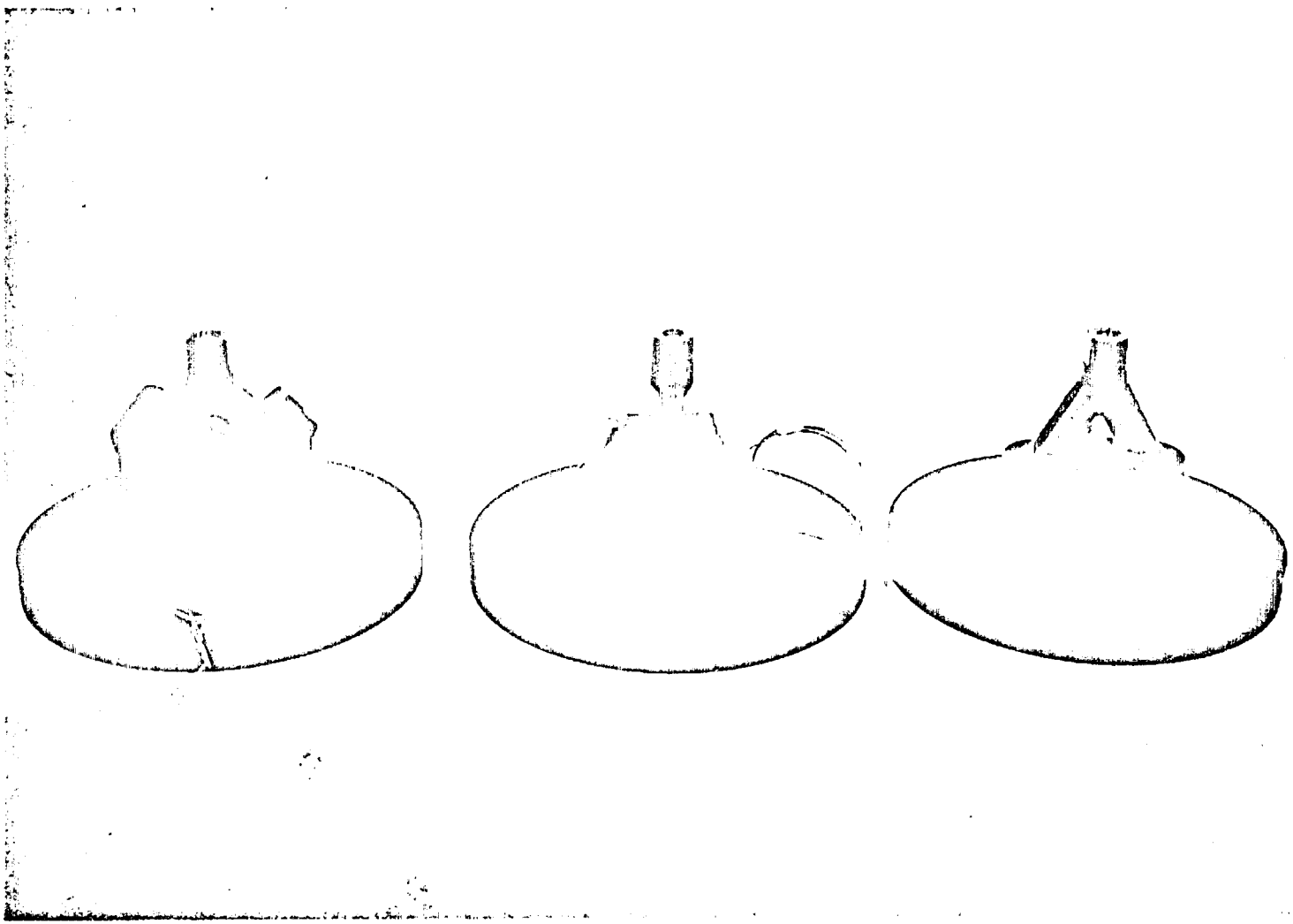

Fig. 4 Mounting Configurations for Elastomer Test Specimen in Compression, Shear and Combined Compression-Shear Loading (right to left)

MTI-13294

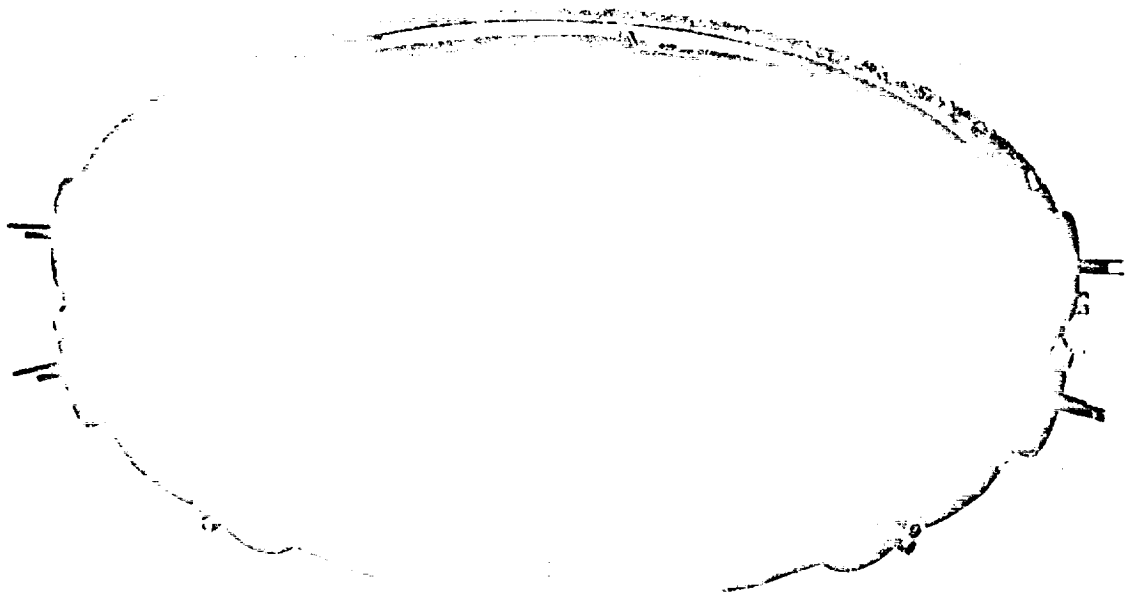

Fig. 5 Radial Guide Bearing

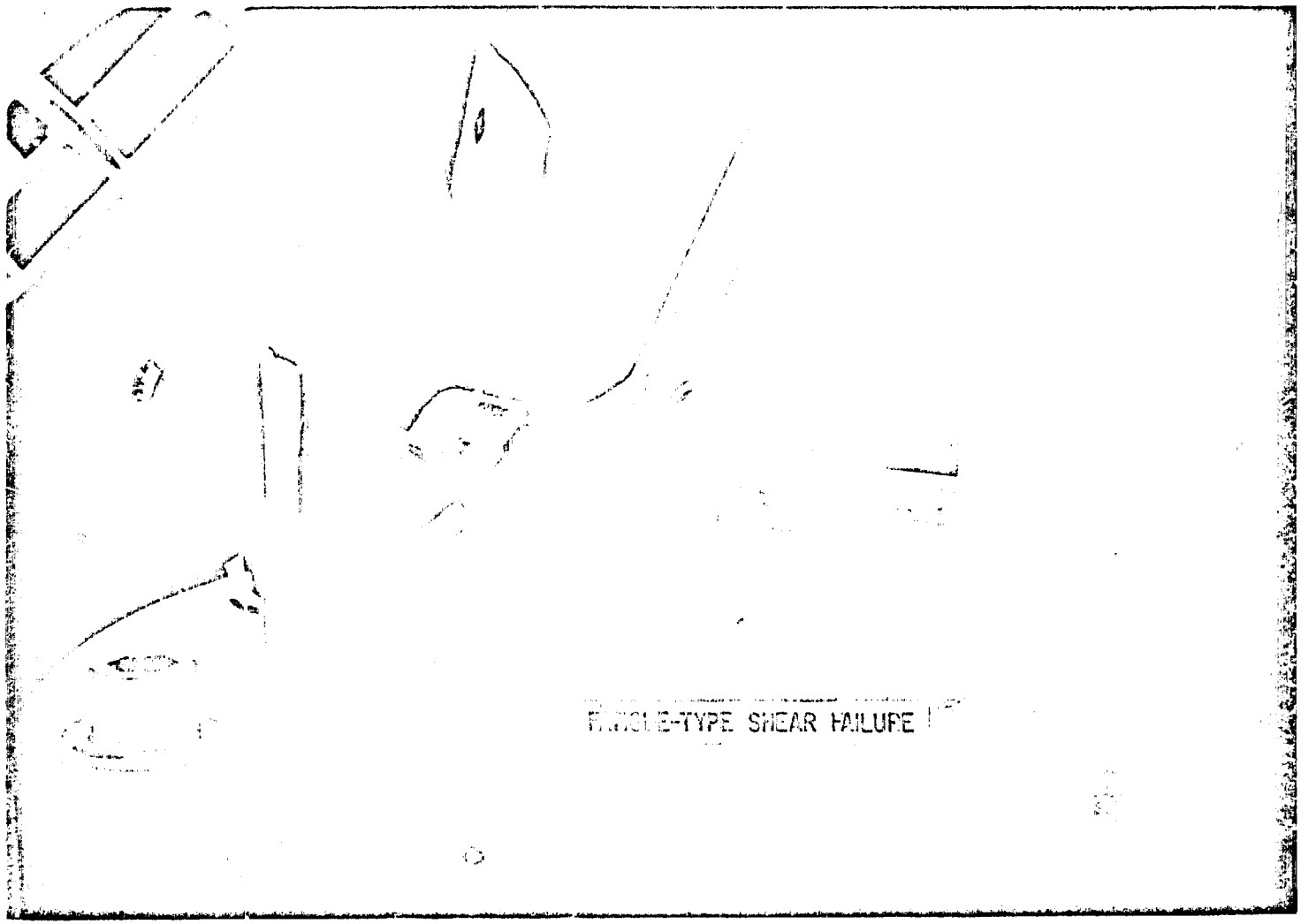

Fig. 6 Urethane Compression Test Sample After Failure

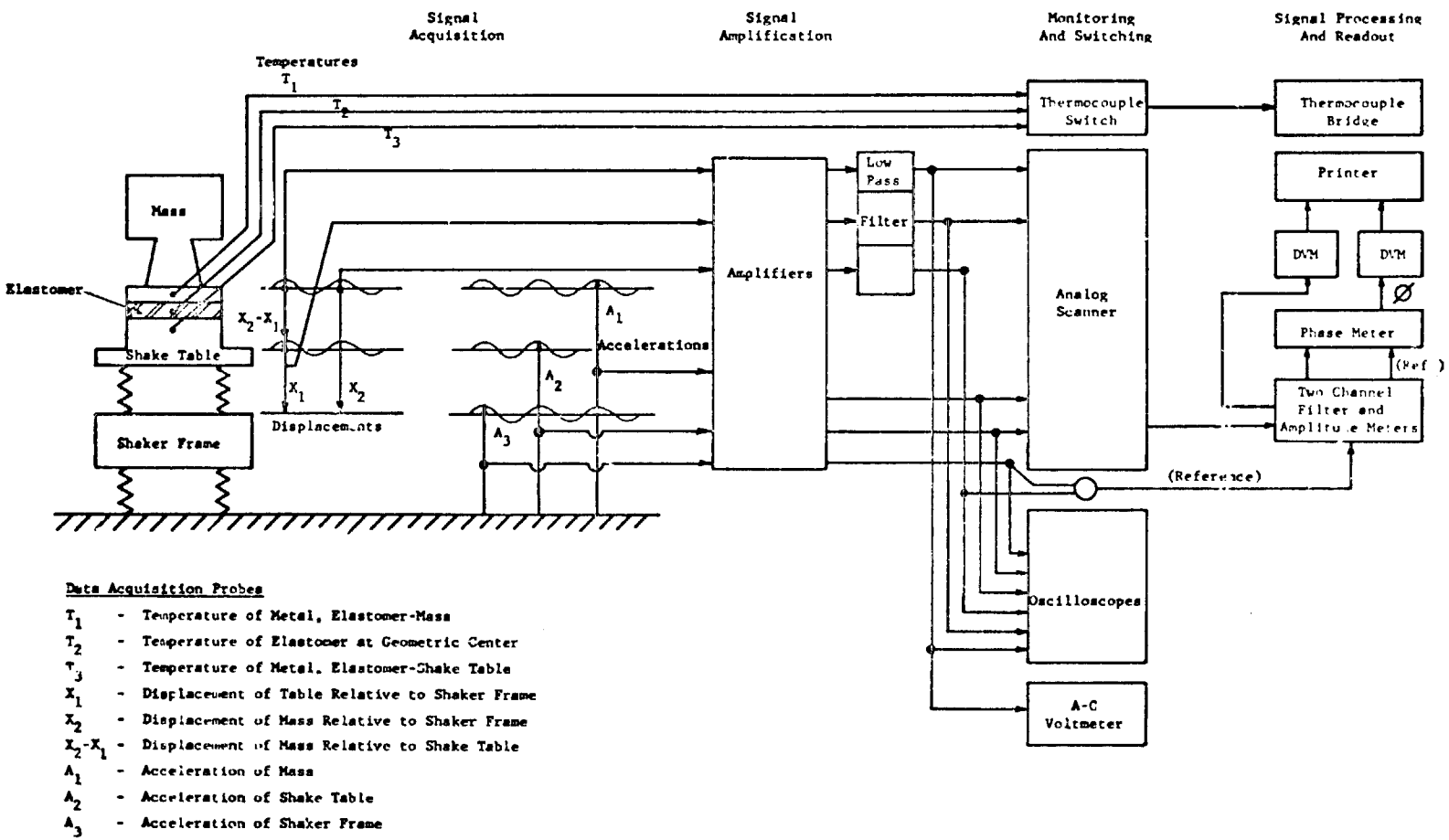

Fig. 7 Schematic of Data Acquisition System for Analytical and Experimental Investigations of Elastomeric Damping Materials

Scanner Channel (1)	Phase Angle (Channel 3 Ref.) (2)	Amplitude Signal (3)	Signal Identification (4)
3	0 0 0 0 0 0 0 0 0 0 .8 0°	0 0 2 3 1	Mass amplitude
2	0 0 0 0 0 0 0 1 6 9 .1 0°	0 1 5 2 0	Table amplitude
1	0 0 0 0 0 0 0 0 2 0 .0 0°	0 1 6 9 5	$(X_2 - X_1)$
	200 Hz (5)		

NOTES: (1) Printout occurred in 1-2-3 sequence.

(2) Phase angle was measured with Channel 3 (mass amplitude signal) as reference. The first reading of 0.8° indicates inherent instrument inaccuracy. Readings of tenths of degrees were ignored for data evaluation. The second reading of 169.1° is the desired phase angle between mass and table amplitude signals. The third reading from the top (scanner channel 1) is of no interest here, since it indicates the angle between signals $(X_2 - X_1)$ and the mass amplitude signal.

(3) Individual calibration factors apply.

(4) Mass amplitude and table amplitude signals were either accelerometer or displacement probe signals as noted at beginning of test.

(5) Shake table frequency was recorded by hand for each data point.

Fig. 8 Data Printout Sample

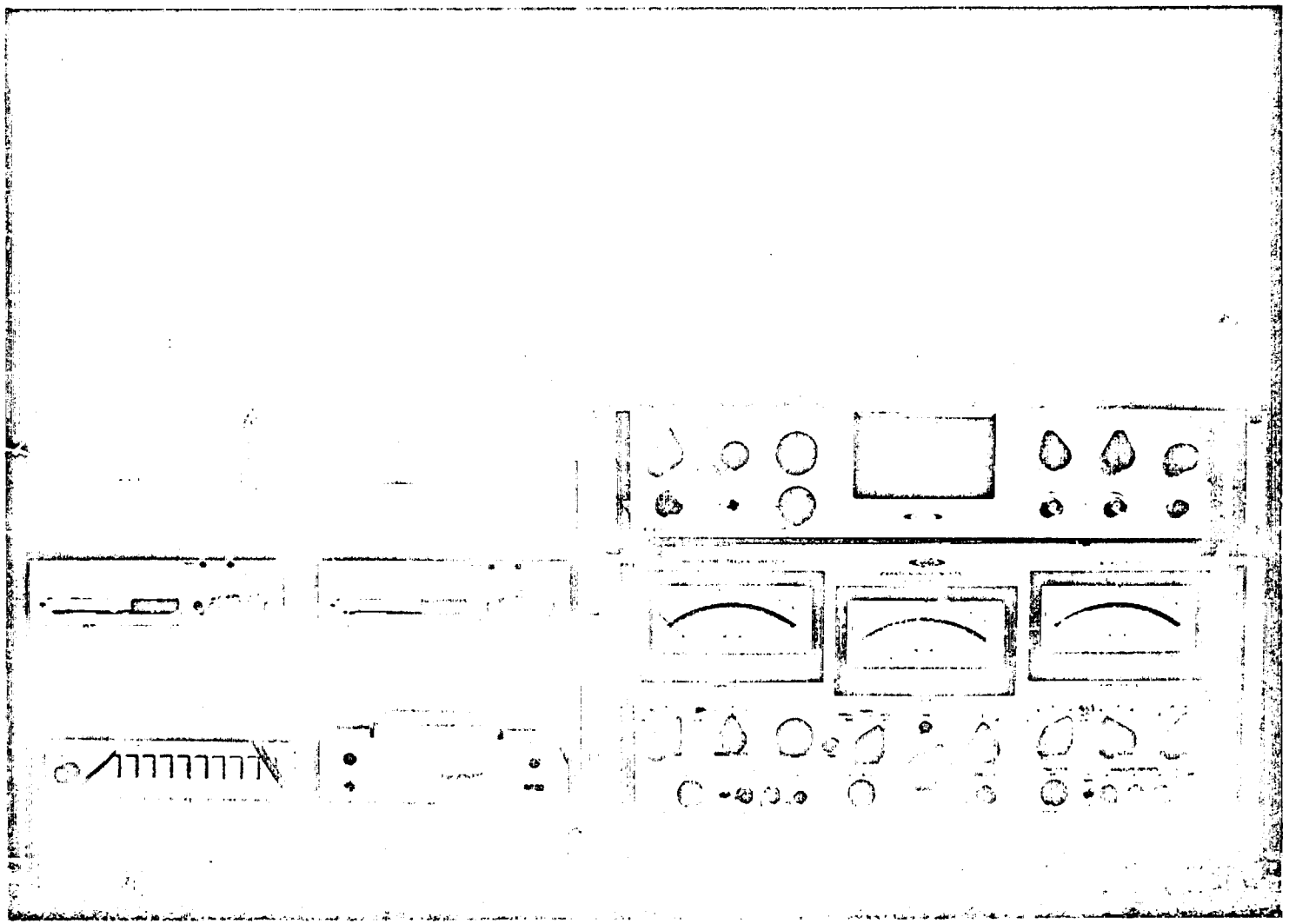

Fig. 9 Data Acquisition Instrumentation

MTI-13291

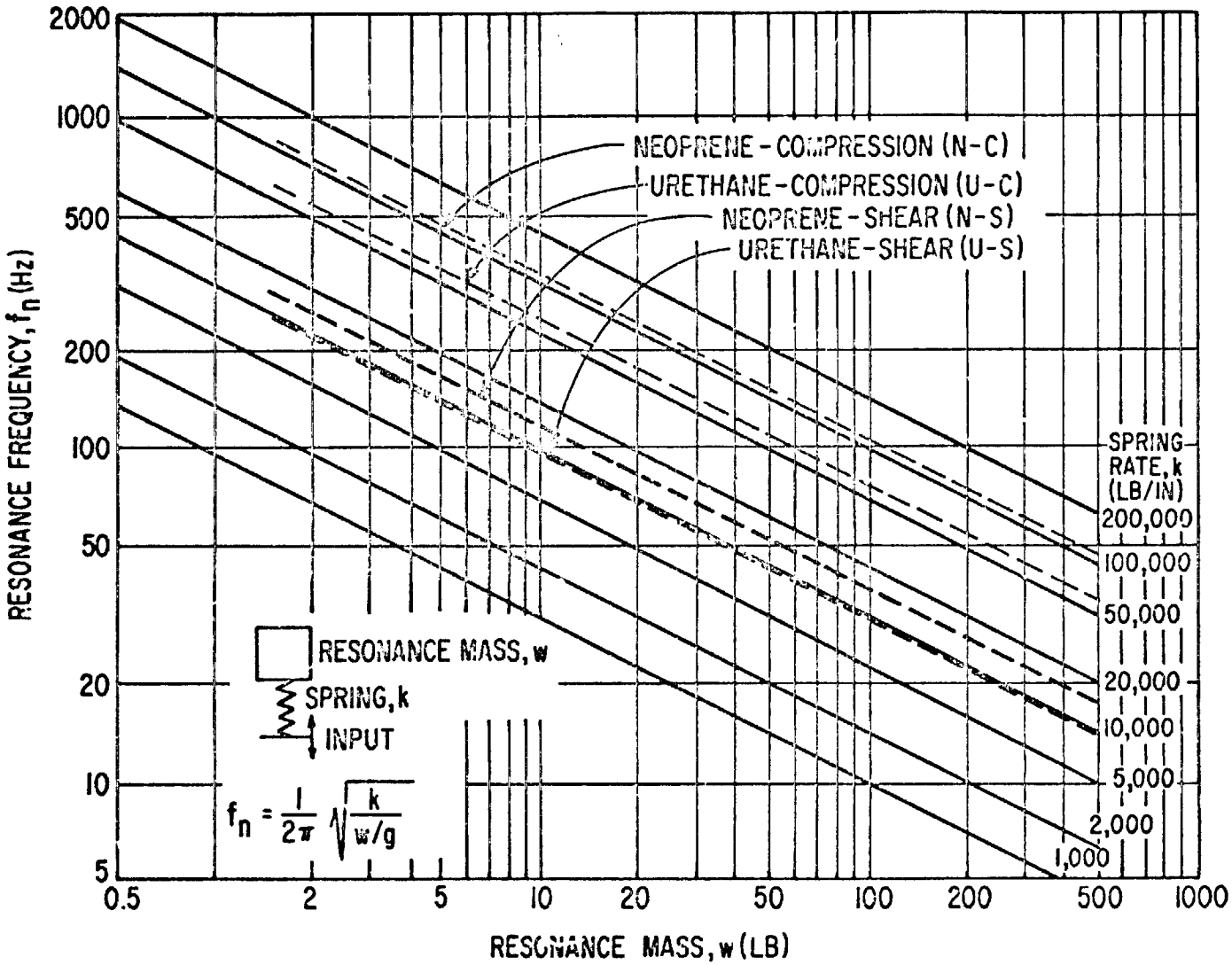

Fig. 10 Resonance Frequency vs. Resonance Mass for Various Spring Rates, Including Approximate Stiffness Values for Neoprene and Urethane Cylindrical Test Specimens 2 Inches (5 cm) in Diameter and 0.50 Inches (1.27 cm) Long

MTI-13304

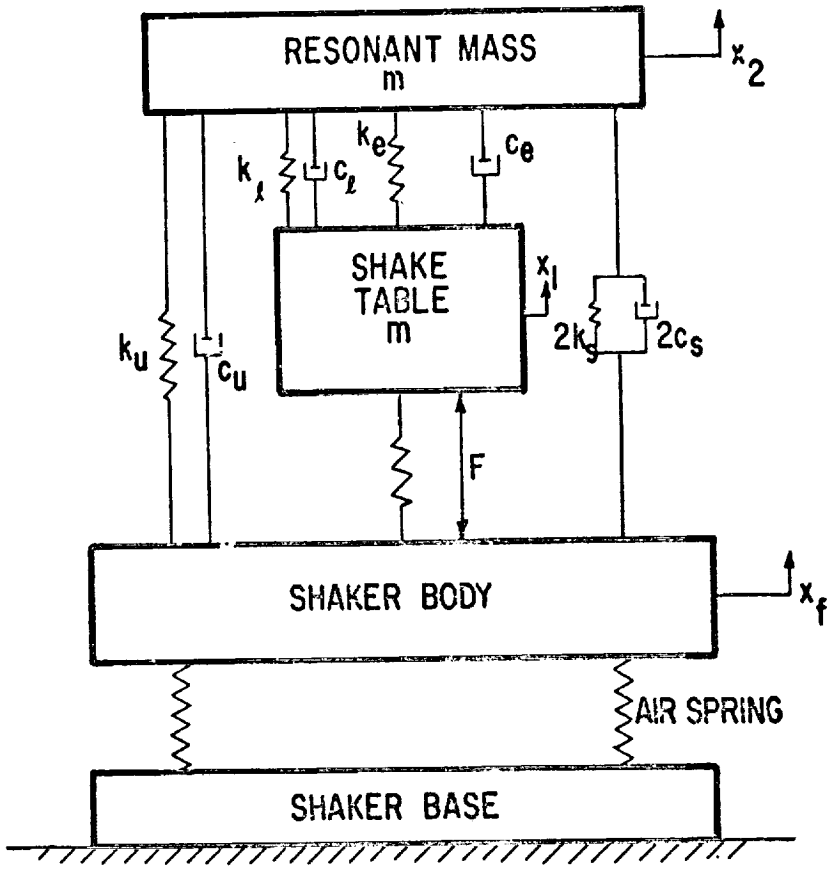

Fig. 11 A Diagram Illustrating the Dynamic Elements of the Test Rig

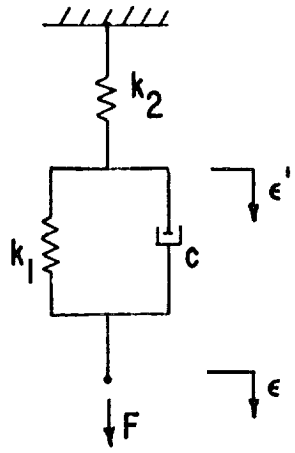

Fig. 12 Three-Element Viscoelastic Model

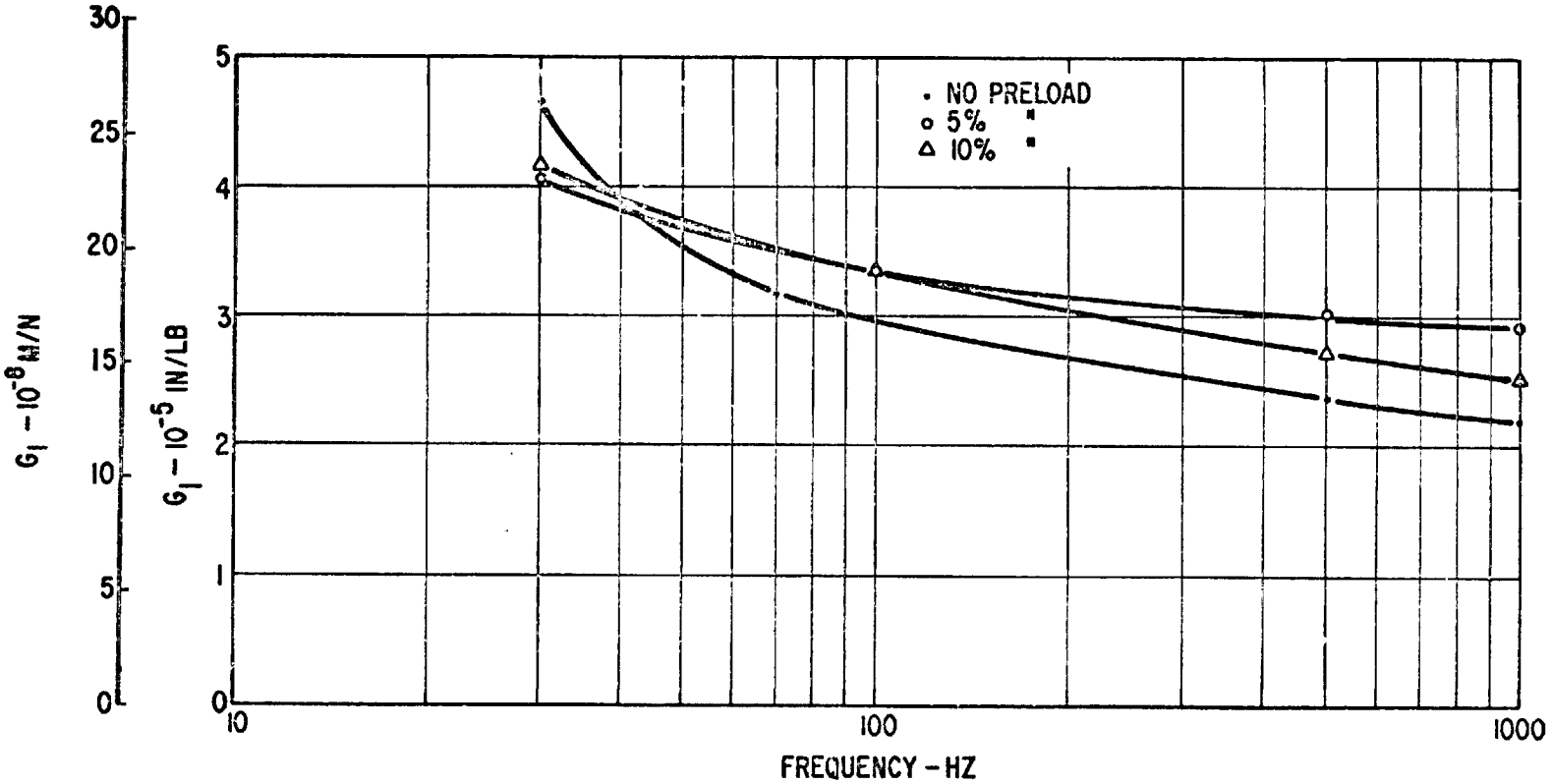

Fig. 13 Real Part of Complex Compliance Function Versus Frequency for Urethane Sample Under Shear Loading at Peak-to-Peak Amplitude of 0.001 in. (0.025 mm)

MTI-13352

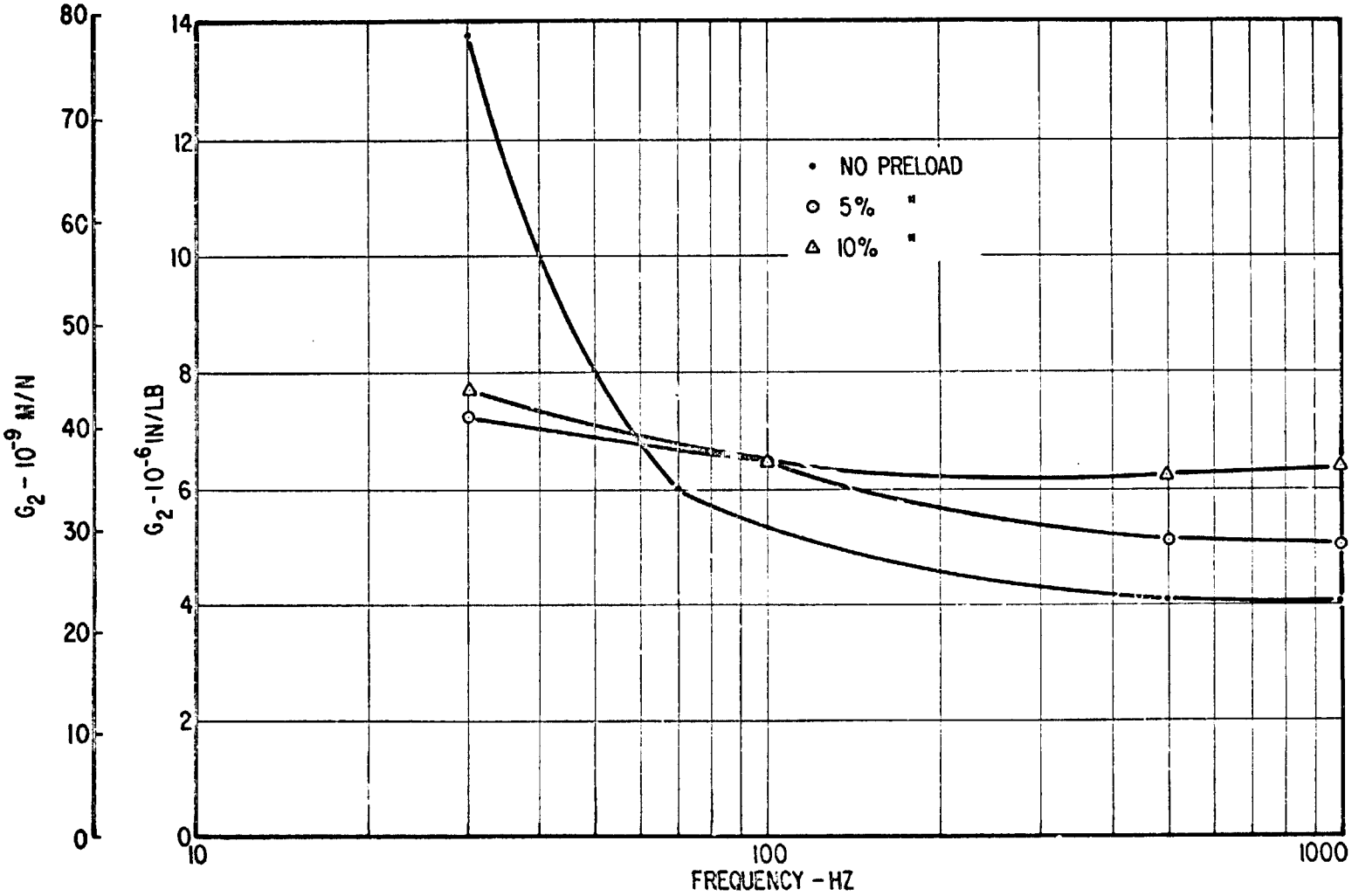

Fig. 14 Imaginary Part of Complex Compliance Function Versus Frequency for Urethane Sample Under Shear Loading at Peak-to-Peak Amplitude of 0.001 in (0.025 mm)

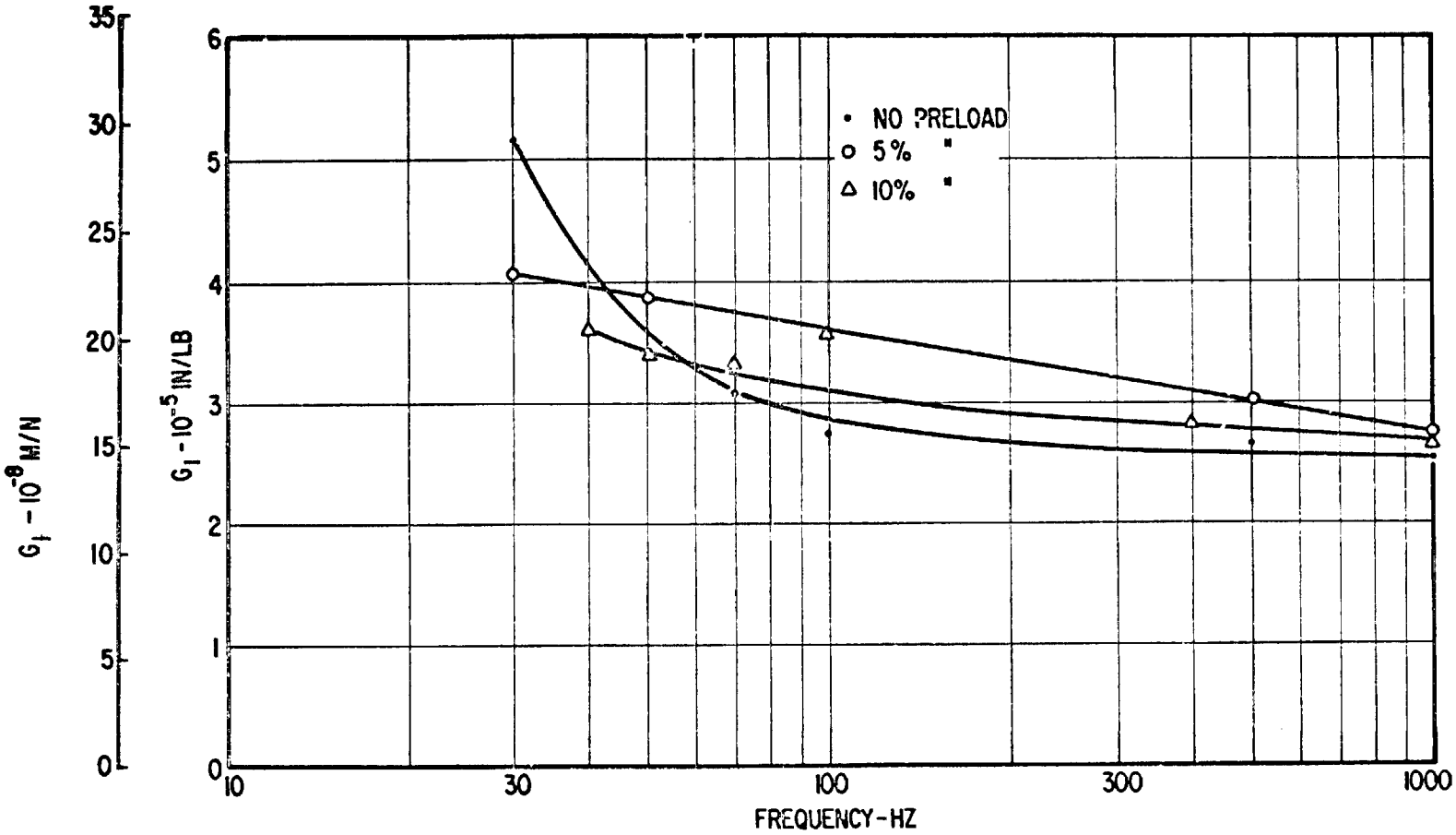

Fig. 15 Real Part of Complex Compliance Function Versus Frequency for Urethane Sample Under Shear Loading at Peak-to-Peak Amplitude of 0.0015 in. (0.038 mm)

MTT-13339

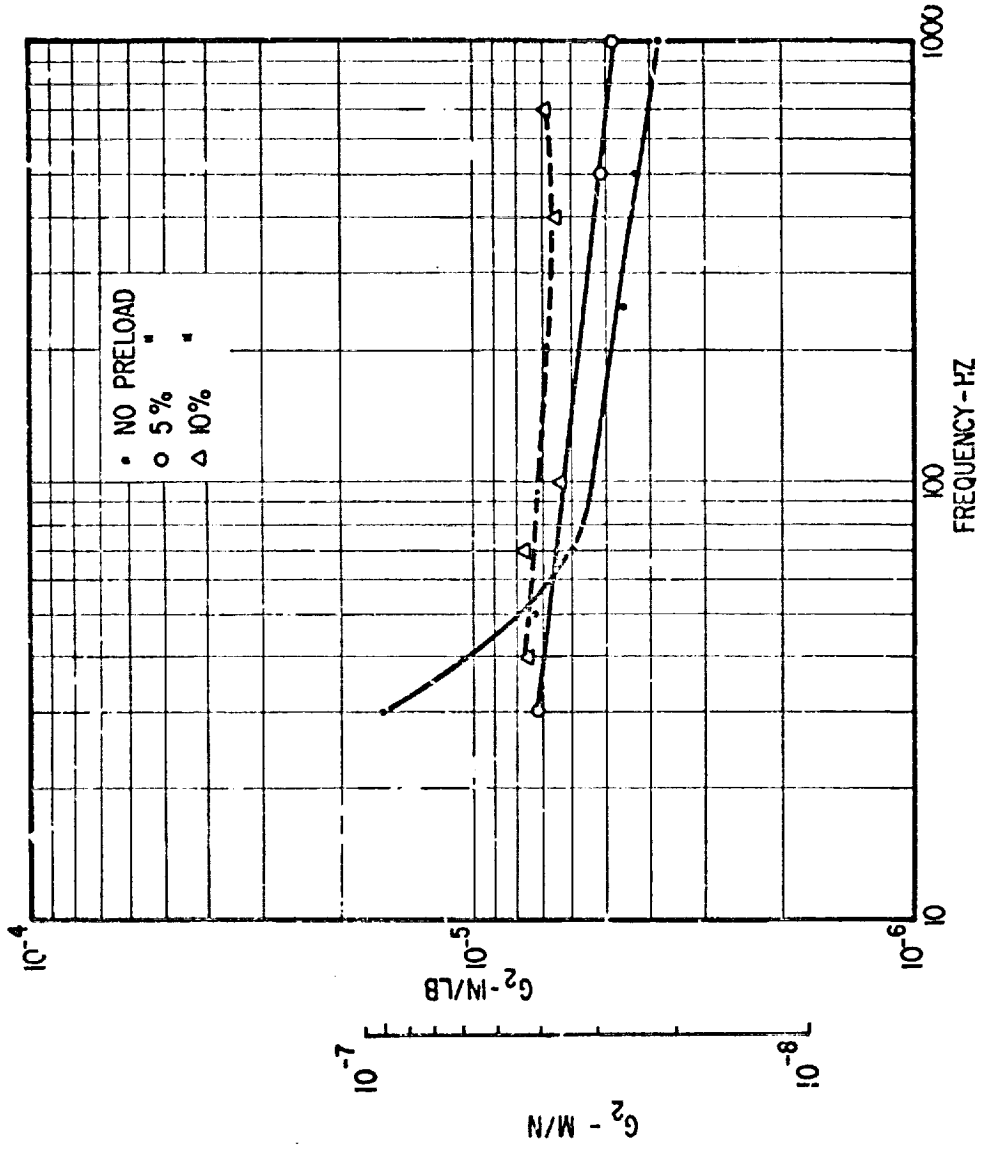

Fig. 16 Imaginary Part of Complex Compliance Function Versus Frequency for Urethane Sample Under Shear Loading at Peak-to-Peak Amplitude of 0.0015 in. (0.038 mm)

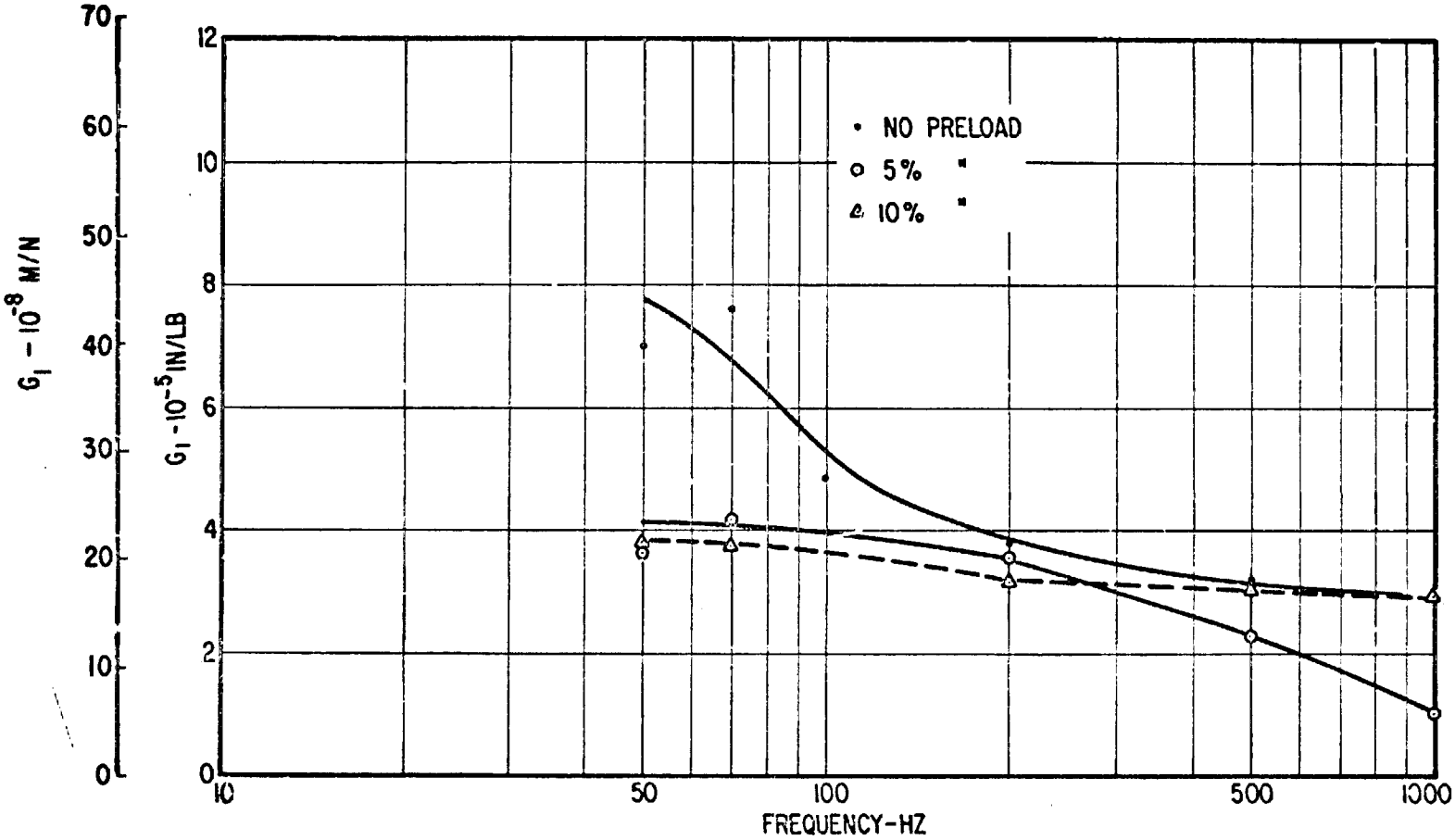

Fig. 17 Real Part of Complex Compliarce Functior Versus Frequency for Neoprene Sample Under Shear Loading at Peak-to-Peak Amplitude of 0.001 in. (0.025 mm)

MTI-13343

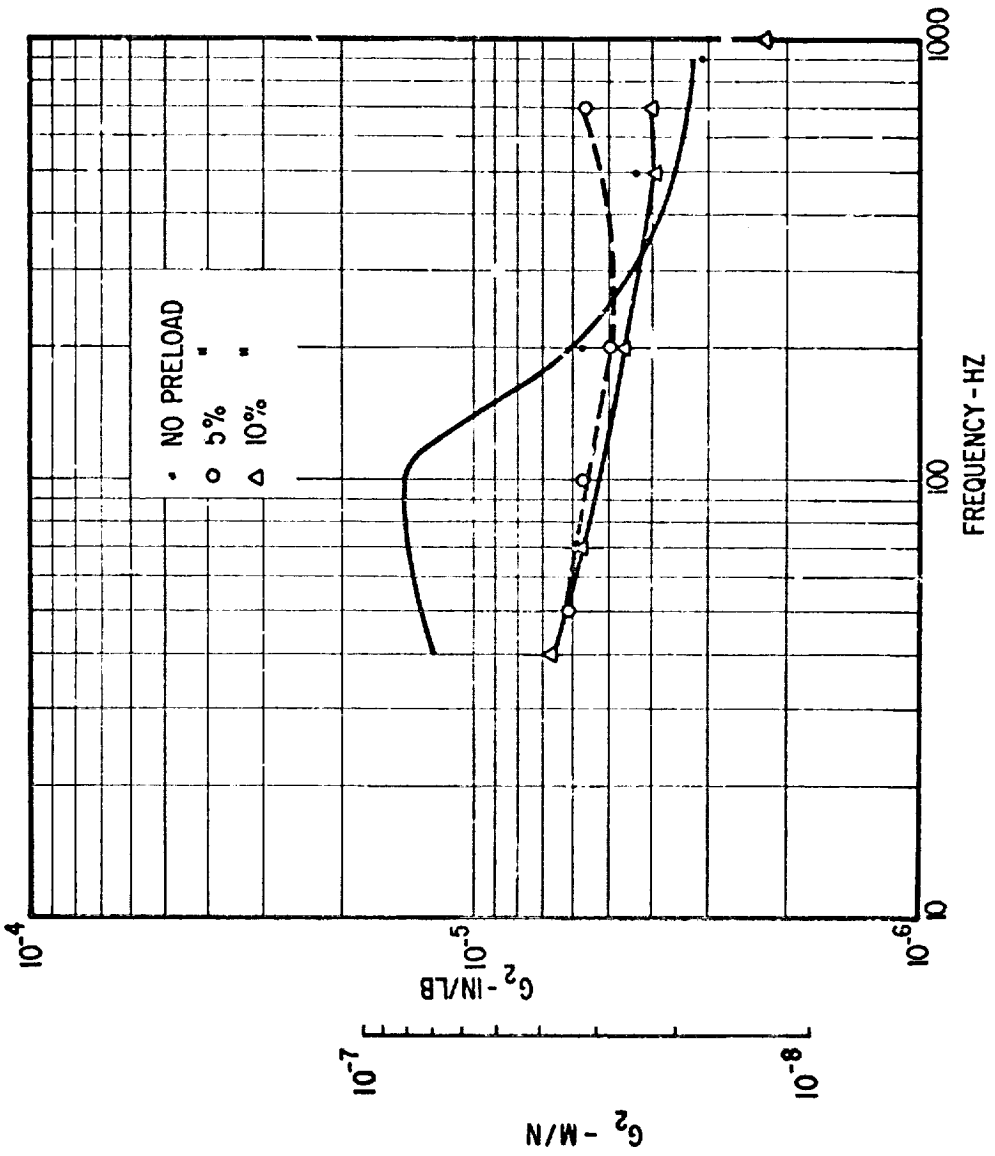

Fig. 18 Imaginary Part of Complex Compliance Function Versus Frequency for Neoprene Sample Under Shear Loading at Peak-to-Peak Amplitude of 0.001 in. (0.025 mm)

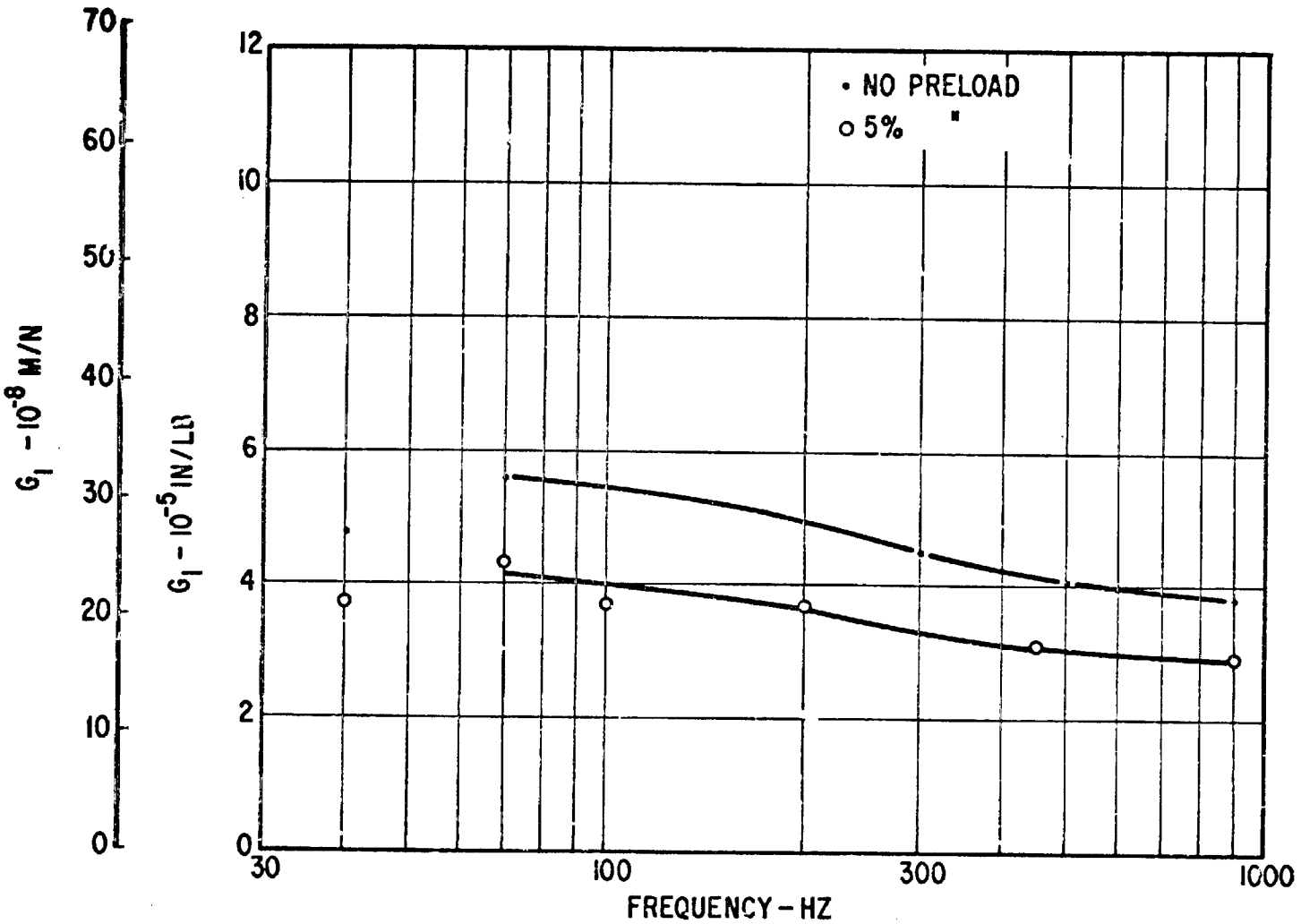

Fig. 19 Real Part of Complex Compliance Function Versus Frequency for Necprene Sample Under Shear Loading at Peak-to-Peak Amplitude of 0.003 in. (0.076 mm)

MTI-13305

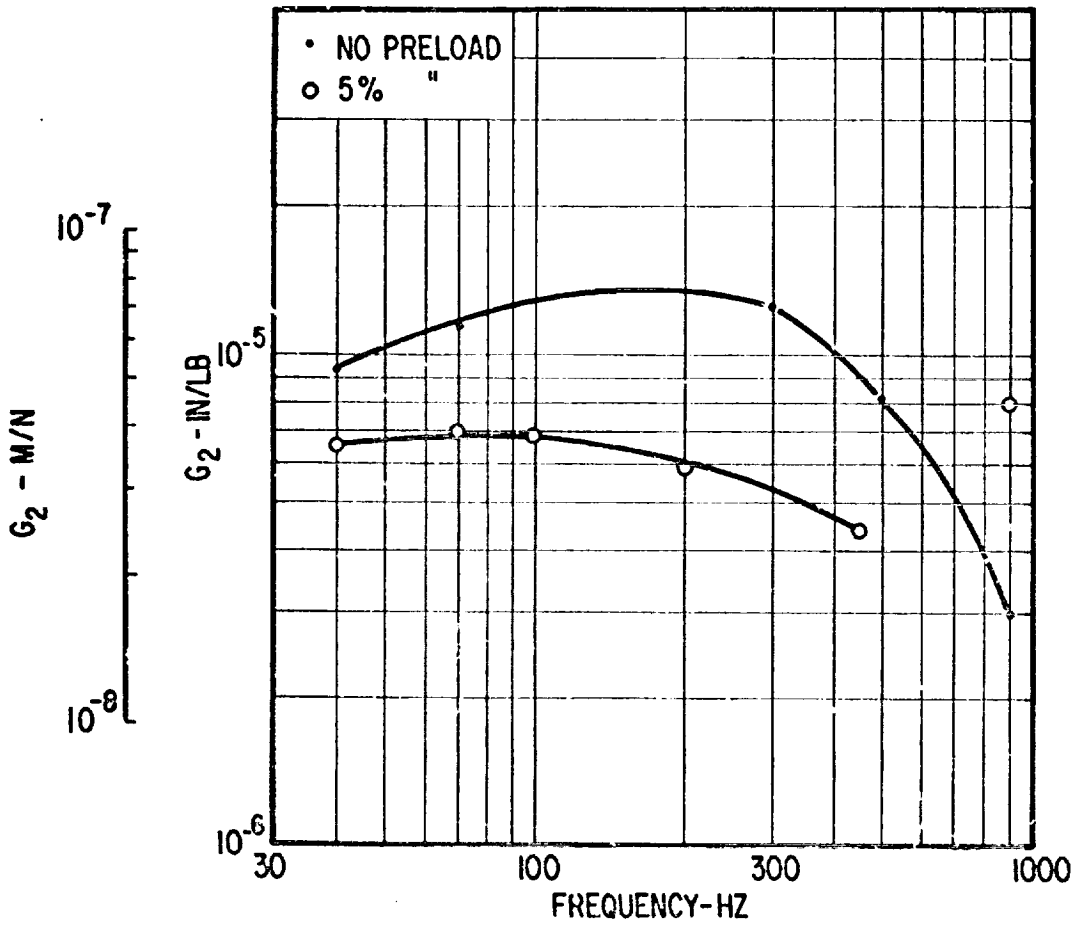

Fig. 20 Imaginary Part of Complex Compliance Function Versus Frequency for Neoprene Sample Under Shear Loading at Peak-to-Peak Amplitude of 0.003 in (0.076 mm)

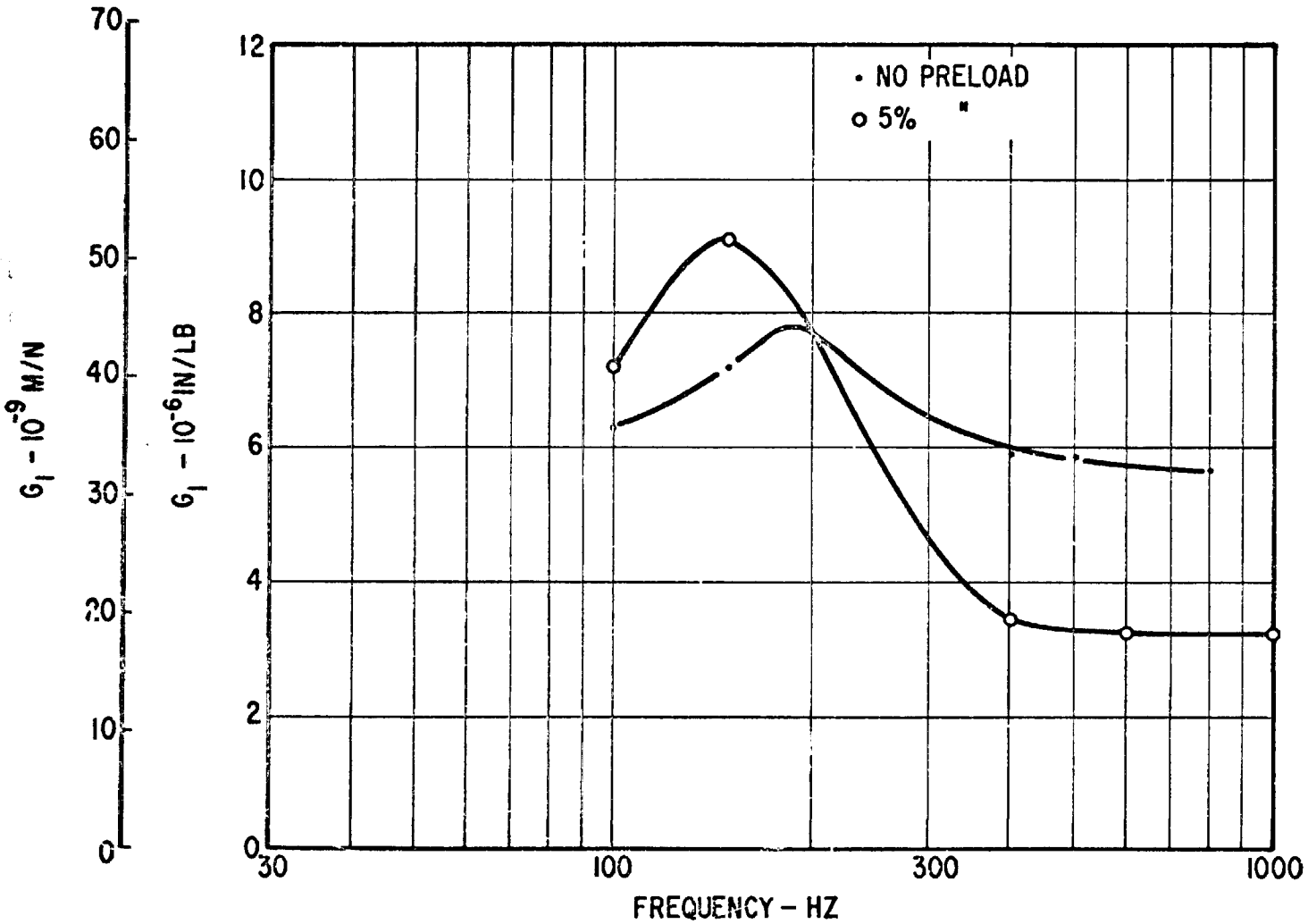

Fig. 21 Real Part of Complex Compliance Function Versus Frequency for Neoprene Sample Under Compression Loading at Peak-to-Peak Amplitude of 0.001 in. (0.025 mm)

MTI-13334

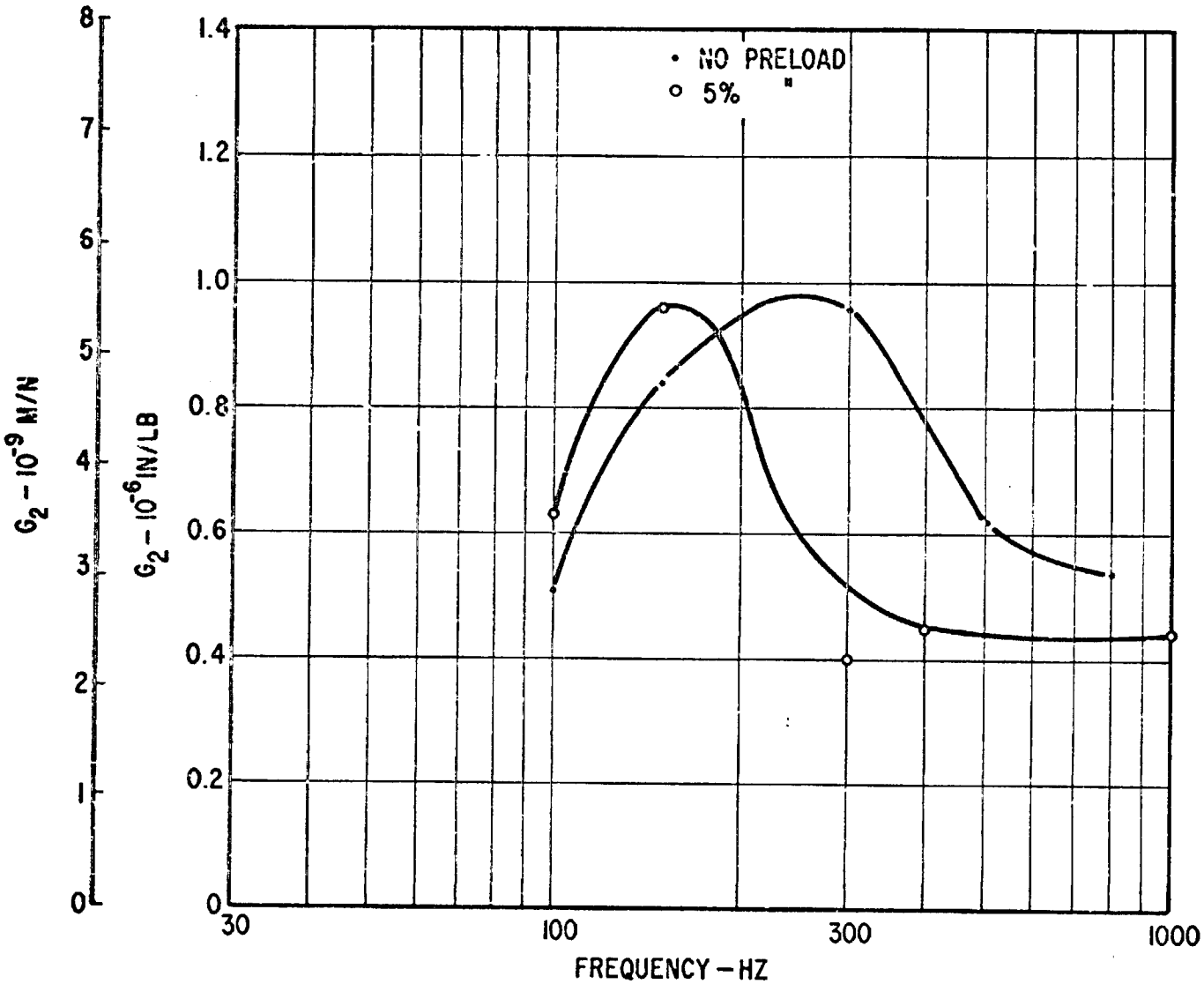

Fig. 22 Imaginary Part of Complex Compliance Function Versus Frequency for Neoprene Sample Under Compression Loading at Peak-to-Peak Amplitude of 0.001 in. (0.025 mm)

MTI-13345

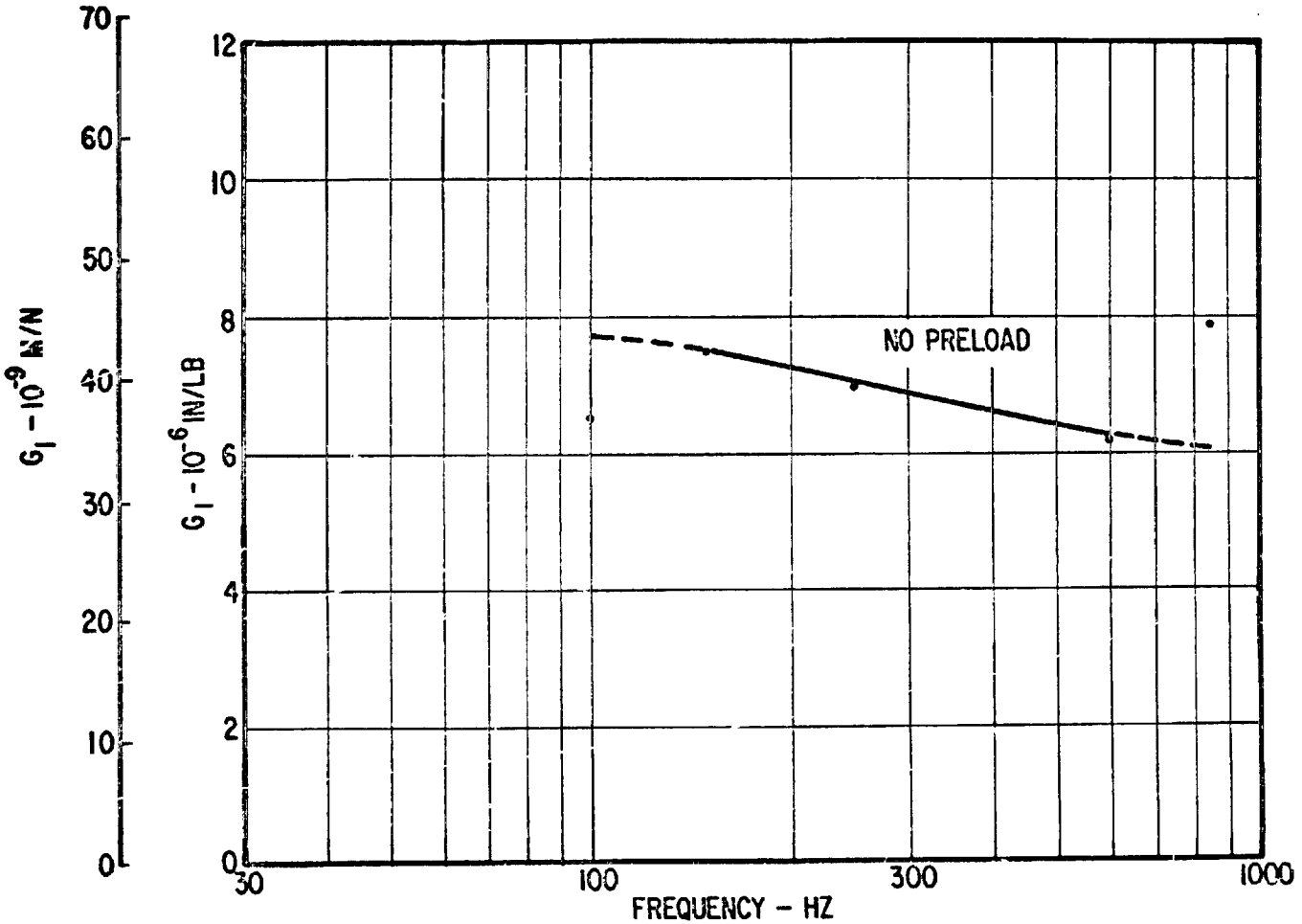

Fig. 23 Real Part of Complex Compliance Function Versus Frequency for Neoprene Sample Under Compression Loading at Peak-to-Peak Amplitude of 0.0015 in. (0.038 mm)

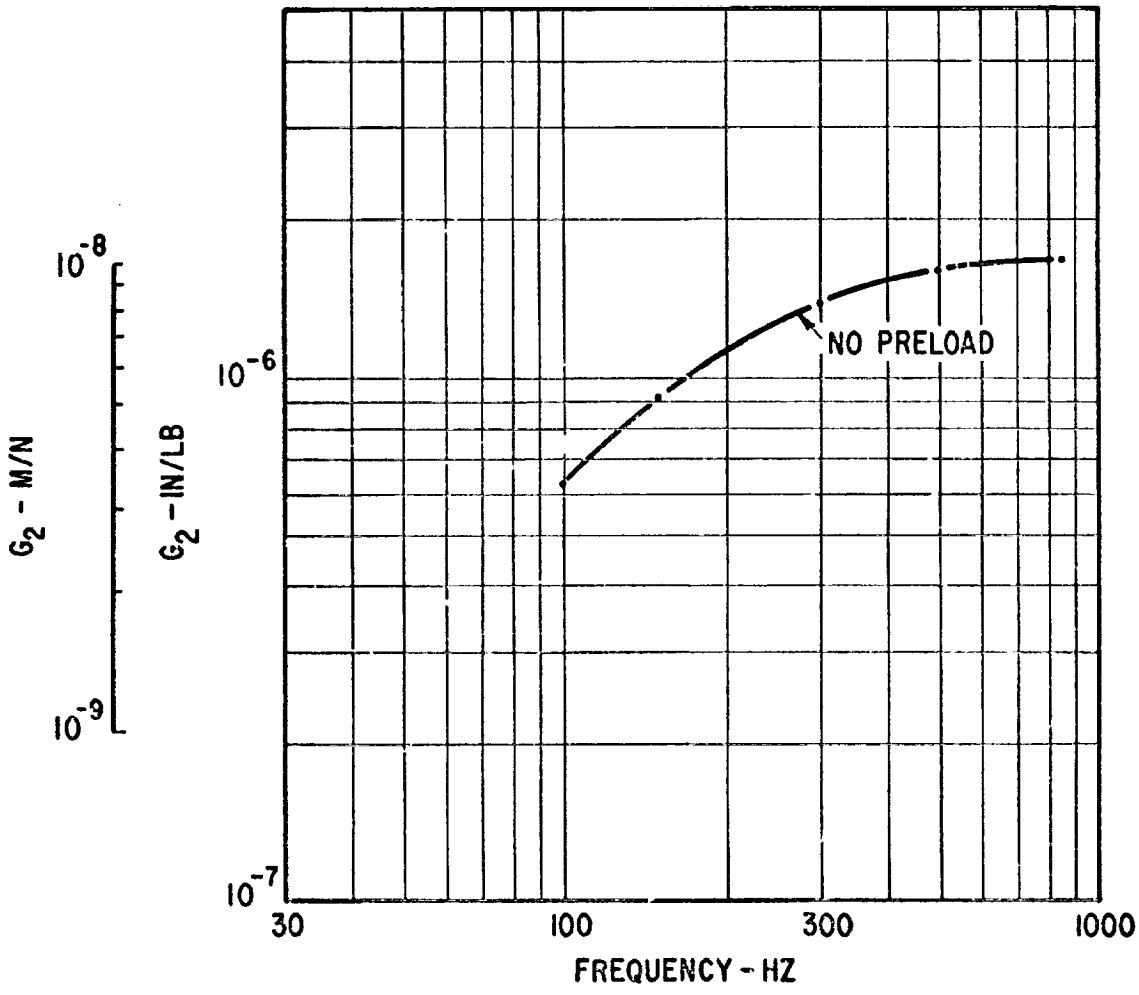

Fig. 24 Imaginary Part of Complex Compliance Function Versus Frequency for Neoprene Sample Under Compression Loading at Peak-to-Peak Amplitude of 0.0015 in. (0.038 mm)

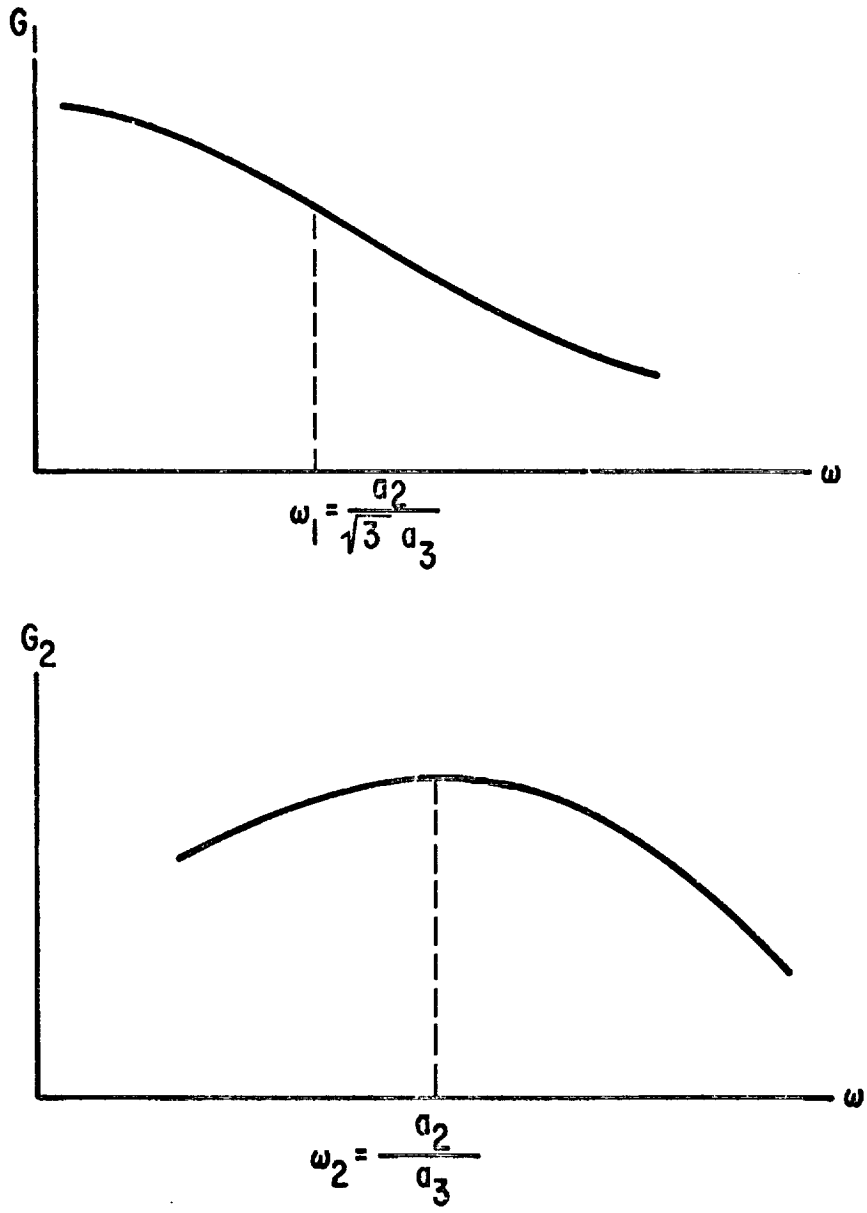

Fig. 25 Qualitative Sketches of G_1 and G_2 According to Equation (32)

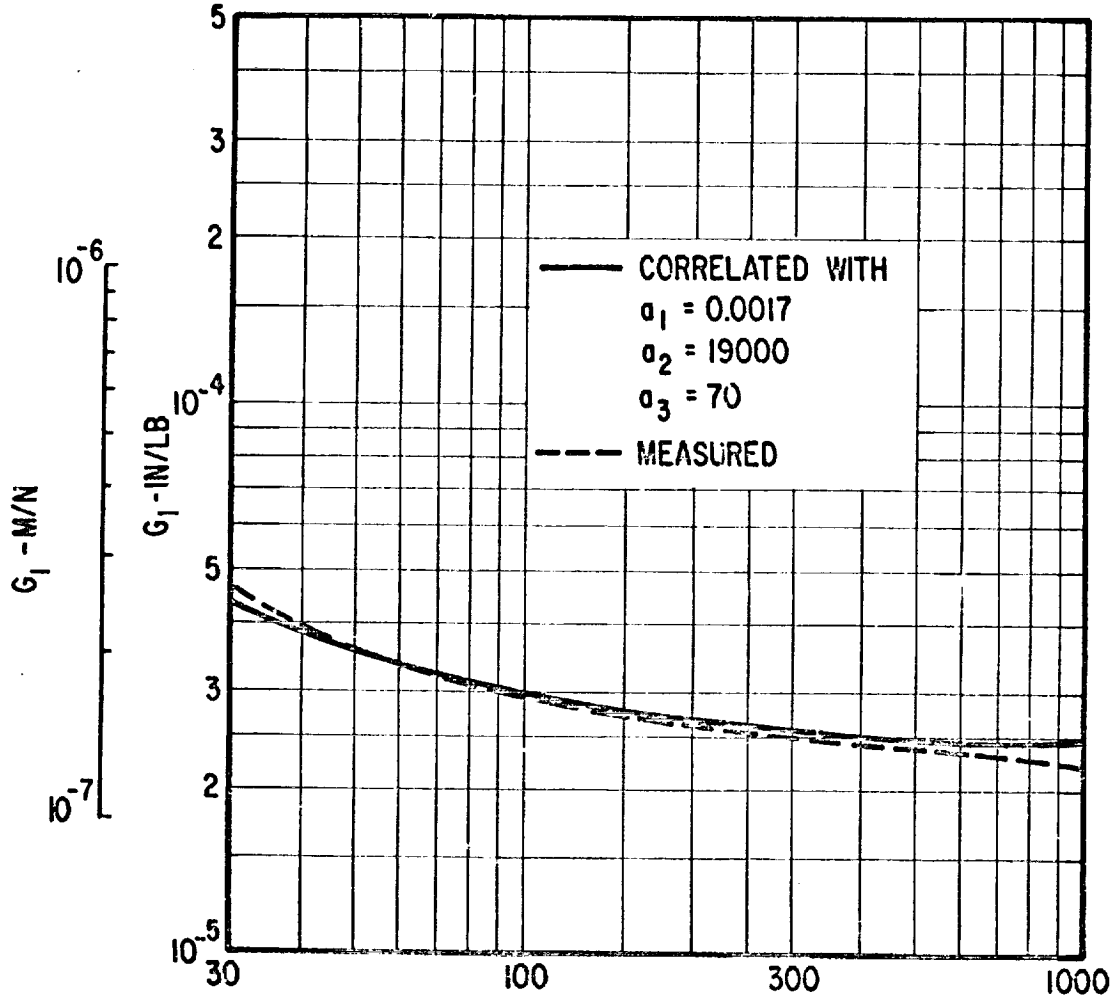

Fig. 26 Comparison of the Correlated and Measured G_1 Functions for Urethane Sample Under Shear Loading at 0.001 in. (0.025 mm) Amplitude and No Preload

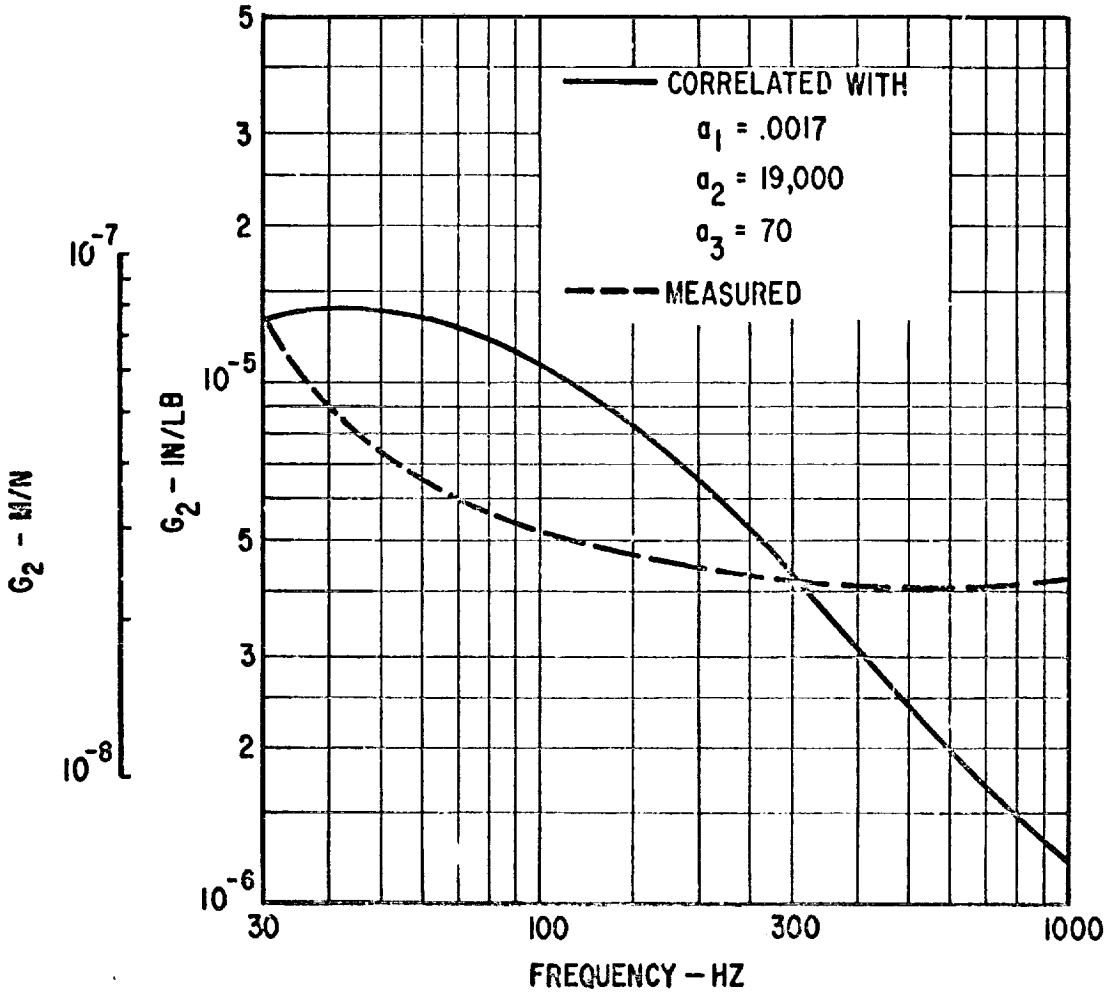

Fig. 27 Comparison of the Correlated and Measured G_2 Functions for Urethane Sample Under Shear Loading at 0.001 in. (0.025 mm) Amplitude and No Preload

MTI-13349

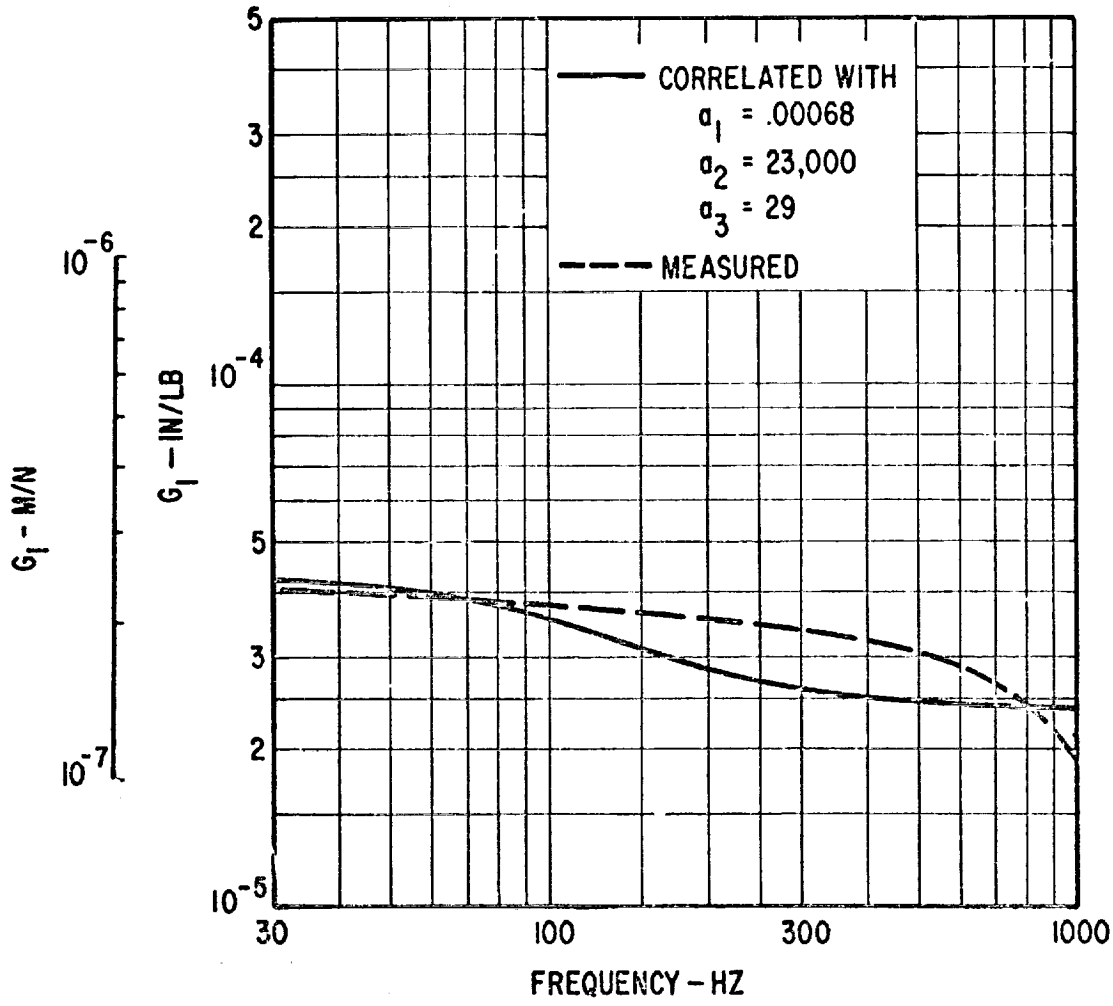

Fig. 28 Comparison of the Correlated and Measured G_1 Functions for Urethane Sample Under Shear Loading at 0.001 in. (0.025 mm) Amplitude and 5% Preload

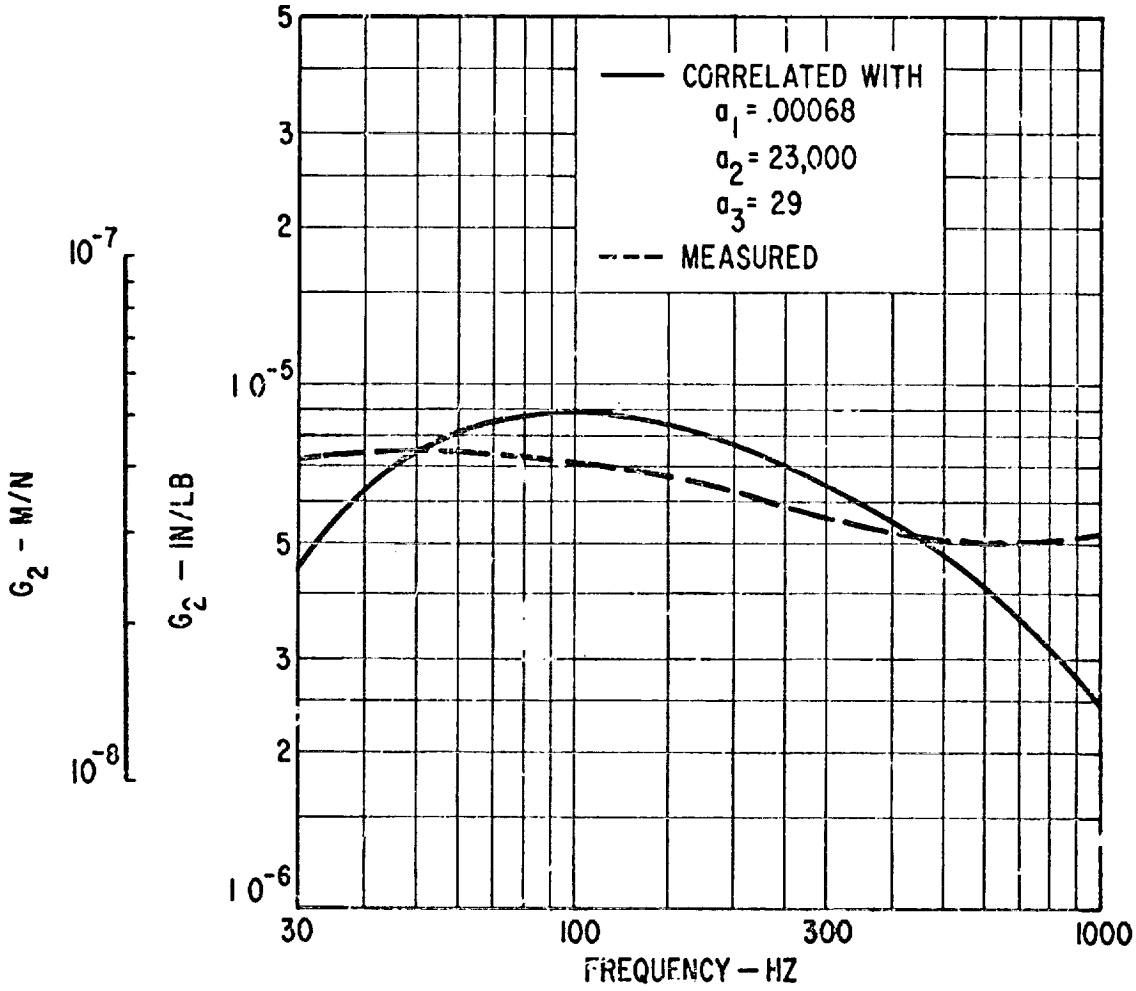

Fig. 29 Comparison of the Correlated and Measured G_2 Functions for Urethane Sample Under Shear Loading at 0.001 in. (0.025 mm) Amplitude and 5 % Preload

MTI-13347

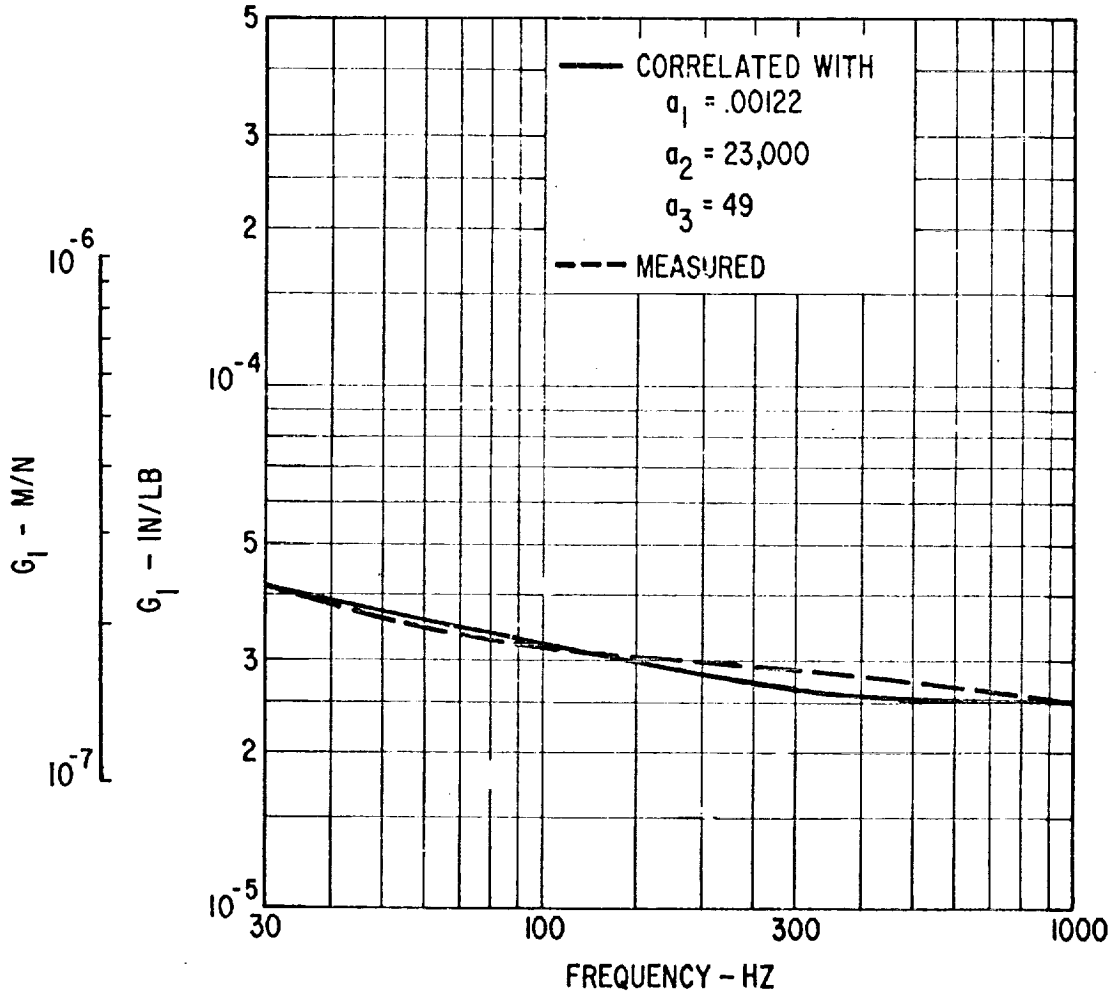

Fig. 30 Comparison of the Correlated and Measured G_1 Functions for Urethane Sample Under Shear Loading at 0.001 in. (0.025 mm) Amplitude and 10% Preload

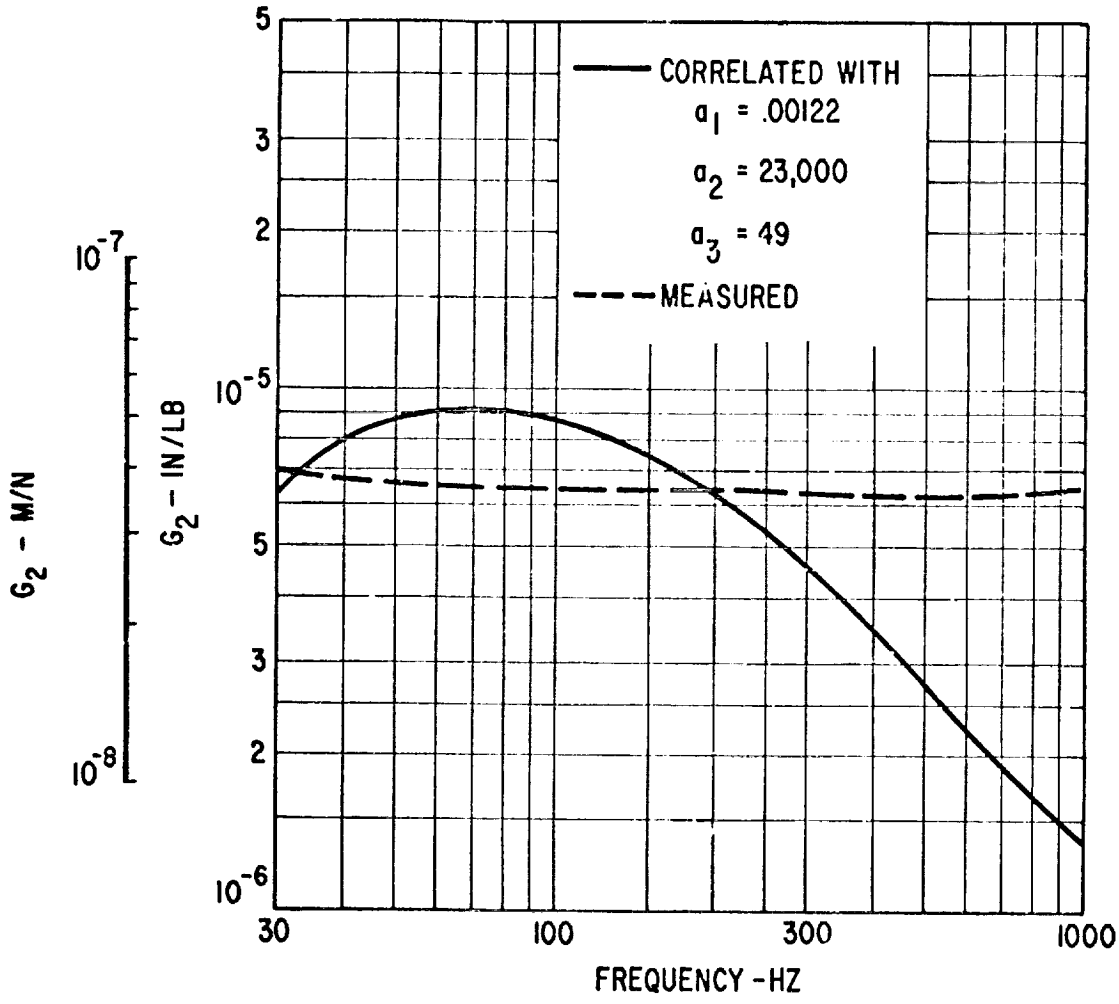

Fig. 31 Comparison of the Correlated and Measured G_2 Functions for Urethane Sample Under Shear Loading at 0.001 in. (0.025 mm) Amplitude and 10% Preload

MTI-13341

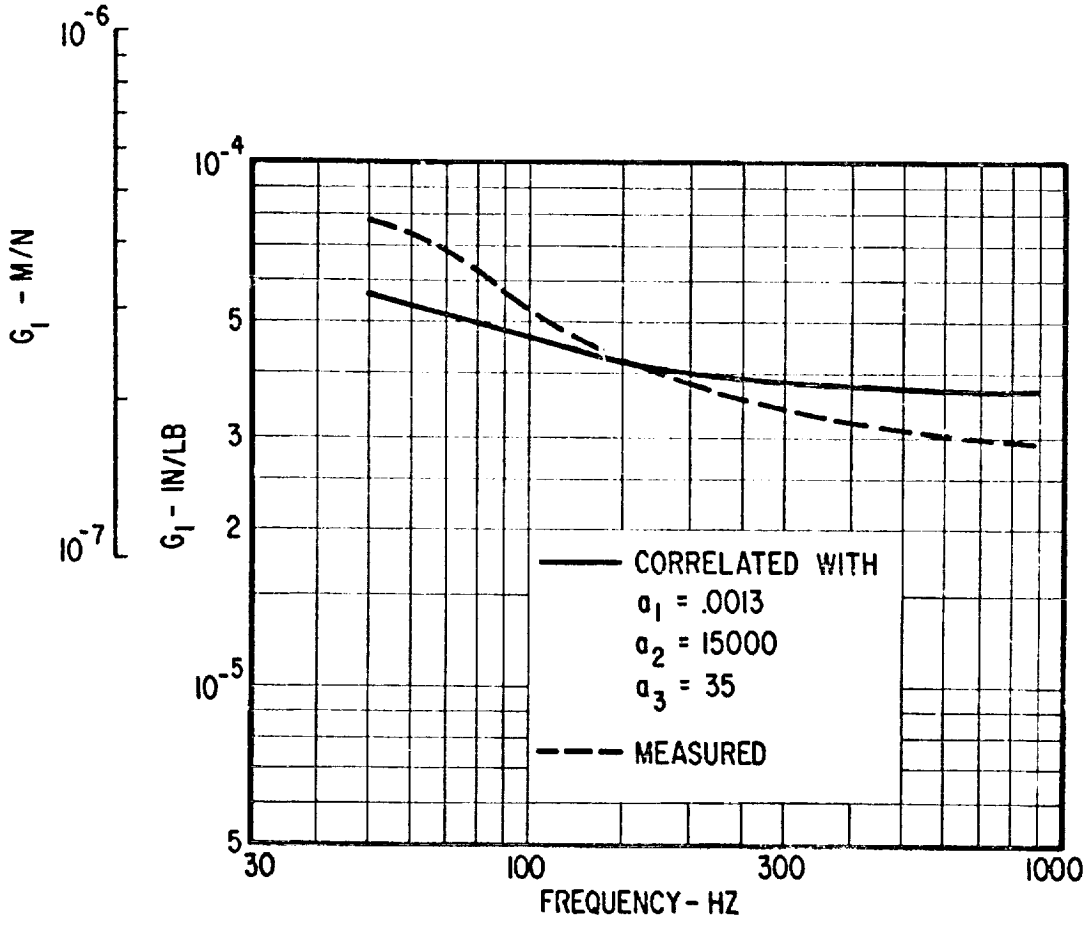

Fig. 32 Comparison of the Correlated and Measured G_1 Functions for Neoprene Sample Under Shear Loading at 0.001 in. (0.025 mm) Amplitude and No Preload

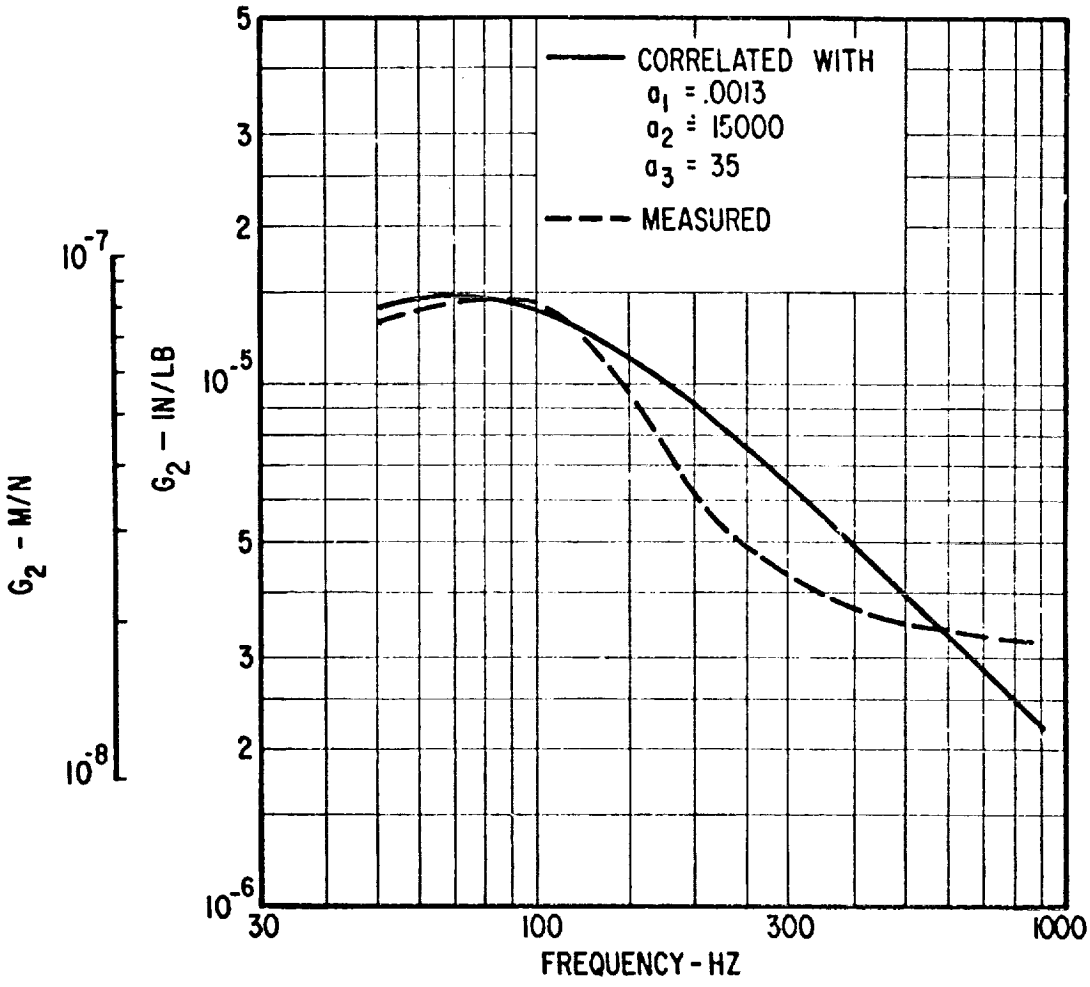

Fig. 33 Comparison of the Correlated and Measured G_2 Functions for Neoprene Sample Under Shear Loading at 0.001 in. (0.025 mm) Amplitude and No Preload

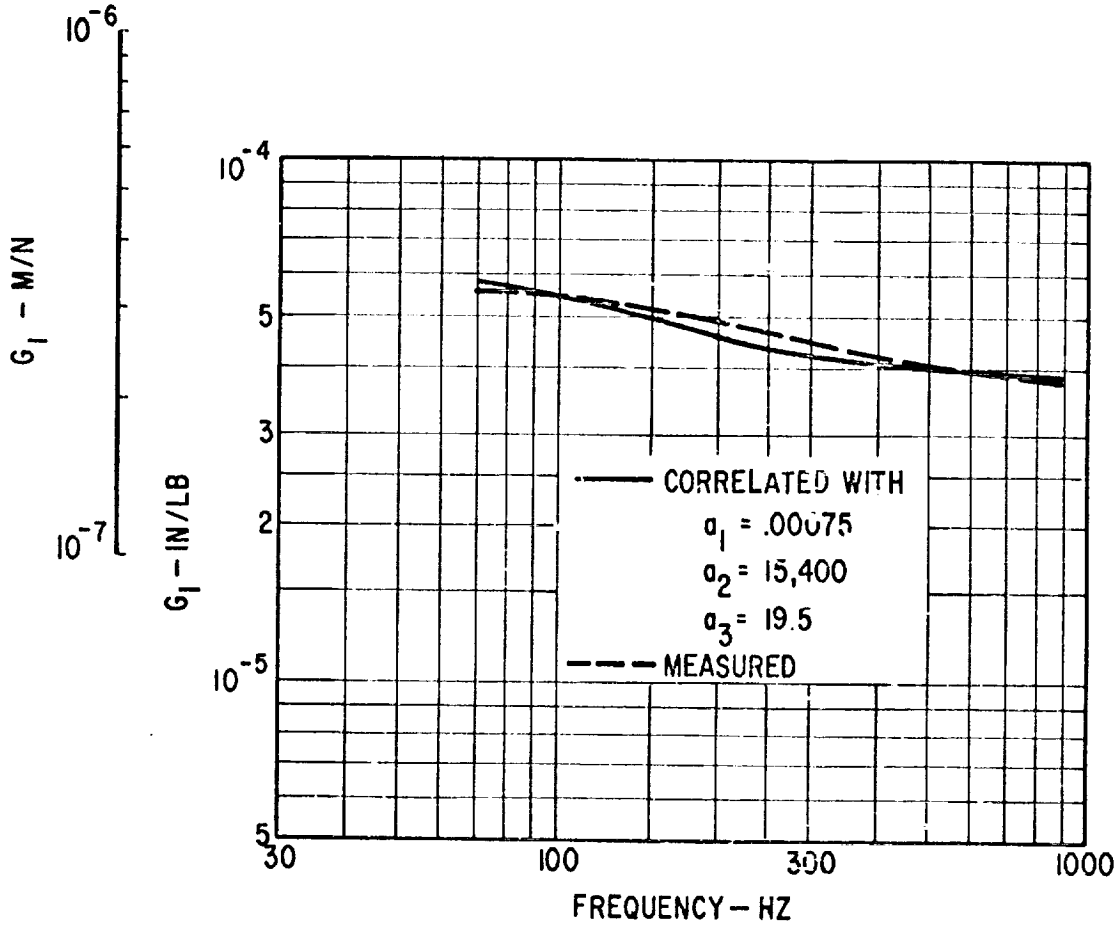

Fig. 34 Comparison of the Correlated and Measured G_1 Functions for Neoprene Sample Under Shear Loading at 0.003 in. (0.076 mm) Amplitude and No Preload

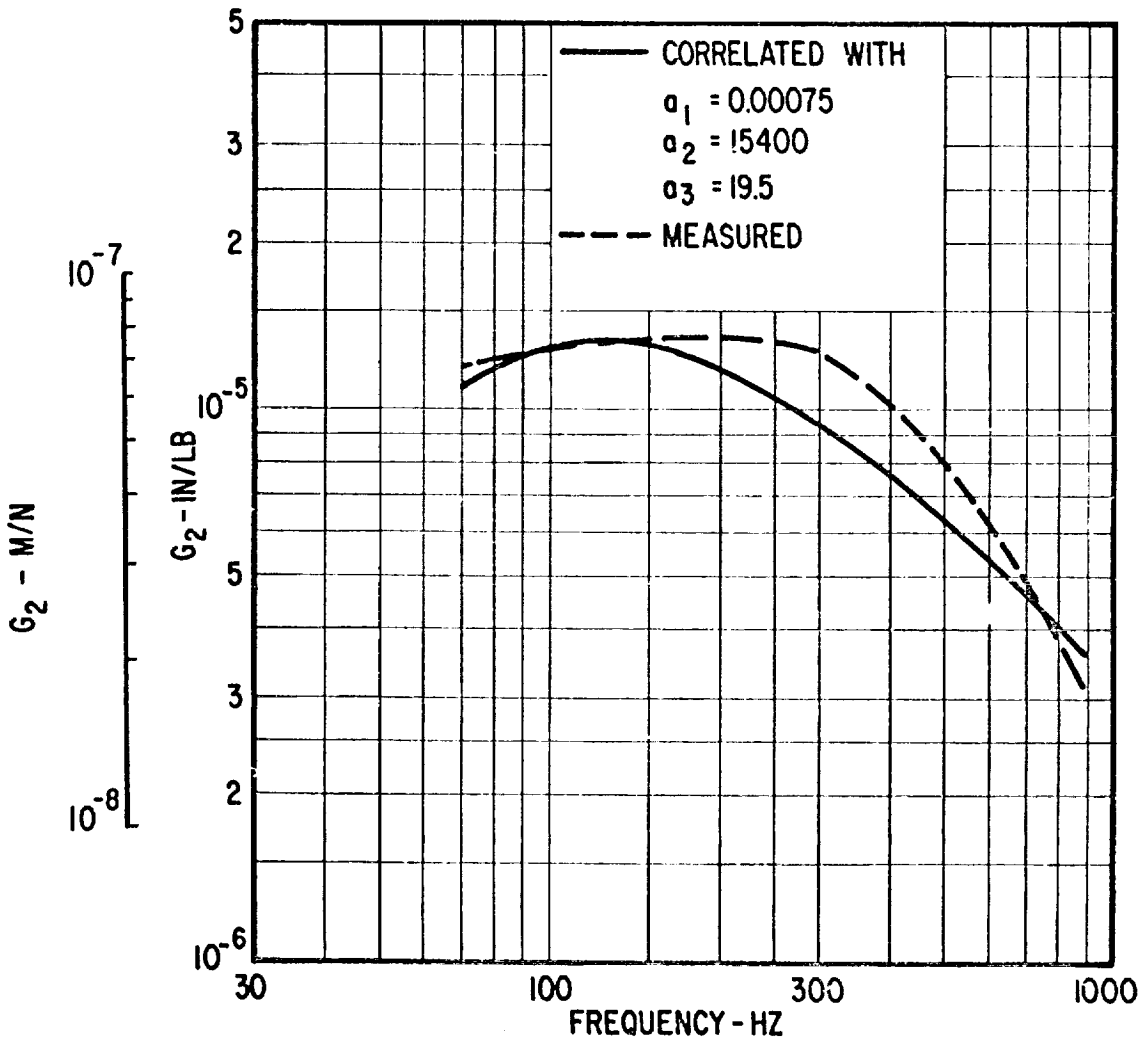

Fig. 35 Comparison of the Correlated and Measured G_2 Functions for Neoprene Sample Under Shear Loading at 0.003 in. (0.076 mm) Amplitude and No Preload

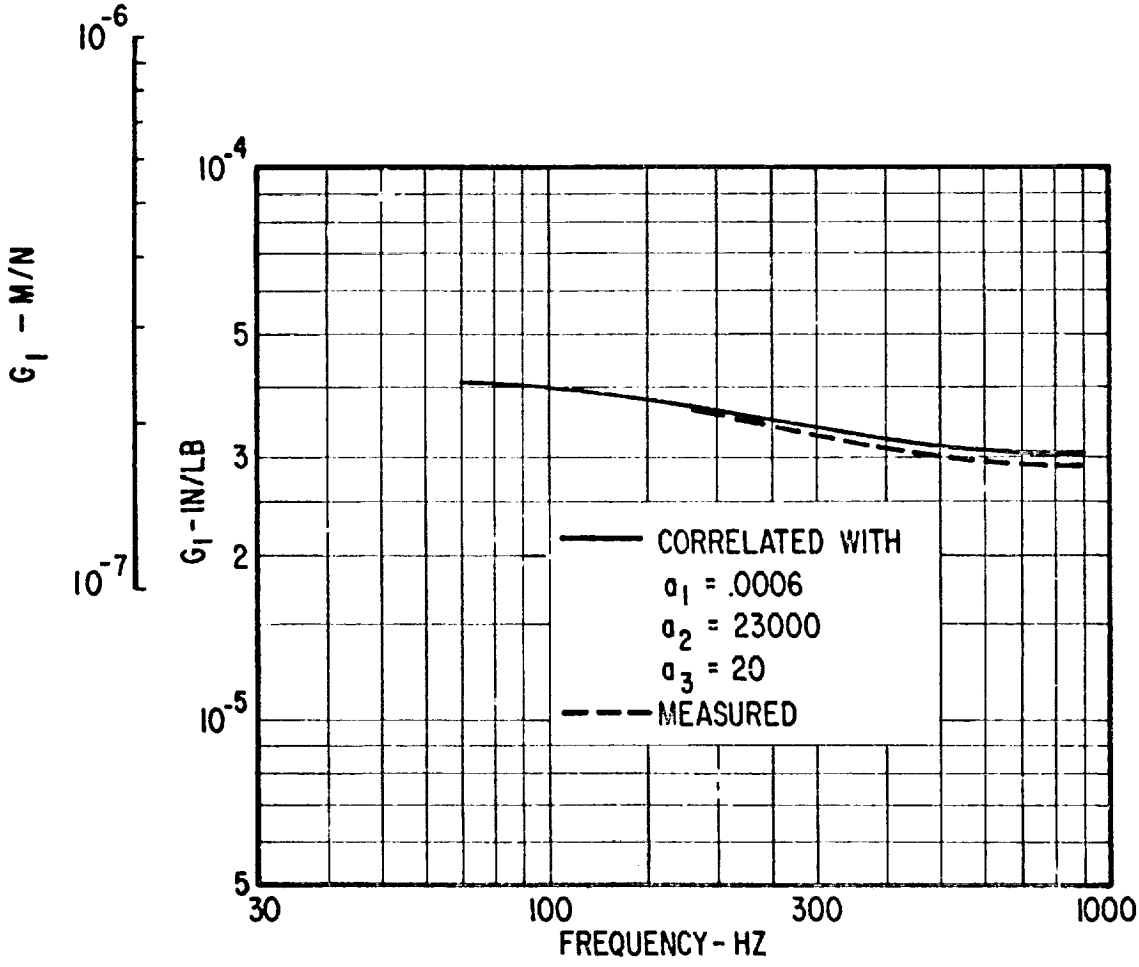

Fig. 36 Comparison of the Correlated and Measured G_1 Functions for Neoprene Sample Under Shear Loading at 0.003 in. (0.076 mm) Amplitude and 5% Preload

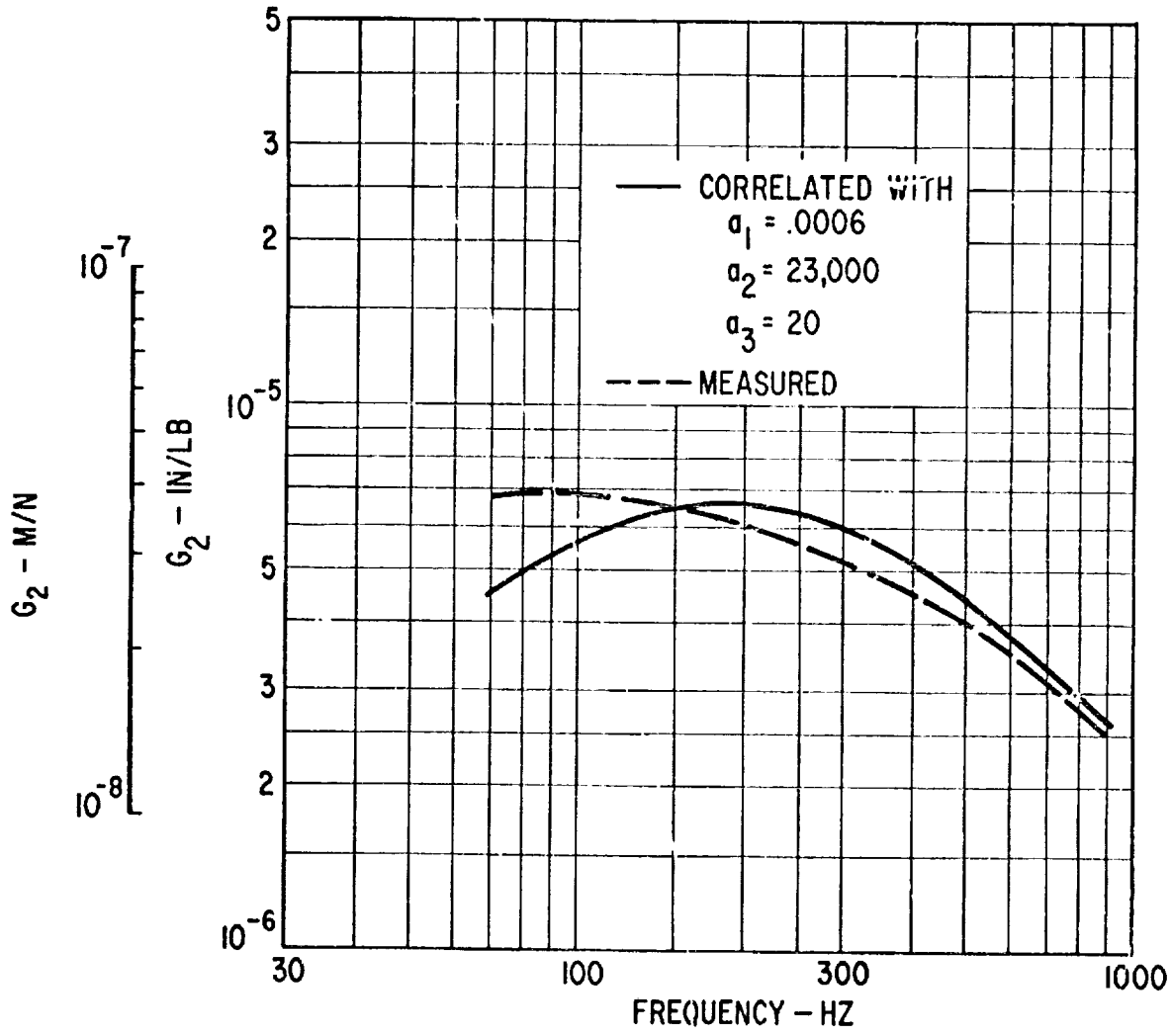

Fig. 37 Comparison of the Correlated and Measured G_2 Functions for Neoprene Sample Under Shear Loading at 0.003 in. (0.076 mm) Amplitude and 5% Preload

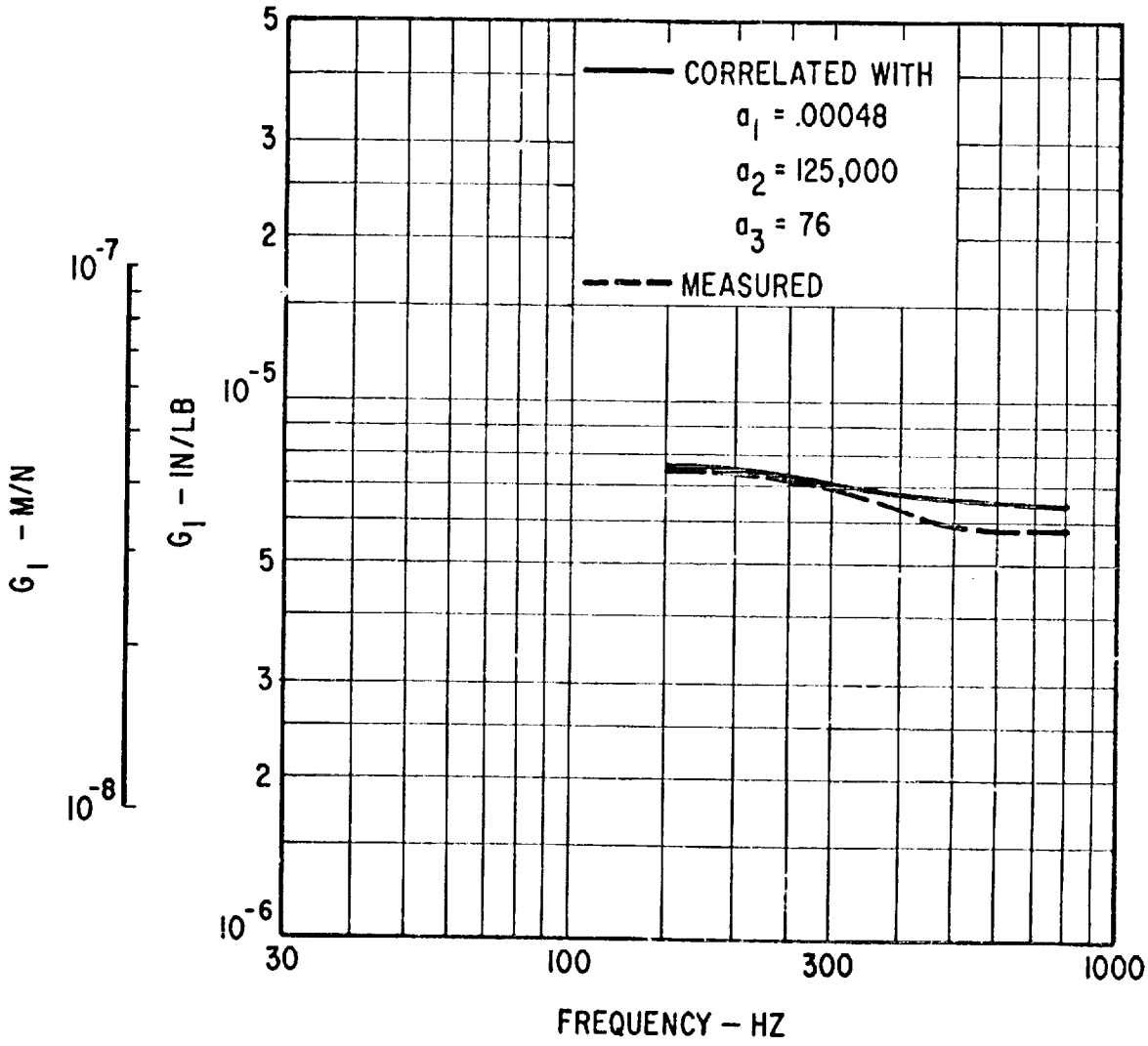

Fig. 38 Comparison of the Correlated and Measured G_1 Functions for Neoprene Sample Under Compression Loading at 0.001 in. (0.025 mm) Amplitude and No Preload

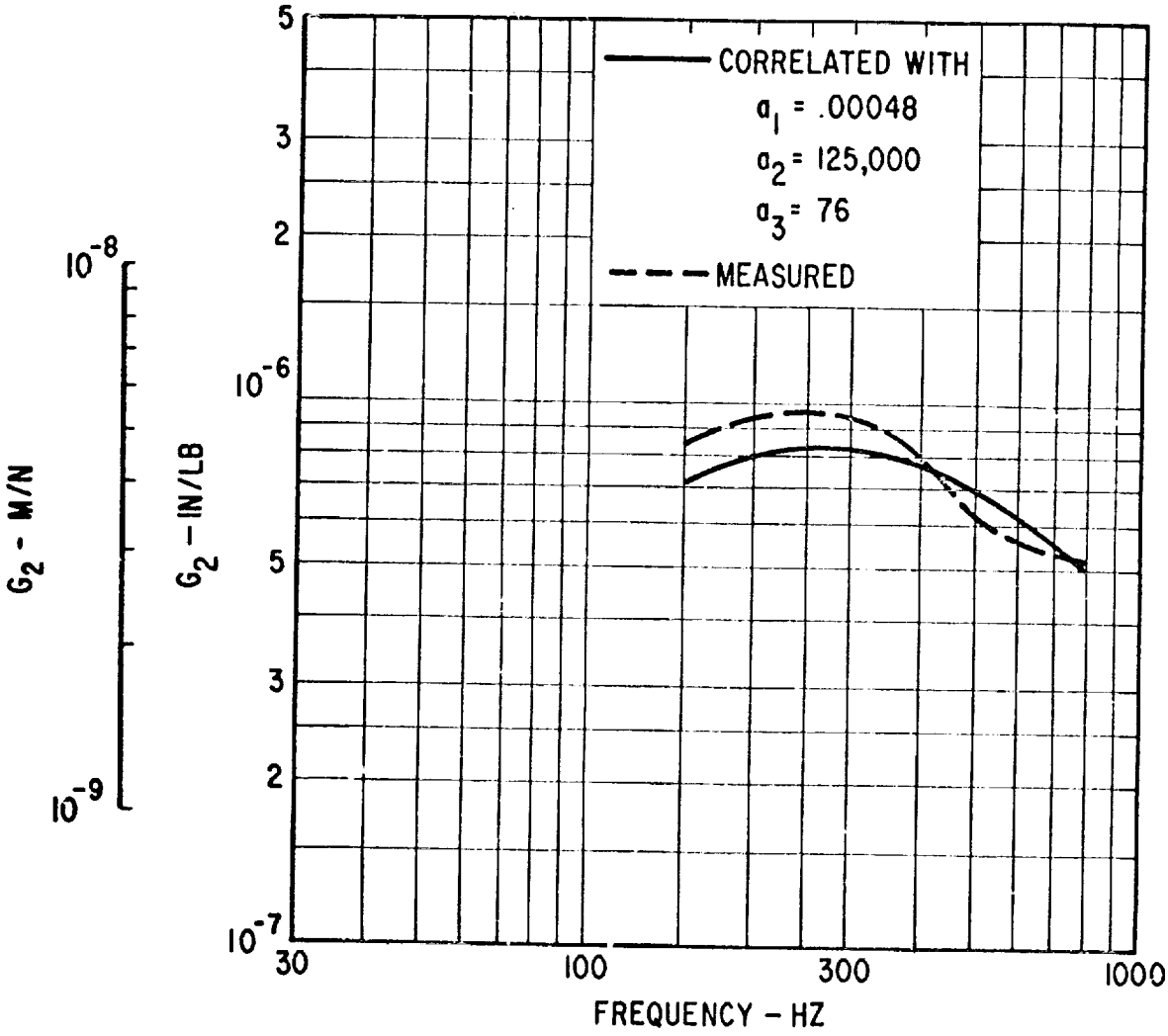

Fig. 39 Comparison of the Correlated and Measured G_2 Functions for Neoprene Sample Under Compression Loading at 0.001 in. (0.025 mm) Amplitude and No Preload

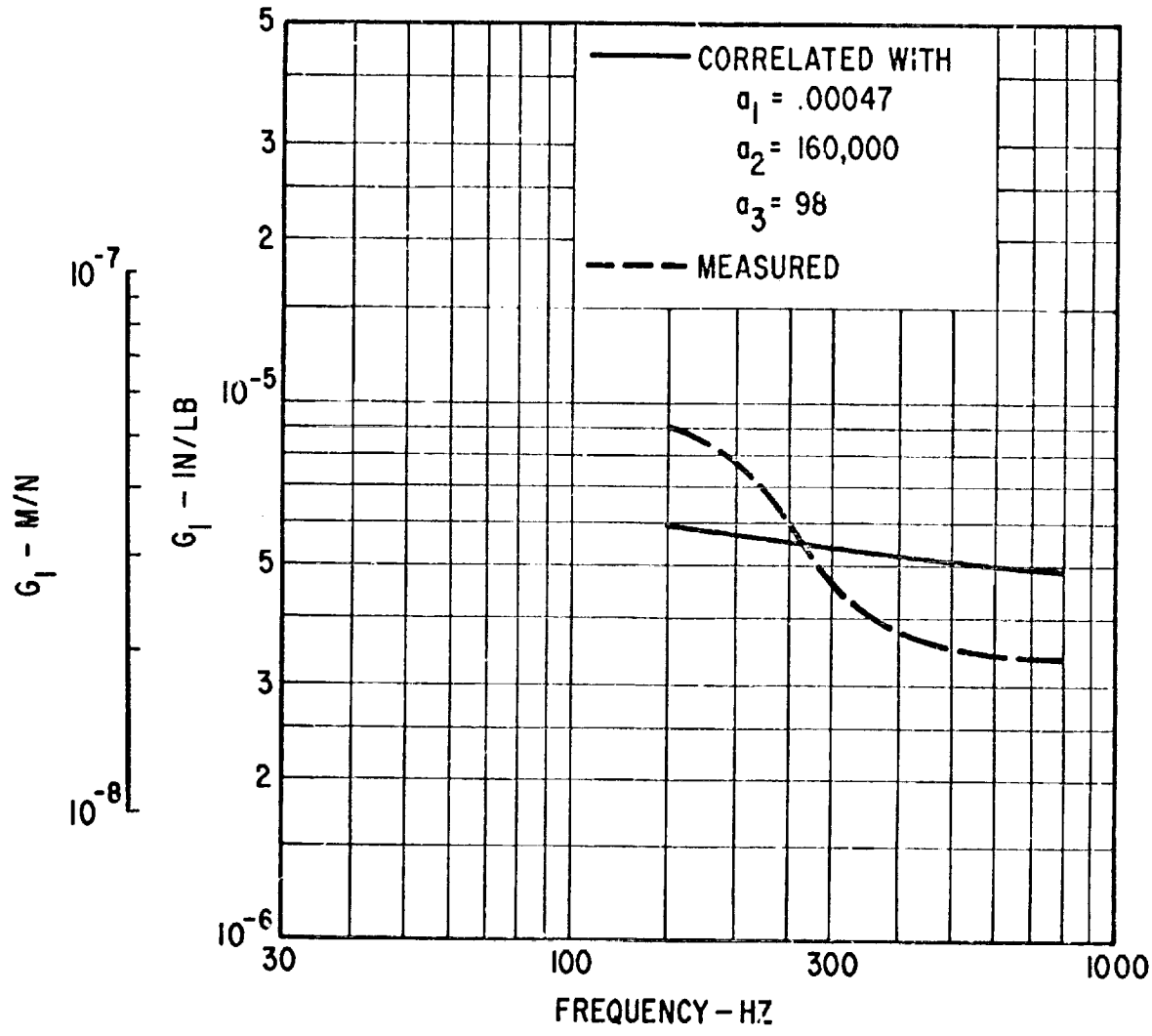

Fig. 40 Comparison of the Correlated and Measured G_1 Functions for Neoprene Sample Under Compression Loading at 0.001 in. (0.025 mm) Amplitude and 5% Preload

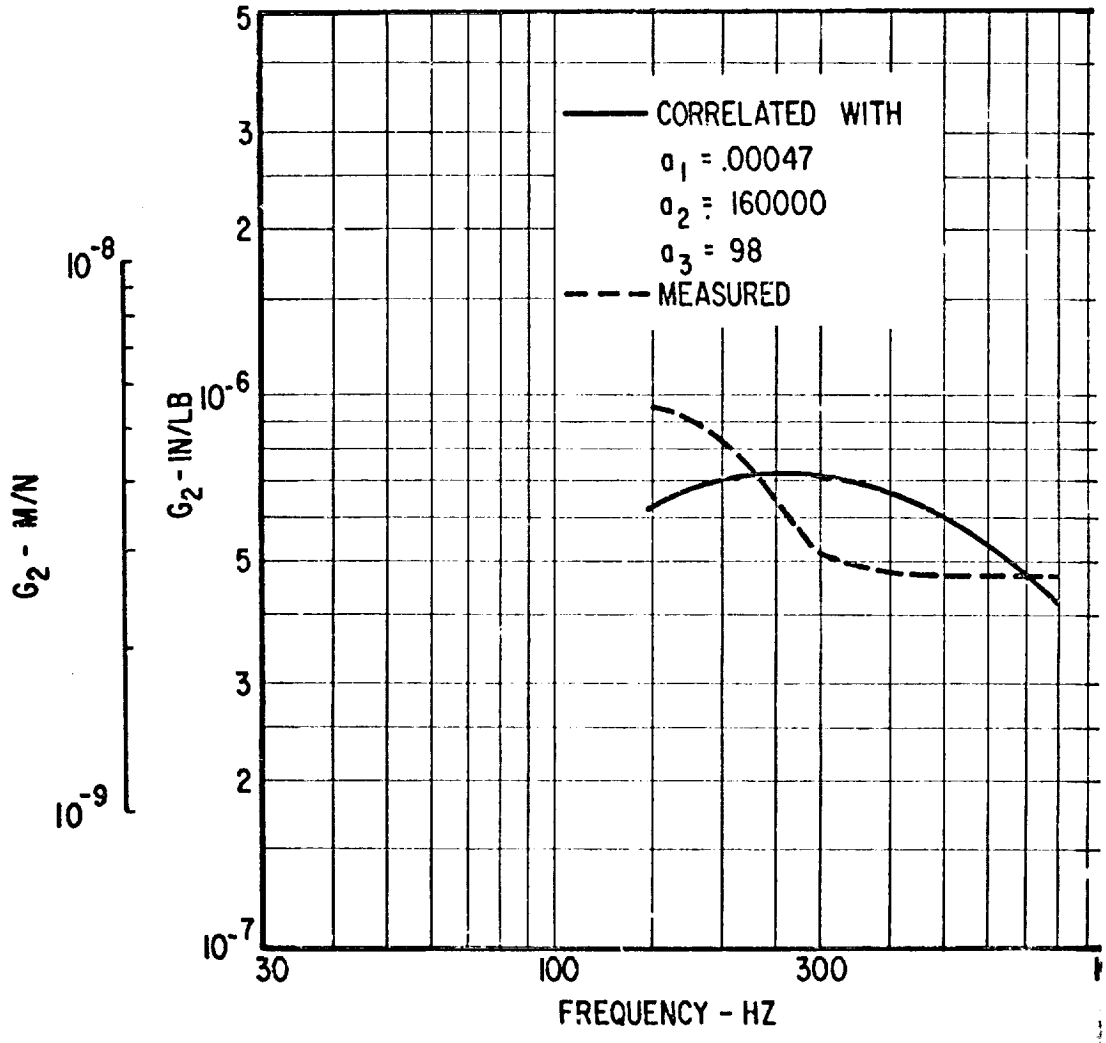

Fig. 41 Comparison of the Correlated and Measured G_2 Functions for Neopren Sample Under Compression Loading at 0.001 in. (0.025 mm) Amplitude and 5% Preload

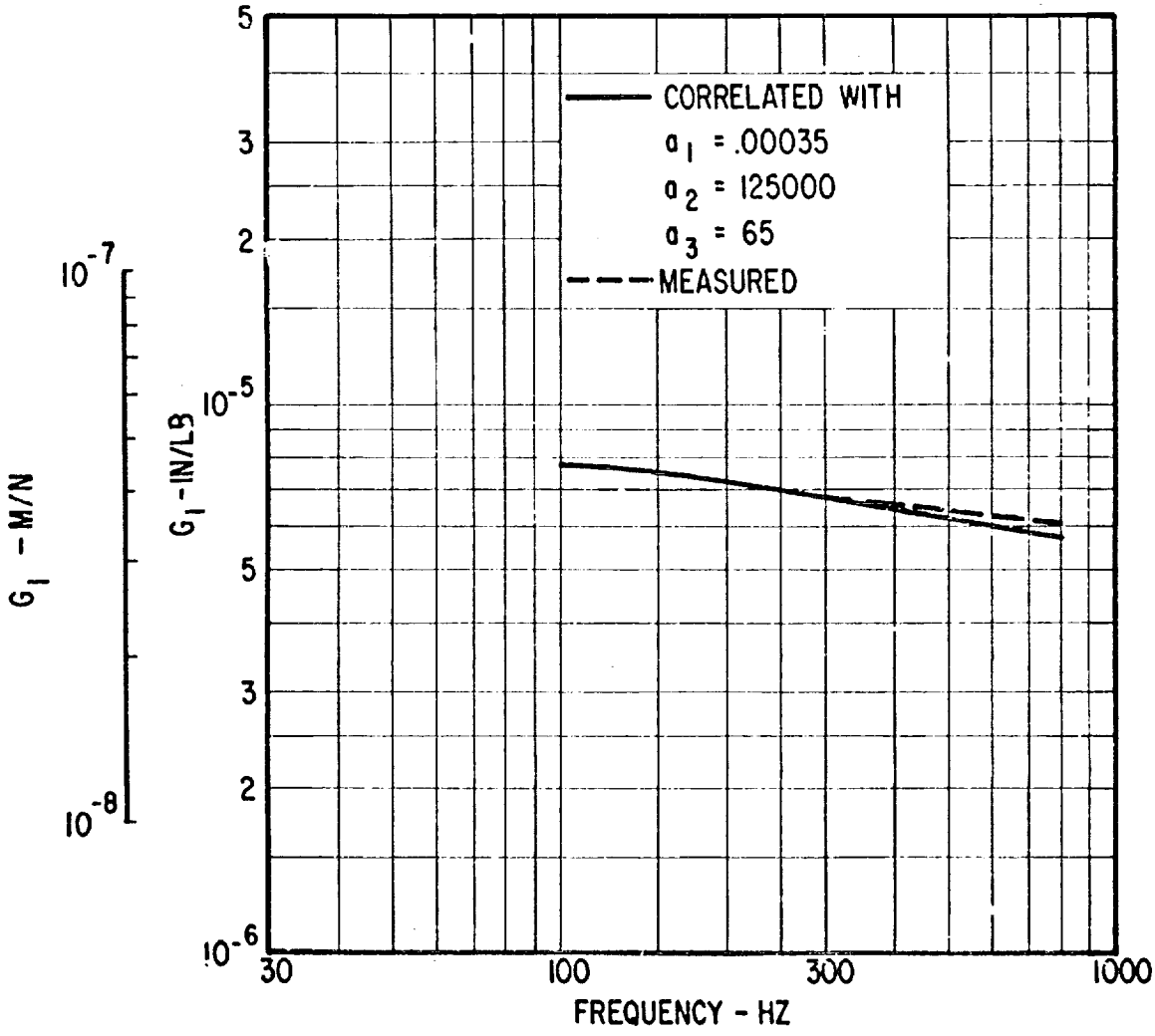

Fig. 42 Comparison of the Correlated and Measured G_1 Functions for Neoprene Sample Under Compression Loading at 0.0015 in. (0.038 mm) Amplitude and No Preload

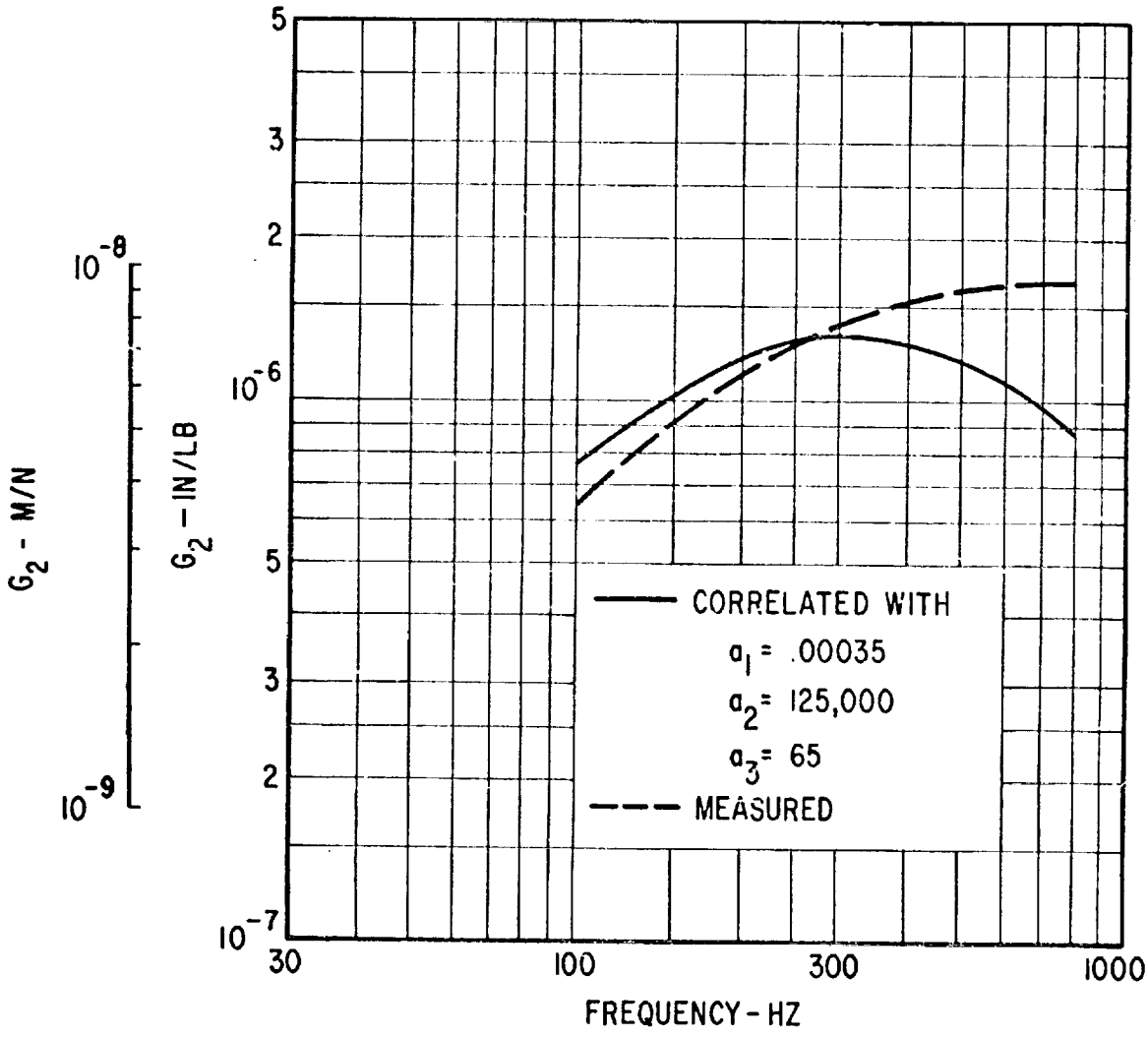

Fig. 43 Comparison of the Correlated and Measured G_2 Functions for Neoprene Sample Under Compression Loading at 0.0015 in. (0.038 mm) Amplitude and No Preload

END

DATE

FILMED

JAN 3 1973